Energy Efficiency of Below-Grade Envelope of the Stanley-Pauley Engineering Building in Winnipeg

by

Kirill Bobko

A thesis report submitted to the faculty of graduate studies of

The University of Manitoba

in partial fulfillment of the requirements for the degree of

MASTER OF SCIENCE

Department of Civil Engineering

University of Manitoba

Winnipeg

Abstract

This work investigates the energy performance of the basement structure of the Stanley Pauley Engineering Building located at the Fort-Garry campus at the University of Manitoba. Particularly, the effect of seasonal freezing and variation of thermal properties of surrounding soils on heat loss through the basement structure is assessed. For this purpose, two approaches have been considered. The first approach treats soil as a solid material with constant thermal properties in an unfrozen state while the second approach takes into account the effects of redistribution of partially unfrozen water and ice content during freezing and thawing cycles in the soil by considering the phase change mechanism. Thermal and physical properties of soil samples collected from the construction site were measured in the lab and used in numerical simulations.

It was concluded that the phase change of pore-water affects significantly the heat loss through the basement enclosure. The second approach considering variable thermal properties for soil resulted in higher heat losses compared to the model with constant properties. Additionally, three alternatives were suggested to reduce heat dissipation. Finally, energy savings are discussed.

Keywords: heat transfer in soils, heat loss, energy performance, insulation, cost analysis.

Acknowledgement

To my supervisor Dr. Pooneh Maghoul for infinite patience to my efforts to fulfill this thesis. With a sincere feeling of gratitude for the time being our group leader and guidance provided over the time at school. For knowledge, you shared with me and time management and strategies I learned from you.

I would like to thank superintendent Evan Fuller from BIRD and lab technician Kerry Lynch for their technical assistance on field and time consulting me and answering my emails. To my friend Hongwei Liu for his friendship and kindness. For his assistance in lab and class as he was every time ready to help me with challenging tasks.

I would not imagine finishing this degree without support from my parents. They were the first who convinced me to start this degree and were always by my side providing great encouragement and care and finally made this research possible. I hope I made this dream come true.

To my wife Vera who put so much love and efforts sacrificing her time supporting me in this program.

Kirill Bobko

List of variables

ξ	distance to freezing front	*m*
Ψ	negative pore-water pressure head	*m*
ρ	density	Kg/m^3
Θ	total volumetric water content	*1*
θ_i	volumetric ice content	*1*
θ_r	residual volumetric water content	*1*
θ_s	saturated volumetric water content	*1*
θ_w	initial unfrozen volumetric water content	*1*
θ_{w1}	unfrozen water content at freezing temperature	*1*
C_{pp}	apparent heat capacity	*J/kgK*
C_p	specific heat	*J/kg-K*
k	thermal conductivity	*W/m-K*
T	temperature	*K*
T_a	air temperature	*K*
T_m	melting temperature	*K*
T_s	surface temperature of the pavement	*K*
L_f	latent heat	kJ/kg
h_{conv}	heat-transfer coefficient, convection conductance	W/m^2K
q_c	net energy conductive flux	*W/m2]*

Table of Content

List of Tables

List of Figures

List of Appendices

List of Copyrighted Material for which Permission was Obtained

1. Facade of Stanley Pauley building. Appears as Fig. 4
2. Plan view of basement floor of Stanley Pauley building. Appears as Fig. 5
3. Fragment of campus key plan. Appears as Fig. 6

Introduction

Recent design practice of “green” buildings is targeted to make zero footprints of carbon dioxide in the environment. This dictates more and more strict rules for energy efficiency of the systems motivating people all around the globe to study solutions for better energy use, recovery and storage. Nowadays public buildings can be equipped with a number of options which allow minimizing energy demands such as the use of renewable sources like solar and geothermal energy and use of ventilation recovery systems when purged to outside stale air exchanges temperature with fresh air coming inside. At the same time, all above-mentioned systems will not be able to function properly without one key parameter: thermal insulation.

It is believed that foundations in cold regions should be buried until frost-free depth to avoid structural damage due to destructive frost action. There was a certain trend of last century to erect light buildings on so-called slab-on-grade foundations combined with edge beams. Foundations with reduced depth observed in some regions of Sweden are assumed to release heat accumulated in building and direct it towards freezing front with the purpose to reduce frost penetration. Also, such foundations were used for relatively “light” (residential) buildings, that exert small pressure to the base (Farouki, 1992). Some other European standards assume that buildings with heated

basements have lower frost penetration depth which is associated with heat released from the building.

The idea of low energy demand dwellings has become a pressing question for families with lower income since valuable maintenance expenses account for energy bills. Government of Canada acting through Indigenous Services Canada (ISC) funded over $600 million in budgets of 2017 and 2018 to improve housing for First Nations people living in reserves ("First Nations housing," 2018). The high standard requirements were established in one particular project associated with construction of 150 new houses in growing Tla-o-qui-aht Nation reserve on the West coast of Canada in Clayoqout Sound (Vancouver Island). Report namely addresses eco-friendly requirements for dwellings as follows: "The ultimate goal of the project is to ensure that newly constructed houses provide the healthiest living environment possible, reduce long-term costs required for heating and water usage, reduce impact on the environment, remain healthy living spaces for longer than current designs and incorporate cultural features that increase pride of ownership." (Taylor, 2012). A growth in new households on reserves was estimated as 4500 per year in a period of 2008-2018 (Taylor, 2012). The same tendency in growing number of residents was observed beyond reserve population. Population of aboriginal people accounted in census agglomeration area of Prince George (BC) has risen in five years until 8855 which is 11% of growth from 2001 to 2006 (Milligan, 2010). At the same time, the number of houses occupied by aboriginal people where major repairs are required also has risen from 12.6% to 15.3% over the same time. Construction of new houses with low energy demands for Indigenous people in reserves is dictated by modern social programs driven by Government of Canada.

Nowadays the necessity of proper insulation of below-grade structures is implied more by a desire to minimize heat loss rather than use heat as a remedy to resist frost action. Modern building

became so thermally insulated in their superstructure that heat often escapes through uninsulated parts of the basement. That is why great interest was attracted to problems associated with the prediction of heat loss through the basement part of the buildings.

Engineering practice sometimes consists of simplified thermal calculations of structural build-up interacting with the ground. Apart from structural materials, it is often assumed in building energy simulation programs, such as EnergyPlus and TRNSYS, that thermal properties of soils are constant, which means that they do not depend on such factors as seasonal freeze-thaw cycles and variations in water content. However, it is shown that this assumption cannot appropriately predict the actual heat loss through the below-grade building envelope (Bobko, Maghoul, & Kavgic, 2018).

This work aims to study the energy efficiency of the below-grade envelope of the new Stanley-Pauley Engineering Building in the Fort-Gary campus in Winnipeg. This case study will help to predict heat loss of the basement and find a solution for energy loss mitigation. The steps to achieve this purpose are described below.

Objectives and Scopes

In order to evaluate the energy performance of the below-grade structure of the Stanley Pauley Engineering building in Winnipeg, Canada, the following steps are taken:

1. Conducting soil investigation of the construction site by testing required number of samples. Primary interest is soil's thermal properties such as thermal conductivity, heat capacity and other physical characteristics.

2. Performing two numerical models and study heat transfer in a quantitative way by calculating energy loss of the basement part of the building. The first model consists of the assumption that soil's thermal properties (the one measured in lab) are constant and do not change during freeze and thaw seasonal cycles. The second approach treats soil as a mixture of three aggregates: solid particles, water and ice. Each component contributes to thermal property by volumetric weight. Additionally, and most importantly the phase change of porewater is considered when soil is subjected to freeze. Heat exchange between the below-grade enclosure and soil is studied.
3. Performing a comparative analysis of methods described above and suggests alternative insulation solution taken from national regulatory manuals. Position of additional insulation is speculated in a way to minimize heat exchange between structure and surrounding soil.
4. Calculating energy savings due to insulation installation and other options.

Thesis Organization

Chapter 1

This chapter consists of literature review which addresses the problem of heat transfer in soils. Importance of groundwater in freezing and thawing cycles is discussed. This chapter provides a review of mechanisms of water migration in freezing soils and physics involved in it. This chapter touches upon the subject of numerical modelling of heat transfer in soil by means of different software such as COMSOL Multiphysics, TRNSYS, and FlexPDE.

Chapter 2

This chapter describes results of soil investigation performed in August 2017 during massive ground excavations of the study area. Soil samples were collected in specific locations and tested in the laboratory to obtain their thermal properties. An excessive number of specimens and measurements allowed to exclude samples with obviously untypical properties. Measurements were made in natural and frozen conditions. Measured properties were used in numerical simulations described in Chapter 3.

Chapter 3

The two numerical models implemented in COMSOL Multiphysics are described in this chapter. The objective is to predict heat loss of below-grade structure over the period of one year after eleven years of simulation. The first model (Approach 1) treats soils' thermal properties as constant values which do not change during freezing and thawing seasonal cycles. It uses measured thermal properties summarized in Chapter 2 in heat transfer equation to evaluate heat flux through the basement floor and wall. The second model (Approach 2) takes into account phase change of porewater when it experiences freezing during cold seasons. Approach 2 calculates thermal properties of soil based on the proportion of water, ice and solid particles in unit volume. Latent heat is considered during phase change. Additionally, calculations are made for two designs: first one is a base design when basement is not insulated, the second type of design is made in line with project documentation (insulated basement, used as a reference case). Results are summarized in a way of quantitative overall energy loss and thermal fluxes, as well as expressed as cost demands for both Approaches and two types of insulation design.

Chapter 4

This chapter is dedicated to study alternative insulation solutions (1) to mitigate energy dissipation through the underground envelope. It also studies the effect of snow pack (2) around the building and use of granular backfilling (3). Outcomes of all three models were referenced to the original design, then comparative analysis was introduced to study the effect of all three modifications.

Chapter 5

This chapter summaries the main conclusions of the project, introduce limitations and describe recommendations for future work.

Dissemination

The outcomes of this research have been disseminated as follows:

Journal paper:

1. **Bobko K.**, Maghoul P., Kavgic M., 2018. Energy Performance of Below-Grade Envelope of an Institutional Building in Cold Regions, Building and Environment (Elsevier), To be submitted.

Conference papers:

2. **Bobko K.**, Maghoul P., Kavgic M., 2018. Energy Performance of Below-Grade Envelope of Stanley-Pauley Building in Winnipeg, 71st Canadian Geotechnical Conference (GeoEdmonton 2018), Edmonton, Canada.
3. Maghoul P., Kavgic M., and **Bobko K.**, 2017. Modelling of Thermal Performance of Foundation Walls in a Cold Climate, 70th Canadian Geotechnical Conference (GeoOttawa 2017), Ottawa, Canada

1. Literature review

1.1. Introduction

Nowadays, design of buildings faces energy-conscious requirements regarding heat losses. Modern construction techniques allow performing insulation of building to minimize heat loss from the superstructure. However, uninsulated structure below ground level might contribute considerable heat loss compare with above grade structure. Due to the absence of proper insulation in some cases up to 30% of total heat loss over the one heat season might be released throughout foundation part of the building (Hagentoft, 1988). Due to this fact, the necessity to reduce energy emission from building via foundations can no longer be disregarded. Seasonal ground frost penetration increases heat flux out of the basement which leads to increased heat loss. Additionally, freeze and thaw cycles in soils might significantly change their thermal properties which also affects energy dissipation. On the other hand, in warm-climate countries, ground-coupled structures might be cooled by lower earth temperature. In this case, ground appears as a heat exchanger with enormously big potential for cooling.

Heat transfer in ground-coupled conditions is a subject for further discussions. Optimization of foundation insulation might bring cost-effective results during building service, in other words, improve energy efficiency of the building.

Starting with physics and processes taking place in freezing soils, this chapter will guide through mathematical computations of ice content, heat flux and other parameters necessary for energy performance analysis. It also shares experience of numerical modelling using different software. After all, some exerts from standards are given about international experience of foundation design in cold regions.

1.1. Mechanism of Heat Transfer in the Ground

The process of heat transfer in the ground is dependent on many factors such as physical properties of soil as a porous material, groundwater level and flow, moisture content and so on. Farouki (1982) collected experimental data of thermal conductivity and capacity of the soil. The thermal conductivities of dry and wet sands can differ up to a factor of ten. Similarly, the thermal conductivity of dry and wet loams can change up to a factor of five. The variances in thermal capacity are less manifest, but it is still doubles or triples from dry to wet state (Janssen, Carmeliet, & Hens, 2004).

The other aspect of heat transfer to be considered is a forced convection. Forced convection is described by M. Zhang, Yuan, & Wang (2011) as “heat transfer phenomena”. It has been classified by other scientists Smith and Chapman (1983) into three main categories. The first one is when hydraulic gradient is orientated against the upcoming vertical conductive gradient (↑↓). In this case, water flow will resist convective transport and as a result, increasing temperature gradient

with depth. The second mechanism is reverse to the first one showing groundwater flow collinear to the temperature profile (↑↑). Such case decreases temperature gradient with increasing depth. The third class of forced convection happens when hydraulic gradient and the temperature gradient are normal to each other (↑←) in this case water flows collinear to isotherms of heat conduction, consequently, convective transfer is eliminated (Domenico & Schwartz, 1998). The three types of forced convection should be considered while modelling heat transfer which makes every project solution tied to local geological conditions.

Nowadays, numerous attempts have been made to simulate thawing and freezing cycles and study behavior of water flow in these conditions. Hansson used formulated by Beskow fundamental principles, in their attempt to express mathematically and simulate the effect of freezing in the soil numerically. It has been observed that water moves towards and accumulates in freezing front. Secondly, water in pores does not freeze at 0ºC but depends on freezing-point depression caused by interaction of water, soil particles, and solutes (Beskow, 1935).

The experiment carried out on a freezing soil cylinder by (Hansson, Šimůnek, Mizoguchi, Lundin, & Van Genuchten, 2004) showed the rapid decrease in the total water content at or immediately below the freezing front and the gradual recovery deeper in the column. This experiment was simulated as well using the coupled water, heat, and vapour transport processes incorporated in the numerical HYDRUS-1D subroutine (Šimůnek, Šejna, & Van Genuchten, 1996). Results of the model showed strong convergence to predicted values of water content in frozen soil compared to the laboratory experiment.

Measurement of water movement into the freezing soil is a challenging task. That is why many techniques have been applied by different scientists. Overall, this process is being caused by

temperature magnitude change, and this brings different effects on saturated and unsaturated soils (Islam, 2015). Additionally, certain impact on freezing pace might affect saline concentration. Thus, the experiment based on nuclear magnetic resonance (NMR) technique was implemented to find a relationship between the reduction in temperature and the amount of unfrozen water in a soil sample. Results of the experiment show that the amount of unfrozen water decreased with the lowering of temperature. When a porous medium was saturated with a solution, the amount of unfrozen water increased with higher solute concentration (Watanabe & Wake, 2009).

Many factors such as phase change of water from liquid into ice create some difficulties in calculation of heat transfer as well. Sometimes boundary conditions of the ground surface are simplified and accepted as average for particular design.

1.1.1. Freezing and Thawing Processes in Soils.

Soil's properties are dependent on freezing-thawing processes and temperature changes during cold seasons. Soil becomes highly impervious when freezes this also leads to structural changes which in turn increase the strength of soil (Andersland & Ladanyi, 2013).

To model freezing process in soils, it is of great importance to introduce freezing from a thermodynamic point of view as well as formulate equilibrium relation between ice and water content. Often freezing of soils is associated with the "drying" assumption in unsaturated soils yielding this process to the soil water retention characteristics (SWRC) curve. Combination of thermodynamic equilibrium coupled with soil water retention curve generates an approach to determine the amount of ice content in soil.

Freezing of soils happens during cold seasons and starts when the temperature drops below the freezing point of pore-water. Freezing leads to a volume increase of frozen water by around 9% (Andersland & Ladanyi, 2013), however, in gravel sands, this is not associated with the expansion of voids by the same percent because water is likely to be squeezed out during freezing. Silty soils show different behaviour during freezing and mostly depend on the rate at which the temperature is lowered. Rapid cooling leads to the freezing of in-situ water while graduate lowering of temperature mobilizes big amount of water and causes the formation of ice lenses in frost-susceptible soils (i.e. silty soils). In this case, ice is forming in layers parallel to the frost front. Upward migration of water appears in fine-grain soils such as silts and clays where capillary rise is possible. Thus, ice lenses are formed only in fine-grained soils with lower permeability than sands (Andersland & Ladanyi, 2013). This assumption was proved by a series of experiments called “freezing soil column”. Vertical cylindrical specimens of soil are subjected to freezing from the top surface. Amount of ice formation on top of the specimen is limited by water percolated from the bottom part of the sample and volumetric increase does not exceed 9% of all water retained in the system. Figure 1 illustrates three samples. First specimen constitutes a closed system because all water contributed to ice formation is taken within the system (Andersland & Ladanyi, 2013).

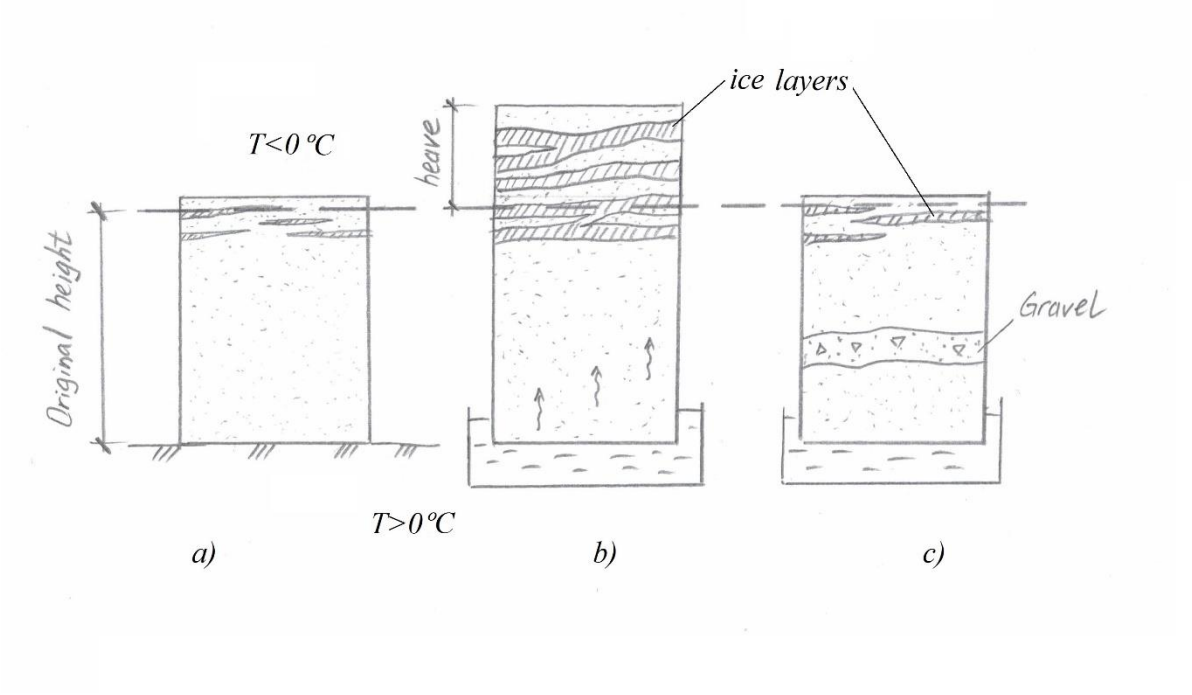

Fig. 1- Ice development in soil's specimens: a) closed system b) open system c) cryo-suction cutoff by gravel layer (adapted from Andersland & Ladanyi, 2013)

The second specimen is called an open system since the lower part of it is exposed to free water. Last will continuously supply water flow to freezing front, and ice lenses would be formed significantly. Andersland and Ladanyi assumed that theoretically ice lenses might grow several meters in thickness. The specimen in part c) demonstrates capillary cut-off of liquid flow by the layer of coarse sandy gravel.

Similar experiment with some modifications using silica flour as a specimen material was carried out by Jame (1977) and later by Hagentoft (1988). Gravimetric moisture content was measured with the gamma-ray method. Results show that redistribution of water content appears during freezing from unfrozen to frozen zones as well (Jame, 1977). These experiments clearly proved groundwater movement during freezing. In the next section, it will be discussed what causes such

moisture redistribution and what are the driving forces behind it. Understanding of mechanism will help to formulate mathematical model with respect to the calculation of heat loss.

1.1.2. Driving Forces of Water Migration during Freezing

A vast number of experiments and observations demonstrated that water movement in freezing soils happens in three different states such as vapour, liquid, and solid (ice). Last only occurs as a result of plastic flow of ice. Such deformations are caused by increasing local stress at points of contact of mineral particles and ice lenses. Plastic redistribution of ice layers may be observed in already frozen soils or permafrost areas due to external loading or even from self-weight (Tsytovich, 1975)

1.1.3. Vaporous Moisture Transfer

Evaporation of moisture in freezing soils may also contribute into heat transfer. Vapour may condensate not only into the water but straight to the ice increasing ice content at frost front. Vaporous transport may occur even at constant temperature. Ice vapour has a lower density than vapour of water, meeting each other they create density-driven flow. Rate of vapour migration is proportional to the pressure difference at the certain point of the domain. Since Clausius-Clapeyron equation relates change in pressure of two phases to the temperature change of the system, then moisture, in its vapour phase, will flow along the drop of the thermal gradient into the freezing front (Newman, 1995). Vapour migration occurs in partially saturated soils while in fully-saturated soils this mechanism may be neglected. In saturated soils, liquid water transport dominates over the other phases (vapour and solid ice), (Tsytovich, 1975). It was mentioned by Jumikis (1966)

that the importance of vaporous heat transfer takes place in soils with large void size and without continuous liquid phase (Newman, 1995).

1.1.4. Liquid Moisture Transfer

It has been discussed that groundwater in freezing soils is driven once the equilibrium conditions are distorted. The reasons causing the unbalanced condition are called as driving forces of moisture migration. There are a number of driving forces described in the literature which causes moisture transfer towards freezing front (Kurylyk & Watanabe, 2013). Advancing freezing makes system thermally imbalanced activating driving forces of moisture migration. They, in turn, create gradients of molecular forces such as adsorption forces of soils skeleton, crystallization potential of ice, less molecular mobility of water at water films close to freezing front (Tsytovich, 1975).

Attraction of water towards freezing front may be explained as an increased suction potential also observed during drying in unsaturated soils. Models, where freezing is associated with drying, have been thoroughly applied by many researchers such as Van Genuchten (1980), Shoop & Bigl (1997), Dall'Amico (2010) and (Krarti, Chuangchid, & Ihm, 2004).

Additionally, structural features of water molecules and molecular mobility is also acknowledged by (Ananyan, 1959) as the driving force of water migration towards freezing fringe. Based on this theory soils with lower temperature would have higher sorption forces of soil skeleton and crystallization potential of ice as well as lower molecular mobility of water. These factors create certain gradients in intermolecular forces towards the source of cold, creating a flow to the freezing front (Tsytovich, 1975).

Water content in soils is often subject to change. There are several mechanisms which drive water to migrate in soils. Evapotranspiration processes caused by precipitations create hydraulic head in top soils, then driven by gravity water redistributes into the lower layers of soil contributing into field capacity of the aquifer. Some of the vadose water is driven towards surface in upward direction by capillary tension or root vegetation intake. Capillary rise also highly depends on soil type and soil's particle size. In sandy soils, capillary rise may reach of 20-50cm when clayey soils demonstrate up to several hundred meters rise (Domenico & Schwartz, 1998).

Presence of water in soils is often described with *soil water retention curve* (SWRC) which is a relation between moisture content θ_w and its matric potential ψ or pore water suction (Fig. 2). During freezing, water content may also be expressed as a function of freezing temperature in *soil freezing characteristic curve* (SFC) (Dall'Amico, 2010). Many of existing models make analogy between two characteristic curves SWRC and SFC. This relationship is explained by the presence of captured liquid water in pores during both "drying=freezing" processes due to sorptive or capillary forces (Kurylyk & Watanabe, 2013). In drying soils evaporated water is substituted with gas phase, similarly in freezing soil, water is substituted with ice. In both cases forces remaining water from draining acting in freezing soil to retain water from freezing which creates suction potential (Fig. 2). Bottom point of all three types of soil in (Fig. 2) represents the residual water content θ_r [-] which is such water content, where the removal of water from soil requires significantly more energy and becomes problematic (Fredlund, Sheng, & Zhao, 2011).

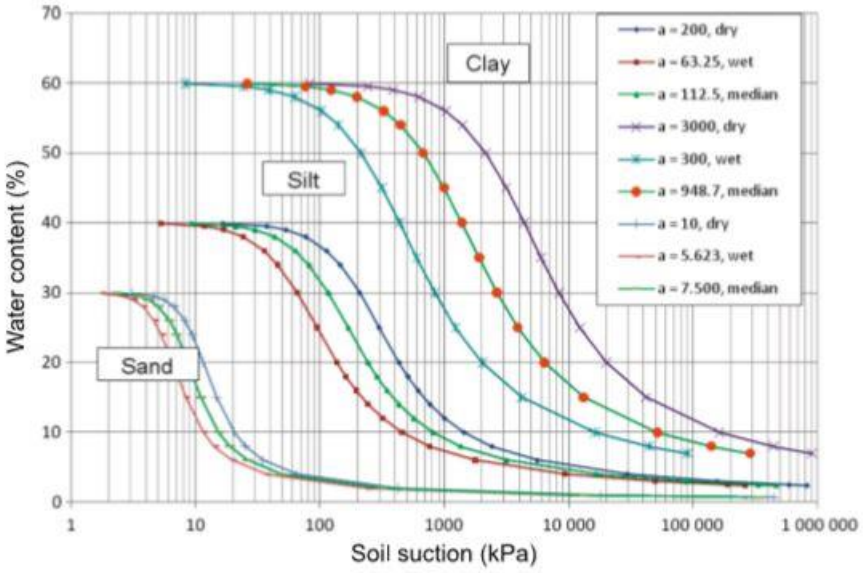

Fig. 2- Drying , wetting and median curves for three types of soil (after Fredlund, Sheng, & Zhao, 2011)

The purpose of the water content formulation in soils is to predict its redistribution based on the soil-water retention characteristics considering hydraulic conductivity dependence of saturated and vadose zones. Brooks & Corey (1964) and Van Genuchten (1980) represented the popular formulation of SWRC for different types of soils. Brooks and Corey (1964) formulated water-soil content as a function of pressure head (h):

$$\Theta = (h/h_b)^{-\lambda}, \qquad [1]$$

where h-is pressure head, h_b-is air entry or bubbling pressuredefined as the pressure head value at which the largest pores begin to drain and λ- is soil characteristic parameter. Later Van Genuchten (1980) has made an extensive analysis based on Mualem (1976) formulation and reached more smooth agreement between soil-water retention curve with experimental data of different types of soils. Van Genuchten (1980) formulation of conductivity model contains a closed-form equation

with three independent parameters α, n, m (Van Genuchten, 1980). Water content in soil as a function of suction potential is expressed in Eq [2].

$$\theta_w = \theta_r + \frac{\theta_s - \theta_r}{[1 + \left(-\alpha(\Psi)\right)^n]^m} \quad [2]$$

where θ_w [-] is volumetric water content; θ_r[-] is the residual volumetric water content; θ_s[-] is the saturated volumetric water content; Ψ [m] is negative pore-water pressure head (similar to h in Eq.[1]); α [1/m], n and m are independent curve fitting parameters.

Flerchinger, Seyfried, & Hardegree (2006) proved reasonable accuracy between SWRC and SFC for loamy sand soil, a slight bias toward higher water potentials was observed for the sandy loam and silt loam. SFC curve may be plotted as water content related to either matric potential or temperature (Fig. 2). Similarly to Eq.[2] unfrozen water content in freezing soils was made by Zhu & Michalowski (2005) in Eq. [3] using SFC. Exponential function can accommodate most of the soils by treating three parameter θ_r, θ_w, a.

$$\theta_{w1} = \theta_r + (\theta_w - \theta_r)e^{a(T-T_0)} \quad [3]$$

where in this study, $\theta_r = 0.05$ [-] is residual unfrozen water content, $a = 0.16$ is curvature coefficient, $\theta_w = \theta_s = 0.535$ [-] is unfrozen water content at the freezing temperature T_0. Additionally, it complies fully saturated condition when temperature remains positive.

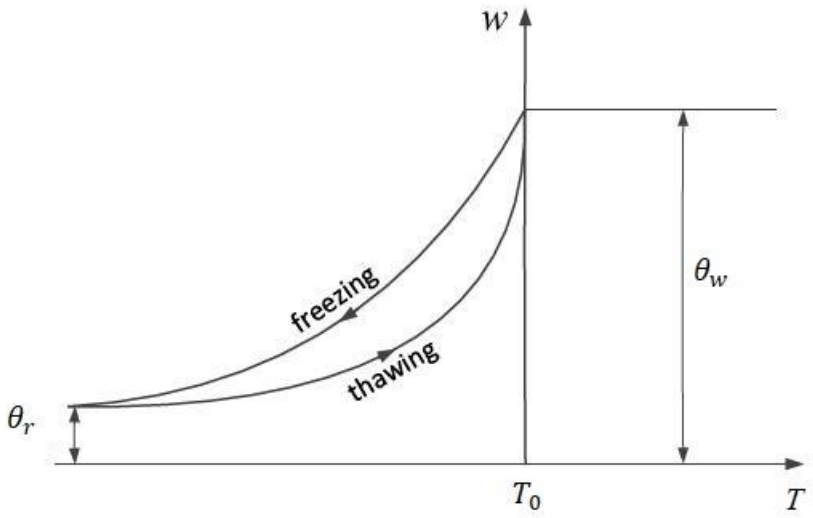

Fig. 3- Unfrozen water content curve (adopted after Y. Zhang, 2014)

The hysteresis-like behaviour of unfrozen water content Fig. 3 was admitted by (Tian, Wei, Wei, & Zhou, 2014; Parkin, von Bertoldi, & McCoy, 2013).They assumed freezing and thawing curves are equal and hysteresis effect is neglected.

1.2.Problem of Phase Change

The problem of phase change was addressed by many authors considering two matters with different thermal properties separated by floating boundary condition of the phase change. The phase change is usually introduced as moving surface between two phases where heat is liberated or absorbed (Dall'Amico, 2010). Stefan formulated equation of thermal balance on the boarder of two phases considering latent heat of two matters. Nowadays, similar moving-boundary problems are often called as Stefan's problem. Early attempts to formulate natural freezing of soils (or water) were introduced in analytical solution of Stefan's problem. It describes mechanism of moving freezing front in medium with applied temperature inlet fluxes and temperature of phase change.

Experimentally Stefan's problem may be described as ice block thermally insulated on sides with initial temperature T and applied constant relatively high temperature on top. With time ice would melt from top to the bottom generating melting front ξ moving in downward direction. Position of phase change front x= ξ (right side of equation [4]) would be described as function of inlet heat flow generated by applied temperature u (left side of equation [4]). Indexes 1 and 2 denote ambience 1 and 2 respectively.

$$\begin{cases} \frac{\partial T_1}{\partial t} = \frac{\partial^2 T_1}{\partial x^2}, & 0 < x < \xi \\ \frac{\partial T_2}{\partial t} = \frac{\partial^2 T_2}{\partial x^2}, & \xi < x < \infty \end{cases} \qquad [4]$$

Difference in the heat p/assing throught one phase into another should be compensated by latent heat term L_f. It is important to state that temperature of phase change boundary located at some distance x= ξ would remain constant value. Assuming freezing/melting temperature equal 0ºC after some time t equation [4] at phase change boundary located at x= ξ would be written as (Rubinšteĭn, 1971).

$$k_1 \frac{\partial u}{\partial x}\Big|_{x=\xi} - k_2 \frac{\partial u}{\partial x}\Big|_{x=\xi} = \rho L_f \frac{d\xi}{dt}, \qquad [5]$$

where $k_1$and k_2 are thermal conductivities of water and ice. General solution of equation [5] gives relationship between the pace of advancing freezing front ξ over the time as well as position of freezing front $\xi = \alpha\sqrt{t}$. Here α is a fitting constant. As can be seen from solution of Stefan's problem position of freezing front is proportional to square root of time and temperature gradient applied. Latent heat of phase change is an important criteria for consideration when determining position of 0ºC isotherm (Rubinšteĭn, 1971).

1.3.Factors Affecting Heat Loss through the Basement Enclosure

Heat accumulated inside the building might be released out of the building in many ways. Since buildings are not completely airtight the heated air may leave the room through gaps in the structure and be replaced by colder air due to ventilation needs. This process is called as ventilation heat loss (M. Deru, 2003). The other way how heat escapes the building is through the materials using three well-known mechanisms: convection, conduction and radiation. Those three processes have been thoroughly studied and heat transfer through structural materials like copper, concrete and glass is well known. However, soil as a foundation material for almost all Civil Engineering structures is also well known for its high uncertainty in properties, which makes prediction of heat flux complex.

The studies of heat transfer through the basement structure includes three approaches: analytical solutions, numerical formulation and direct measurements. The majority of studies were focused on solving steady-state and two-dimensional problems with an infinite slab (Hagentoft, 1988). Hagentoft measuring ground temperatures and calculating heat flux of ground-coupled structure proved that simple conduction calculation gives mainly over-predicted results of heat loss.

Study made by Spiga and Vocale admits that heat transfer coefficient h may be reduced by about 8% if a 10mm-thick insulation is applied for the vertical surface of the ground slab. However, increasing the thickness of the insulation layer, h may be further diminished only by 13% considering an 80mm-thick piece of insulation (Spiga & Vocale, 2014).

1.3.1. Moisture Content

One of the most significant factors which influence heat transfer in the ground is the moisture content of soils. Numerous studies were dedicated to highlight relationship between the thermal conductivity of the soil and its moisture content. Deru (2003) points out that moisture content might increase the effective thermal conductivity by a factor of ten. That is why for those calculations where moisture content is taken as constant the error occurs to be valuable (M. Deru, 2003). Additionally, M. Deru (2003) studied effect of added water (precipitation) to the ground surface on heat transfer from slab-on-grade and basement. Results of his study showed that basement is very sensitive to surface moisture conditions at summer time and the most affected by its variation. In contrast, basement floor is less prominent to short-term moisture variation at the surface, but more related to deep ground conditions, such as groundwater (M. Deru, 2003).

Janssen studied influence of the coupling between heat and moisture transfer in the soil and at the surface. Simulating two coupled and uncoupled models with a specified number of simplifications (e.g. homogeneous and isotropic deposits, evapotranspiration and root uptake were not accounted) the results showed that effect of moisture content has not to be disregarded since it has a non-negligible influence on foundation heat loss. Moisture content effectively increases heat flow in the soil deposit (Janssen et al., 2004).

1.3.2. Boundary Conditions

Boundary conditions generally depend on the particular case of study and in many cases inevitable assumptions are taken to simplify or neglect the minor impact of certain conditions. Generally, boundary conditions are applied on the soil surface exposed to the ambient air, surfaces between foundation and soil.

A good attempt made by (Krarti et al., 2004) was focused on modelling of foundation slab under the refrigerated warehouse. Heat and mass boundary conditions for both foundation and soil surfaces were used in the calculation. To represent heat flux and express total thermal conductivity of soil a convective heat transfer coefficient, *h*, were used. As an assumption, the moisture transfer along the concrete slab was not considered. However, moisture evaporation on surface soil exposed to the ambient outdoor surface was controlled.

Another study made by Spiga and Vocale was focused on how the geometry of raft foundation influences heat transfer to the ground. The symmetrical 3D model of soil with slab on the top was solved in COMSOL Multiphysics software using governing Fourier equation for heat flux. The soil was considered homogeneous with constant thermal conductivity and volumetric heat capacity. The boundary condition at the external and internal zone (floor and walls) and at ground surface outside the building considers both convection and radiation. External convection was expressed through the convective coefficient h_{ce} which is a function of wind speed. Far away from building the temperature is assumed undisturbed by building and expressed as a function of outside temperature and depth of soil (Spiga & Vocale, 2014)

1.4. Heat and Mass Transfer Modeling in Soils in Different Software

Excessive and thorough study of two- and three-dimensional movement of heat, water and solutes in porous medium was made by Šimůnek, Van Genuchten and Šejna (1996). Results were implemented in software package HYDRIS which solves Richardson's equation for variably-saturated soils. It also summaries numerous equations for unsaturated hydraulic soils transport parameters from the transient flow. HYDRIS successfully has solved various problems of coupled

heat and mass transport in soils using closed-form equation to predict hydraulic conductivity of unsaturated soils (Van Genuchten, 1980).

Shoop & Bigl, (1997) tried to define moisture regime in unsaturated soils with large-scale experiments comparing results with outcomes from FROSTB software. Freeze-thaw effect was predicted in frost susceptible silty sands overlaying gravel sands with total depth of up to three meters. The model uses Darcy's law for mass transport and one-dimensional thermodynamic equation to accommodate heat transfer and phase change. FROSTB also calculated liquid flow potential as a function of the three-phase system (air, water, ice). Here two new terms were introduced; they are *flow potential in an air- water-soil system* and *flow potential in an ice- water-soil system.* Authors state that model overpredict ice formation, which delays thawing period in turn. Also, moisture content of thawed soils was better predicted in problems with shallow water table while with deeper water table moisture content was overestimated.

1.5.Building Energy Software

Spiga & Vocale (2014) studied the effect of floor geometry on building heat loss through the ground. They used commercial software COMSOL Multiphysics to solve finite element code. Method was validated based on International Standard ISO 10211. Results proved that heat exchange becomes dependent on the floor geometry of the foundation. Merely changing configuration and proportion of foundation slab the heat transfer may be adjusted to minimize heat flux. The numerical solution of this problem was addressed to slab on grade foundation. Depends on the variable aspect ratio of the foundation slab (width related to length) from γ =0.16 to γ =0.25 and from γ =0.25 to γ = 0.39 the steady-state ground global heat transfer coefficient decreases by about 6%. Reaching aspect ratio close to square footing (γ =0.39-1.0) the geometry effect becomes

smaller. However, ranging from a narrow rectangular floor (8 m × 50 m) to a square one (20 m × 20 m) the steady-state ground global heat transfer coefficient decreases by about 15% (Spiga & Vocale, 2014).

Energy performance of underground buildings was studied in 2D by Maghoul, Kavgic, et. al (2017) using finite element model builder FlexPDE 6. Unsaturated conditions were formulated by SWRC curve obtained from Van Genuchten (1980) approach. The governing equations for freezing soil include the conservation of total mass (water and ice), conservation of energy, flux laws for liquid water (Richards' equations) and heat (Fourier's law), and thermodynamic relationships with respect to pressure and temperature under phase change (freezing/thawing) conditions (Pooneh Maghoul, 2017)

Another whole building energy simulation package TRNSYS is available to simulate ground coupled foundation and solve energy-related problems. Engine is able to solve implicitly the three-dimensional finite difference soil domain (Duffy, Hiller, Bradley, Keilholz, & Thornton, 2009).

EnergyPlus focuses on whole building modelling to evaluate energy consumption of building for heating, cooling, ventilation etc. purposes. Heat and mass modules take into account movement of the air between building zones. For underground structures such as basement walls and floor a C- and F-factor approaches are used. The monthly ground temperature is required as input for calculation. C-factor approach uses time rate of steady-state heat flow through unit area of the construction, caused by temperature difference. F-factor represents the heat transfer through the floor, induced by a unit temperature difference between the outside and inside air temperature, on the per linear length of the exposed perimeter of the floor (*EnergyPlus. Version 8.9.0 Documentation*, 2018).

Overall, analyzing above-mentioned technics there is a certain tendency to take into account variability of soil properties due to seasonal temperature changes, as this creates strongly-coupled, non-linear moisture and heat flow. Considering soil properties as constant value gives underestimated results of energy loss.

1.6. Below-Grade Enclosure Insulation: Standards and Practices

Building erection in cold regions have its own practice and regulated by local national Codes. Both construction on permafrost and soils with seasonal freezing depth follows the same concept of rational use of heat from the building. In permafrost areas foundation is designed in a way to prevent heat exchange between building and soil to avoid thermally induced settlements. For these purposes a ventilated gap between ground and house is built to keep soil in naturally intact conditions. Pile foundation is used as a rule where the first floor rests on top of pile heads tied with beam (Farouki, 1992).

In case with seasonally frozen soils the number of insulation technics varies with types of foundation. Design of foundation depth according to the Codes of Canada, Norway, Sweden and Finland bases upon the value of freezing index [dayC^{o}]. If crawl space is ventilated the design depth might be reduced. Insulation of basements of heated buildings aims the general idea to raise the zero isotherm in the ground above foundation depth and reduce energy dissipation into environment. In most cases insulation is a must do conditions for frost-susceptible soils. Vertical basement walls should be protected with hardboard insulation of 50-100mm depends on designed thermal resistance of the built-up. Insulation should be installed from outside of the basement wall. This will move dewpoint outward and prevent the basement from excessive moisture. Additionally

insulation may be installed horizontally under the wall with the extent to the outer direction of the building for 1.2-1.5m (Farouki, 1992).

In case of frost susceptible soils, the backfill is often replaced with granular material which is capable to drain soil easily making more favourable conditions against frost action. Granular drainage material (sand, gravel) around foundation creates moisture cut off and prevent saturation of concrete by capillary rise. Often in Finnish basements combination of granular backfilling and vertical insulation is used for better frost protection (Farouki, 1992).

2. Site Investigation and Laboratory Work

2.1. Introduction

The aim of this chapter is to give general information about the structural design of the Stanley Pauley Engineering Building and the site investigation and laboratory work performed during this study.

Stanley Pauley Engineering Building (Fig. 4) was named after the graduate student of the Faculty of Engineering of the University of Manitoba with a major in electrical engineering (BSc(EE)/49). Mr. Pauley's contribution into construction estimates valuable $5 million. The transformational gift supported the construction of the building with a new facility designated to house graduate and undergraduate laboratories, provide study space for students and offices for faculty employees (Moore, 2015). The construction of this building started in 2017 and it will be operational by 2019.

2.2. Site Overview of Stanley Pauley Engineering Building

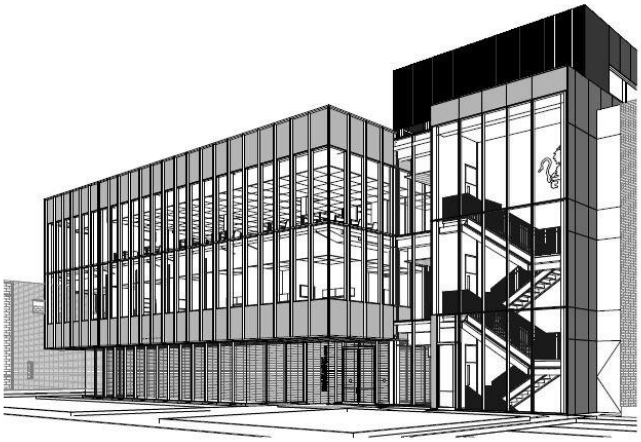

Fig. 4- Facade view of Stanley Pauley Building
(*courtesy of University of Manitoba*)

The new engineering building has four floors including basement floor at elevation -4.250 m below grade. The overall footprint of the building makes more than 900 m^2. Cast in place reinforced concrete beam-and-column frame is situated on pile foundation. Groups of four piles support individual columns. Load from the upper structure is transferred into piles through reinforced pile caps. Exterior basement walls are supported by individual piles arranged in line with variable step (Fig. 5). New building is surrounded by adjacent units of Faculty of Engineering from North and East sides and other University buildings from West as North-West (Fig. 6). East side of the building connects to the adjacent laboratory facilities. South facade faces Dafoe road where the main entrance of the building is located.

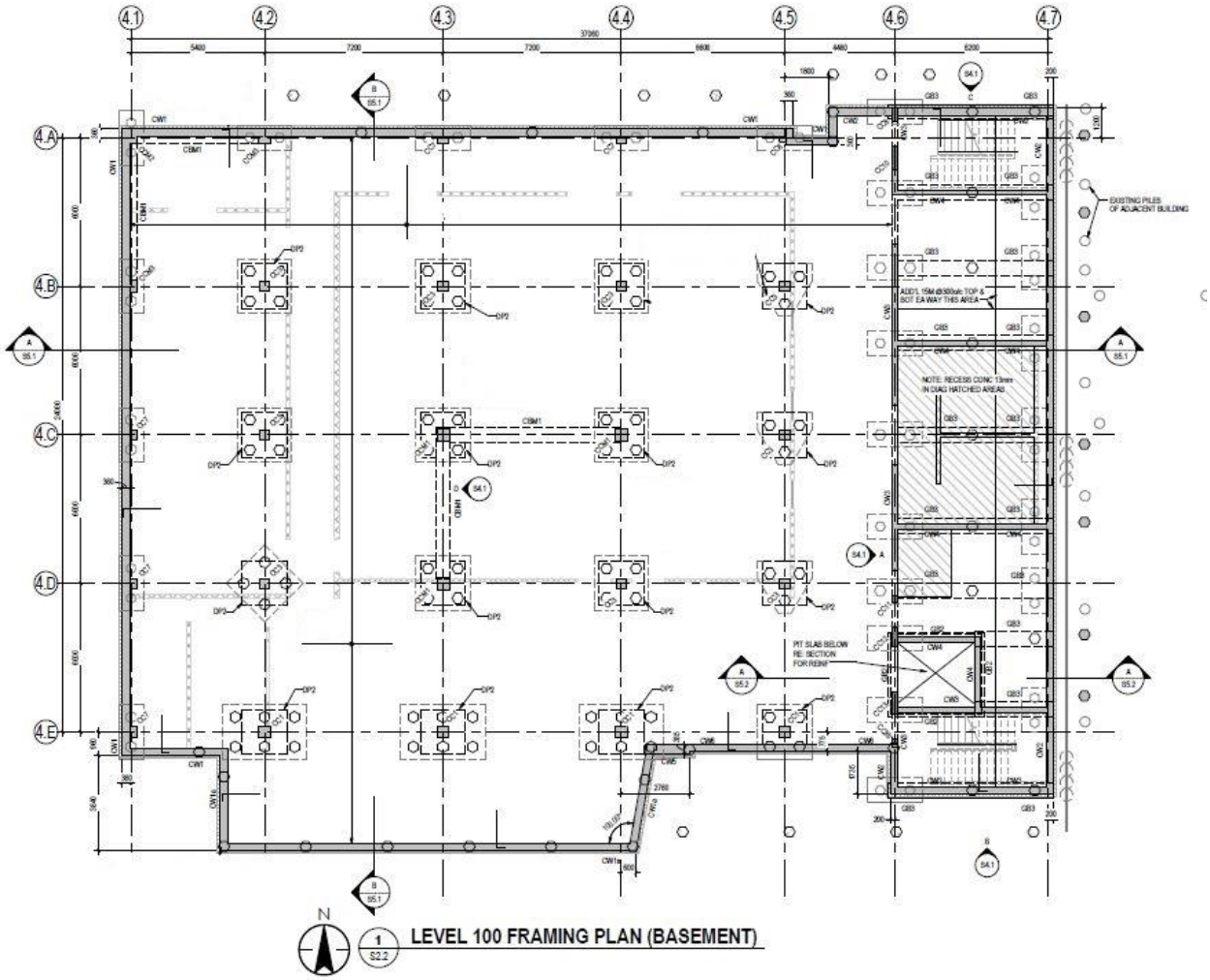

Fig. 5 Basement plan view at elevation -4.250m
(*used with permission*)

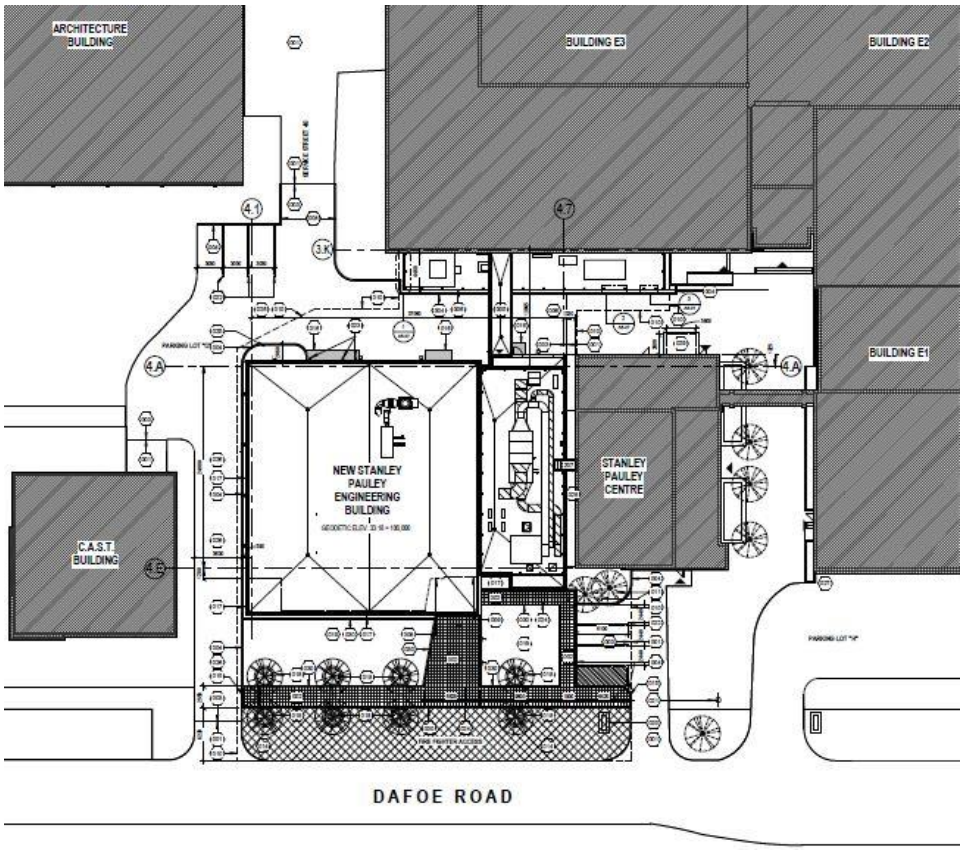

Fig. 6- Fragment of campus key plan with Stanley Pauley Building
(*used with permission*)

2.3. Geotechnical Site Investigation

Winnipeg soil is well known for its fine-grained deposits of glaciolacustrine clays and tills of former Lake Agassiz overlying the Precambrian basement of bedrock. Seasonal freezing in top layers of soil may reach ~1.8m in the Winnipeg area, so moisture regime in this zone is of great interest (Ferguson & Woodbury, 2004).

The purpose of soil investigation was to collect samples and measure its thermal properties and some other parameters necessary to predict thermal transfer from the building. Geotechnical report made in 2015 was consulted prior to the independent soil investigation. Information about borehole

logs was obtained as well as information about groundwater conditions. This was used to identify the most appropriate location for sampling.

Construction site has topsoil cover and asphalt followed by gravel pack of approximately 250mm. Geological profile of the site is represented by three stratigraphic layers, as shown in Fig. 7. They consist of clays of different consistency and depth of the formation. First two meters of clay were black and grey later turning into brown clays of higher moisture content. Clays encountered until depths 16.7m are classified as very soft to very stiff. Moisture content varied from 27% to 61% along the whole profile (Essex et al., 2017).

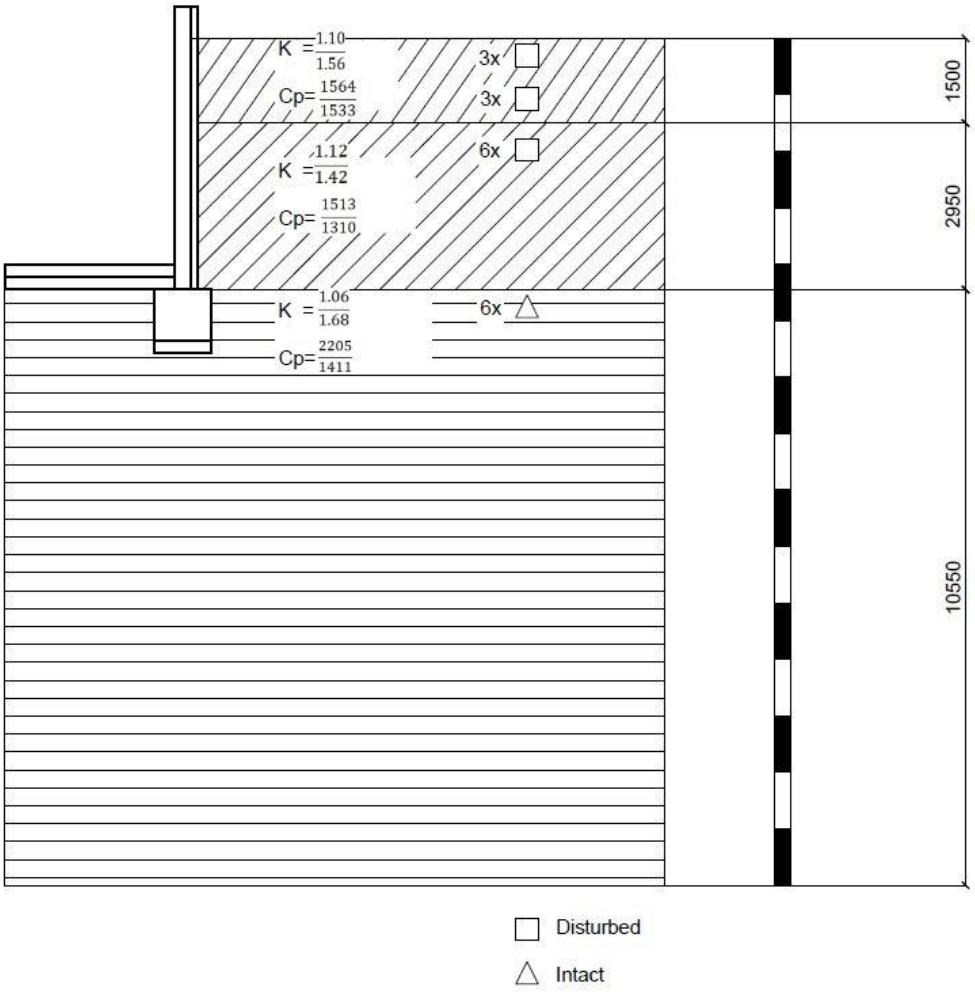

Fig. 7 Geological profile. Location of disturbed and intact samples. Properties are measured in unfrozen (nominator) and frozen conditions (in denominator)

2.4. Soil Sampling

Overall, eighteen samples were retrieved at different locations and depth during the massive excavation of construction site in August 2017. The goal was to obtain samples from different depth to study the variability of soil properties along geological profile as well as to reduce uncertainty of ground conditions. Position of grab samples was scattered at three different locations as indicated in Fig. 8. Samples were taken from three elevations situated at depth 1-1.5

m, 2 m and 4.5 m below grade (Fig. 7). After site analysis, it is noted that the geological profile of the site consists of three layers with the following thicknesses: Layer 1 (1.5m); Layer 2 (2.95m); and Layer 3 (10.55m) as illustrated in Fig. 7

Fig. 8- Grab sample's location

Layer 1 is presented by black and grey clays of soft consistency, with the inclusion of organic material, visibly layered at depth from 0.5 to 1.5 meters below grade. Layer 2 (depth from -1.5m to -4.5m) is presented by brown and grey clays of stiff consistency lasting within the next three meters until the depth -4.5m, soil appeared silty below depth 3.0m.

Disturbed soil sampling in Layers one and two was carried out with consideration of provisions from standards ASTM D4220-14 and ASTM D7015-13. For this purpose, three trenches with depth 1-1.5m and 2m were dug at the locations shown in Fig. 8. Twelve cohesive cubical specimens with side of 20 cm were sampled through the trench cuts (Fig. 9). Samples were preserved and sealed before tests to avoid moisture loss as this significantly affects its thermal conductivity and heat capacity (Fig. 10).

Fig. 9- Cut wall for grab sampling

Fig. 10- Preparation of disturbed (*left*) and intact (*right*) samples for tests

Furthermore, Shelby tubes were used to collect six intact (undisturbed) soil samples from Layer 3 of the excavation at depth -4.00m (Fig. 11). Sampling was made according to ASTM D1587-15

standard where retrieved tubes were preserved and stored in the refrigerator before required tests have been accomplished (Fig. 10).

Stiff tan clay, with trace of organic inclusions, was observed at depth -4.0 m. The bottom of the pit was exposed to the atmosphere for approximately ten days prior sampling. The water table was located at elevation -8.5m based on survey report conducted in 2015 (Essex et al., 2017).

Fig. 11- Shelby tube sampling at the bottom of excavation

2.5. Test Procedures and Results

Above mentioned samples were tested to gain thermal properties at their initial state of moisture content. Measurements were taken with KD2-Pro device by Decagon (Decagon, 2013) previously calibrated in the laboratory according to manufacturing instructions.

Thermal conductivity was measured by sensors with acronyms TR-1 and SH-1 (Fig. 12). Both sensors use transient line heat source technique and consist of the needle with a heater and temperature sensor inside. TR-1 is a single needle sensor (100mm long, 2.4mm diameter) typically used for wide range of porous materials including soils. TR-1 sensor was used to measure thermal properties of all samples. Experiments were accompanied by additional measurements of SH-1 sensor with dual needle. Apart from thermal conductivity, the SH-1 sensor yields the information on diffusivity and volumetric heat capacity (VHC). In SH-1 volumetric heat capacity is measured through the heat impulse induced but needle 1 and captured by needle 2 located in a distance of 6mm. Later VHC will be converted to specific heat $[\frac{J}{kg \cdot K}]$ by dividing VHC value over the bulk density of specimen (Fig. 13).

Fig. 12- TR-1 sensor (*left*) and SH-1 sensor (*right*)

Both TR-1 and SH-1 sensors has *low* and *high-power* modes of operation. Low power mode allows to generating temperature impulse of tiny fractions of degree of Celsius. This allows to conduct measurements in sensitive to temperature substances such as liquids or frozen samples where forced convection may affect results of measurements or sample might partially melt. In contrast, high power mode makes stronger temperature increment more than 1^0C and used in less prominent to temperature changes materials such as rocks and clays. Both power modes were used to measure thermal properties of frozen samples (Fig. 15).

Fig. 13- Disturbed sample during measurement

Fig. 14- Coring frozen sample with steel ring in hydraulic press

Additionally, each thermal measurement was instantly accompanied with test of physical properties. Samples were tested to gain bulk density, water content, dry density and porosity. Results of laboratory experiments were narrowed down to average values and presented in Table 1. More descriptive information is summarized in Table 2-5.

Table 1 –Summary of samples properties in average values

Item	Depth [m]	**k** [W/mK]	**C_p** (Volumetric) [MJ/m^{3}K]	**C_p** [J/kg·K]	**WC** [%]	**ρ** [g/cm^3]	**ρ** (dry) [g/cm^3]	**n** [-]
Layer 1	1.0-1.5	1.10	2.93	1565	39.4-47.1	1.80	1.35	0.32
Layer 2	2	1.12	3.01	1513	45.8-51	1.86	1.34	0.30
Layer 3	4	1.06	3.85	2205	35.9-42.4	1.74	1.14	0.34

Overall, laboratory tests were carried out to determine basic thermal properties of soils. These tests have shown how thermal properties are related to moisture content and density of soil. Measurements made for frozen samples gave an expected response in properties change. This fact can be largely attributed to the presence of frozen water in soil's pores. Frozen soil samples in comparison with unfrozen ones have slightly lower specific heat capacity and valuable 40% higher thermal conductivity (Table 5). Density of soils was less sensitive to variation due to freezing effect. Graphics of lab test are presented in Appendix 1- Graphic Materials of Laboratory Tests.

Table 2 –Layer 1. Black & grey clay (Elevation -1.0÷1.5 m)

Sample #	k [W/mK]		C_p [MJ/m^{3}K]	C_p [J/kg·K]	T_diff [mm^2/s]	WC [%]	γ [g/cm^3]	γ_d [g/cm^3]	n [-]	Temperature TR-1 [ºC]	Temperature SH-1 [ºC]
	TR-1	SH-1									
1	1.200	0.921	2.602	1487.9	0.354	39.370	1.749	1.314	0.339	6.09	7.01
2	1.160	1.008	3.022	1688.1	0.334	42.670	1.790	1.333	0.323	4.67	5.52
3	1.100	1.085	3.038	1712.9	0.357	32.340	-	-	-	10.28	12.40
4	1.054	2.928	1.030	557.9	0.352	47.140	1.846	1.400	0.302	5.96	4.47
5	1.173	1.050	3.002	1284.5	0.350	36.402	-	-	-	5.60	6.22
6	1.295	1.055	3.008	1651.3	0.351	45.170	1.822	1.336	0.312	4.49	5.26

Table 3–Layer 2. Brown clay (Elevation -2.0 m)

Sample #	k [W/mK]		C_p [MJ/m^{3}K]	C_p [J/kg·K]	T_diff [mm^2/s]	WC [%]	γ [g/cm^3]	γ_d [g/cm^3]	n [-]	Temperature TR-1 [ºC]	Temperature SH-1 [ºC]
	TR-1	SH-1									
1	1.273	0.945	2.929	1601.4	0.323	45.770	1.829	1.294	0.309	6.53	7.32
2	1.054	-	-	-	-	-	-	-	-	5.96	
3	1.305	1.102	3.084	1529.8	-	40.023	-	-	-	5.18	7.00
4	1.202	1.019	3.072	1620.5	0.332	51.080	1.896	1.379	0.284	3.94	4.98
5	1.186	1.032	2.802	1217.1	-	37.537	-	-	-	5.14	
6	1.173	1.074	3.155	1598.6	-	37.134	-	-	-	4.73	6.58

Table 4 –Layer 3. Brown clay (Elevation -4.0m)

Sample #	k [W/mK]		C [MJ/m^{3}K]	C_p [J/kg·K]	T_diff [mm^2/s]	WC [%]	γ [g/cm^3]	γ_d [g/cm^3]	n [-]	Temperature TR-1 [ºC]	Temperature SH-1 [ºC]
	TR-1	SH-1									
1	Tested in frozen state (**Table 5**)										
2	1.292	0.889	4.272	2390.9	0.208	42.4	1.787	1.20	0.325	4.37	8.22
3	1.250	0.898	4.510	2617.1	0.199	37.34	1.723	1.11	0.349	9.76	12.27
4	Tested in frozen state (**Table 5**)										
5	1.222	0.917	4.122	2341.1	0.222	40.32	1.761	1.18	0.335	8.44	11.62
6	1.290	0.741	2.514	1473.9	0.295	35.94	1.706	1.08	0.355	6.21	9.26

Table 5–Measurements in frozen state

Sample #	k [W/mK]		C_p [MJ/m^{3}K]	C_p [J/kg·K]	T_diff [mm^2/s]	WC [%]	γ [g/cm^3]	γ_d [g/cm^3]	n [-]	Temperature TR-1 [ºC]	Temperature SH-1 [ºC]
	TR-1	SH-1									
Layer 1 Black cl	-	1.557	2.794	1533.4	0.555	0.35	1.82	1.34	0.31	-	-17.76
Layer 2 Brown cl	-	1.417	2.394	1310.5	0.591	0.33	1.83	1.37	0.31	-	-15.10
Layer 3 Shelby #1	-	1.631	2.327	1411	0.701	57.82	1.72	1.04	0.38	-	-13.16
Layer 3 Shelby #4	-	1.760	2.510	-	0.702	-	-	-	-	-	-14.52

3. Energy Efficiency of Stanley Pauley Building's Basement Structure

3.1. Introduction

This chapter aims to assess heat loss and energy performance of the below-grade envelope of currently under-construction Stanley Pauley Building in the Fort-Garry campus at the University of Manitoba in Winnipeg, Canada. For this purpose, two approaches have been used. The first approach treats soil as a solid material with constant thermal properties regardless of the seasonal temperature change and its effect on soil thermal properties, as it is often assumed in building energy simulation programs such as EnergyPlus and TRNSYS, while the second approach takes into account the effects of redistribution of partially unfrozen water and ice content during freezing-thawing cycles in the soil by considering the phase change mechanism. Both heat transfer models were implemented in COMSOL Multiphysics.

The energy performance of the basement enclosure studied in this chapter comprises two scenarios. The first scenario, called *Base Case*, assumes an uninsulated basement structure, i.e. the basement structure is in direct contact with surrounding foundation soils. The second scenario for

the basement structure is based on the existing structural and architectural plans provided by the Faculty of Engineering of the University of Manitoba which consist of a layer of insulation at the exterior of the basement wall and a layer of honeycomb cardboard below the floor slab. Then, values of obtained heat fluxes and overall energy loss were compared.

3.1.1. Heat Transfer Model: Numerical Implementation and Methodology

In order to study heat losses through the basement wall and floor to the ground as well as heat transfer in surrounding soils, conduction is considered as the primary heat transfer mechanism. This implies several assumptions: (1) soil domain is incompressible, meaning that no stress occurs due to temperature change, (2) soil is homogeneous and isotropic to provide a smooth solution for heat transfer, and (3) phase change is considered when temperature goes beyond freezing point, so energy of enthalpy is required to overcome unfrozen-frozen transition.

3.1.2. First approach: Constant Thermal Properties

In this simplified approach, it is assumed that the thermal parameters in Equations [6] and [7], k and C_p, are constant and correspond to the values observed during laboratory measurements. Soil properties are represented in Table 1. Energy of enthalpy required to overcome unfrozen-frozen transition is not considered. The governing equation for the conductive heat transfer can be written as follows

$$\rho C_p \frac{\partial T}{\partial t} - \nabla \cdot q_c = 0 \qquad [6]$$

where, C_p [J/kg·K] is the specific heat capacity of soil, ρ [kg/m^3] is the density, T [C^0] is the temperature, q_c [W/m^2] is net energy conductive flux through the volume defined by generalized form of Fourier's law as follows:

$$q_c = k\nabla T \quad [7]$$

where k [$\frac{W}{m \cdot K}$] is thermal conductivity of soil, T [K] is temperature, ∇ stands for the gradient operation.

This approach has been used in building energy simulation programs such as EnergyPlus and TRNSYS. Soil might be assigned as variable boundary condition with fixed temperature or treated as solid material where no property change occurs during thawing and freezing rather than proportion of ice and water content.

3.1.3. Second approach: Variable Thermal Properties

Conductive heat transfer through a freezing soil can be expressed by Eq.[8]. In this equation, heat conduction is considered as the governing mechanism. Phase change term is represented by the second addendum.

$$\rho C_p \frac{\partial T}{\partial t} - \rho_i L_f \frac{\partial \theta_i}{\partial t} - \nabla \cdot q_c = 0 \quad [8]$$

in which L_f is the latent heat of fusion (333.5 kJ/kg), ρ [kg/m^3] is density of soil, θ_i [-] is ice content. Index *i* refers to ice, C_p [J/kg·K] is heat capacity, q_c [W/m^2] is the same term expressed above in Eq [7]

Since soil is represented as a mixture of solid particles, ice and water the thermal conductivity will be expressed as a geometric mean of thermal conductivities of each phase weighted by volumetric content (Eq. [9]).

$$k = k_s\theta_s + k_w\theta_w + k_i\theta_i \quad [9]$$

where indexes *s, w, i* refer to solid water and ice phases respectively.

Heat capacity may be expressed as follows:

$$C_{pp} = \rho_s C_s \theta_s + \rho_w C_w \theta_w + \rho_i C_i \theta_i \quad [10]$$

Similar to Eq.[9] density of soil at each time when liquid water content is changing may be expressed as follows:

$$\rho = \rho_s(1-n) + \rho_w \theta_w + \rho_i \theta_i, \quad [11]$$

It is assumed that total water content may be expressed as a summation of ice and liquid water content. Such assumption explains fully saturated condition of soil (Eq [12]). When the temperature drops below freezing point liquid water turns into ice consequently changing its physical properties.

$$n = \theta_w + \theta_i \quad [12]$$

Unfrozen water content is expressed by the following equation (Zhu & Michalowski, 2005):

$$\theta_{w1} = \theta_r + (\theta_{w0} - \theta_r) e^{a(T-T_0)} \quad [13]$$

where, $\theta_r = 0.05$ [-] is residual unfrozen water content, $a = 0.16$ is curvature coefficient, $\theta_{w0} = 0.535$ [-] is unfrozen water content at the freezing temperature T_0. This assumption is made based on the measurements on the soil samples collected from the construction site. Additionally, it conforms with fully saturated condition when temperature remains positive.

3.1.4. Validation

Processes in freezing soils were extensively observed through experiments conducted in last 90 years (Hansson et al., 2004). General procedures for numerical modelling require model validation based on experimental data. For model validation an experiment with freezing soil was simulated in COMSOL Multiphysics (later COMSOL). Originally developed in ABAQUS software

algorithm by Zhu & Michalowski (2005), the similar model was implemented in this study in COMSOL and validated to assure adequate response of the program. Unfrozen water content was controlled by three-parameter function described in Eq.[3]. The parameters used are: $\theta_r = 0.058$, $\theta_w = 0.285$, $T = 0°C$, $e = 0.16$. Outcomes of simulation were compared with real test measurements made by Fukuda & Kim (1997). Results are shown in Fig. 15. Results of simulated unfrozen water content demonstrates good agreement with measured values. Curve were fitted to experimental data by adjusting fitting parameter e.

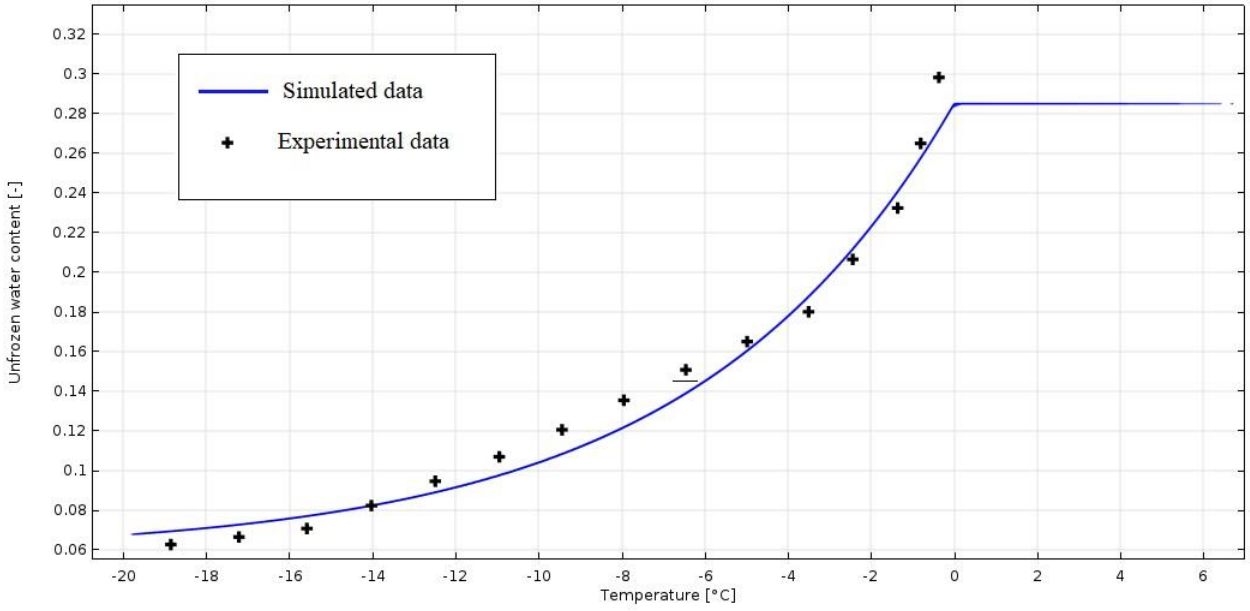

Fig. 15 Predicted and measured unfrozen water content.

3.2. Model Description

The thermal and physical properties of the soil obtained in the lab (Chapter 2), as well as the construction materials used in the basement structure have been used to estimate heat loss of the foundation of Stanley Pauley building by implementing the above-mentioned models in COMSOL Multiphysics® Software.

An axisymmetric condition is considered. The model built in COMSOL represents base case of hypothetical design when basement has no insulation. Concrete walls are in direct contact with soil. Basement cross-section is illustrated in Fig. 16.

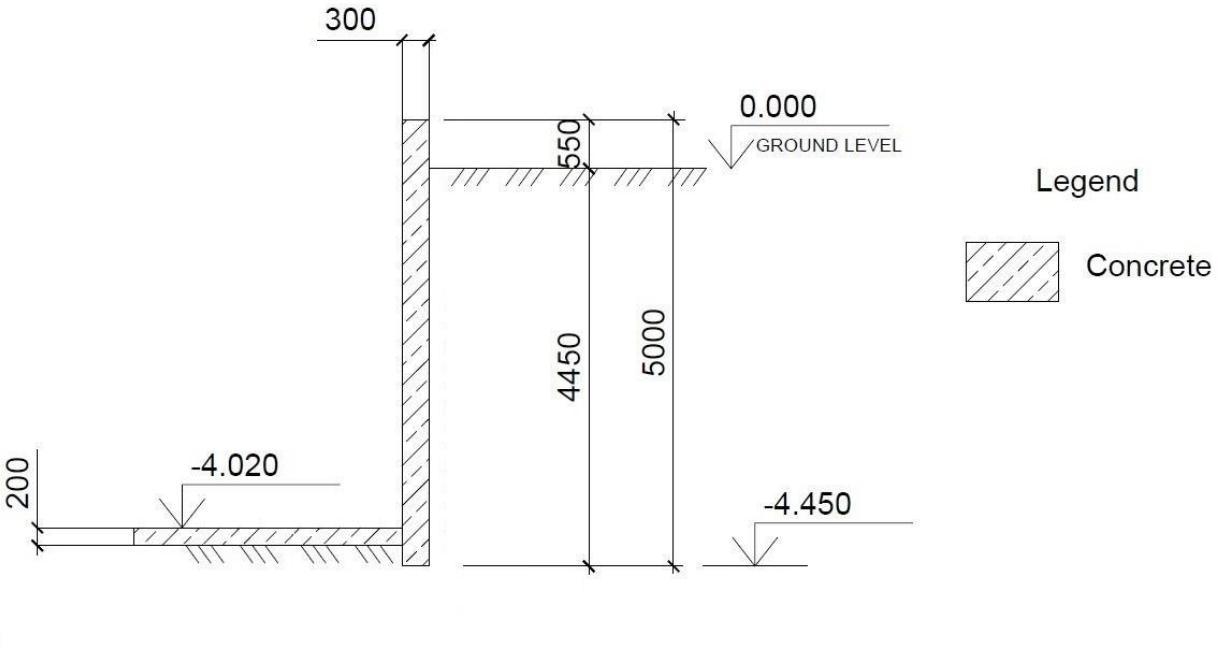

Fig. 16 Cross-section of the basement (in mm)

Soil domain was assumed of three layers according to field investigations described in Chapter 2. Layers 1-3 have thicknesses 1.5 m, 3.0 m and 10.5 m, respectively with properties summarized in Table 1. Concrete has the following properties $k = 1.8$ [W/m·C], $C_p = 880$ [J/kg·C], $\rho = 2300$ kg/m^3].

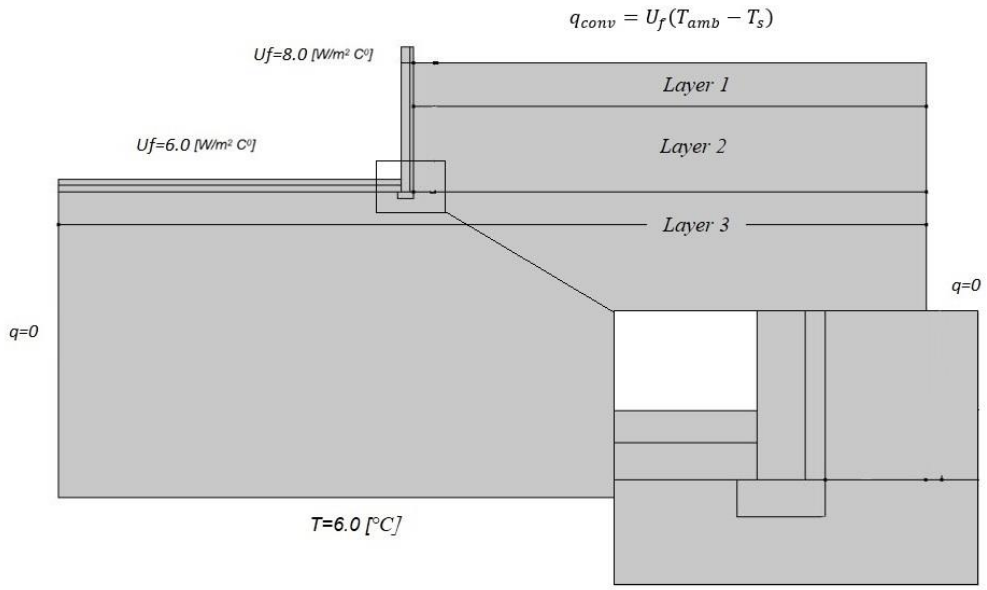

Fig. 17 Boundary conditions of model

3.2.1. Boundary and Initial Conditions

The initial temperature of the structural material is set to 15C°, while soil domain is assumed to be 6 Cº. Upper Carbonate Aquifer beneath Winnipeg has a variable temperature from 5.4 to 14.3 C°. Background temperatures do not exceed 6.0 C° (Ferguson & Woodbury, 2004). Bottom boundary of the domain was assigned with Dirichlet boundary condition which is fixed temperature T=6.0 C°. This explains infinite thermal capacity of ground potential.

Internal temperature of Stanley Pauley building is maintained over the whole annual period in a range of 21-23°C regardless of the energy demand of the building during the year (either cooling or heating). It is assumed that the HVAC system is designed in such way that temperature is

maintained at constant comfortable level. For calculations, the indoor air temperature is assumed 20ºC. Heat flux from building through the floor and basement is introduced through convective heat transfer coefficient U_f equals to 8 and 6 W/m^2 °C for the basement wall and floor slab, respectively (M. P. Deru & Kirkpatrick, 2002). The heat flux from the basement structure into the soil will be expressed as (P. Maghoul, 2017):

$$q_{conv} = U_f(T_{amb} - T_s) \quad [14]$$

where T_s is the temperature of soil surronding the basement.

Adiabatic boundaries were assigned on the left and right sides of the model where no heat flow was assumed. Soil domain extends at a depth of 11 m below foundation and reaches elevation of -15.0 m. On the right side domain spreads for 17m. Distance to boundaries was adjusted to the mentioned above dimensions to minimize the effect of model borders to acceptable limits. The 2D model domain including the boundary conditions is presented in

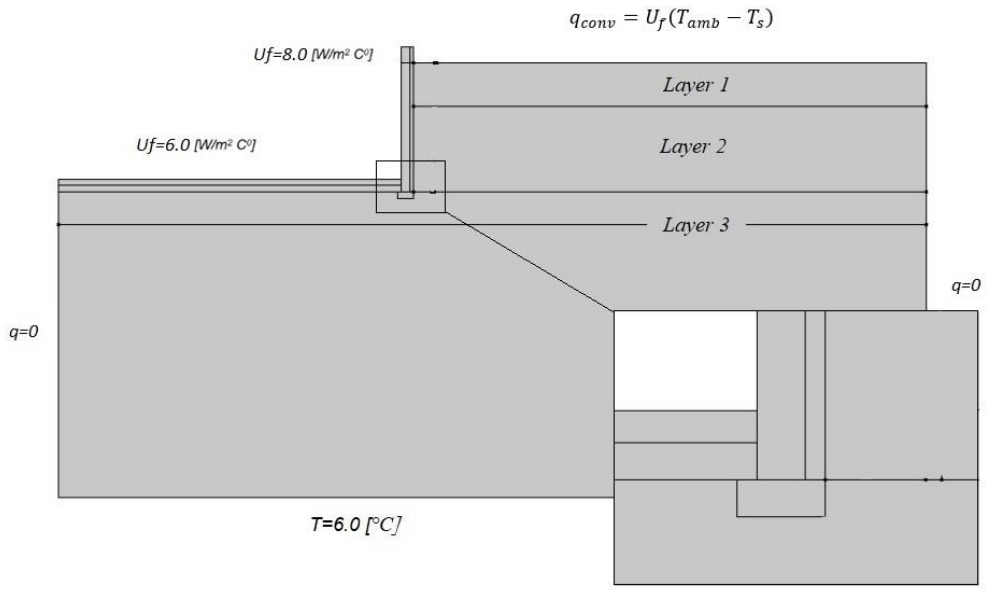

Fig. 17.

Variability of outdoor weather conditions creates great uncertainty for calculation. Apart from variable air temperatures and wind velocities, it is accounted for a dozen of the other factors which influence thermal regime of the system. Precipitation, evaporation, solar radiation and snow cover make assigning of boundary condition very problematic.

To provide robust solution with regard to simplicity of calculation, it is necessary to introduce some limitations and assumptions of the model regarding weather conditions applied. First, since the building is located on campus in the vicinity of other units and at very live pedestrian traffic routes it is assumed that pavement surface will be maintained clean of snow during the whole year. This fact allows to neglect the effect of the snowpack.

Weather data was taken from ASHRAE database for the Winnipeg area in 2013. Wind speed and temperature are assumed as diurnal values and presented in Fig. 18 and Fig. 19 respectively.

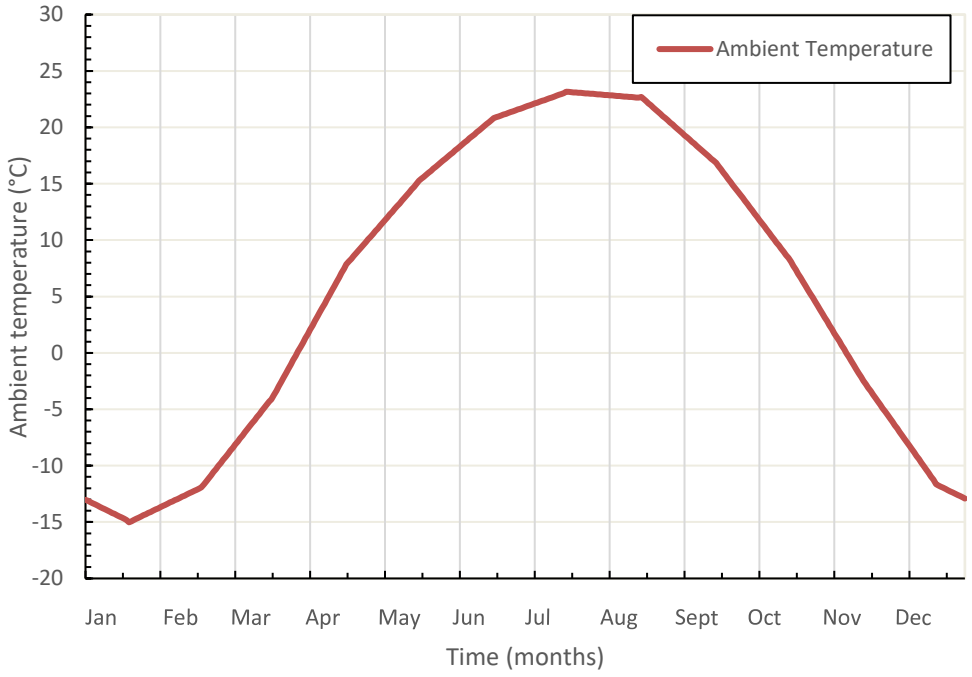

Fig. 18- Ambient temperature distribution over one year (ASHRAE 2013)

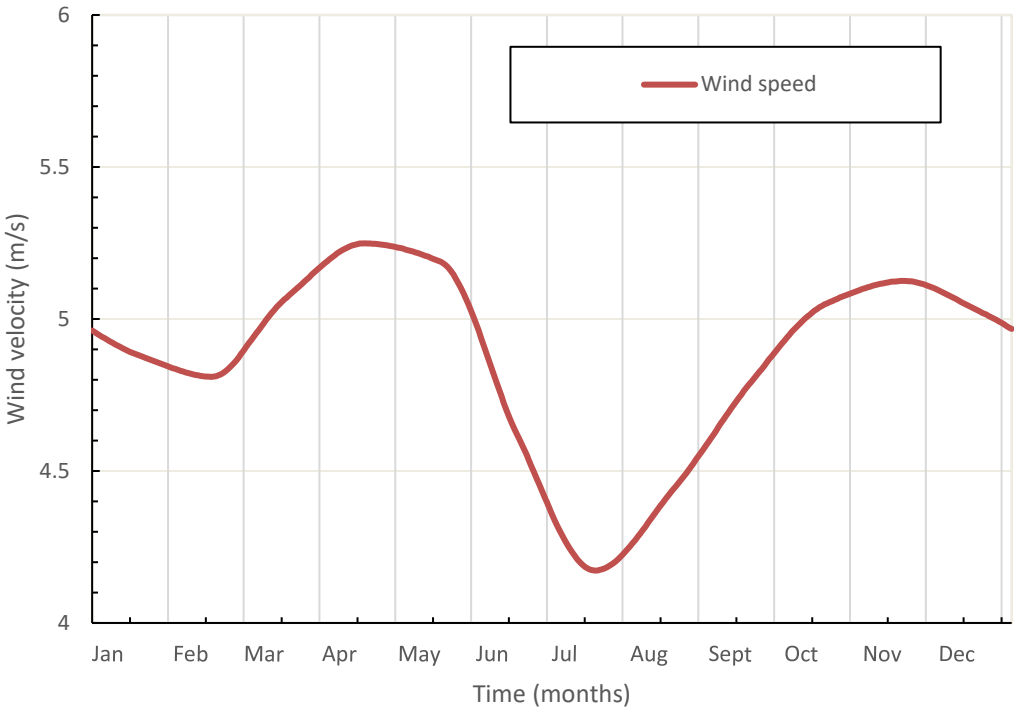

Fig. 19- Wind velocity distribution over one year (ASHRE 2013)

Ambient weather conditions create a heat flux between atmosphere and ground surface. Considering the average values of ambient temperature and daily rates of wind velocity taken from weather station, convective heat flux q_0 [W/m^2] has been defined on the upper boundary at grade level as follows:

$$q_0 = h_{conv}(T_{ext} - T) \qquad [15]$$

where, T_{ext} and T [C^0] are ambient and surface temperatures, h_{conv} [W/m^{2}C^o] is heat transfer coefficient related to wind velocity and temperature. Coefficient h_{conv} is fluid mechanic property (in our case it is air), whereas temperature gradient appeal to thermodynamic quantity (Kays, Crawford, & Weigand, 2005). Coefficient h_{conv} is often related to the Nusselt number (*Nu*) which is ratio of convective and conductive heat transfer across the boundary. General view of Nusselt number takes form as (Gorochov, 2015):

$$Nu = A \cdot Re^{a} \cdot Pr^{b}, \qquad [16]$$

where Pr stands for Prandtl number, R_e is Reynolds number, *A*, *a* and *b* are parameters obtained from experiments. *Nu* coefficient is widely used to describe heat exchange between two interacting ambiences such as air flow and soil material, liquid flow in pipe and wall of the pipe. In hydrotechnical engineering Nusselt number introduce convective heat exchange between rocks and ventilated air in earth-and-rockfill dams. Some typical values of *Nu* coefficient are presented in Table 6 (Gorochov, 2015).

Table 6 –Typical Nusselt coefficients at different problems

Authors		Nusselt number
Air flow through rock surface	(Eckert & Drake, 1961)	$Nu = 0.124Re^{0.8}Pr^{0.33}$
	(Chuhanov, 1974)	$Nu = 0.25Re^{0.86}$
	(Timofeev, 1962)	$Nu = 106Re^{0.67}\ if\ 20 \leq\ Re \leq 200$ $Nu = 0.61Re^{0.67}\ if\ Re > 200$
	(Lebedev & Petrov-Denisov, 1966)	$Nu = 0.166Re^{0.86}$
Turbulent internal flow in smooth pipe	(Kutateladze, 1990)	$Nu = \frac{0{,}023Pr \cdot Re^{0.8}}{1 + 2.14Re^{-0.1}(Pr^{\frac{2}{3}} - 1)} \quad if\ R_e > 5 * 10^5$
	(Kays et al., 2005)	$Nu = \frac{0{,}023Pr \cdot Re^{0.8}Pr}{0.88 + 2.03Re^{-0.1}(Pr^{\frac{2}{3}} - 0.78)}$

To formulate heat transfer from flows (wind) it is important to mention the type of flow that may be either laminar or turbulent. Particularly for this problem h_{conv} as a product of Nusselt number can be written as follows:

$$h_{conv} = 2\frac{k}{L}\left(\frac{0.3387\ Pr^{\frac{1}{3}}Re_L^{0.5}}{\left(1+\left(\frac{0.0468}{Pr}\right)^{\frac{2}{3}}\right)^{\frac{1}{4}}}\right) \quad if\ Re_L \leq 5*10^5$$

$$h_{conv} = 2\frac{k}{L}\ Pr^{\frac{1}{3}}\left(0.037\ Re_L^{\frac{4}{5}} - 871\right) \quad if\ Re_L > 5*10^5 \qquad [17]$$

where k [W/m·K] is thermal conductivity of air; L(m) is characteristic length of the surface in the direction of wind; Pr stands for Prandtl number of air, the ratio of thermal diffusivity to viscosity, taken as 0.7152. And Re_L is Reynolds number based on characteristic length L, calculated as follows:

$$Re_L = VL/\nu_{air} \qquad [18]$$

V is wind velocity along the characteristic length L=17.7m, ν_{air} is kinematic viscosity of air.

3.2.2. Mesh Generation

Automatic physics-controlled sequence type with fine mesh refinement generates mesh as presented in Fig. 20. Size of the mesh is adapted to the size of domain elements, so the meshing becomes denser at smaller elements and corner points.

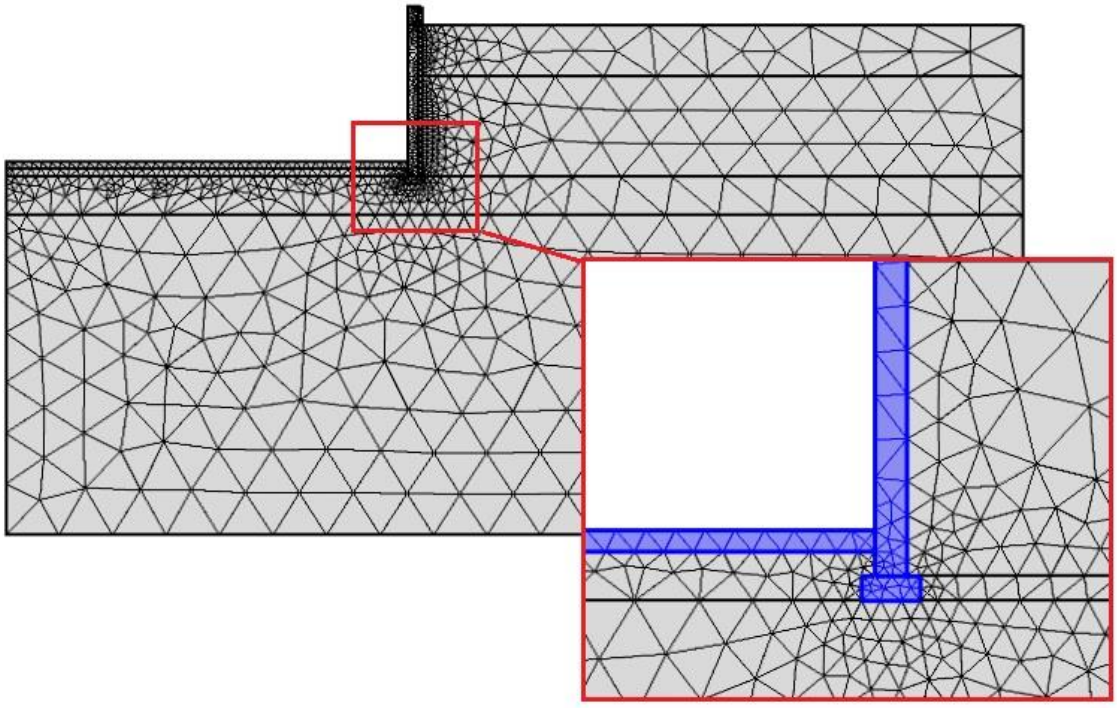

Fig. 20 Mesh refinement of domain

3.2.3. Heat Loss Simulation Using Approach 1

Approach 1 to be applied on base case where foundation is assumed uninsulated and in direct contact with soil. This case to be calculated to understand the magnitude of heat loss when no insulation applied.

To ensure that the results are not affected by the initial temperatures imposed on parts of the field, only 11th year of simulation was analyzed in detail. For example, in both models, it has been observed that within the first ten years, heat flux through the floor were continuously decreasing until it levelled to slightly fluctuating sinusoidal curve due to seasonal temperature variations as shown in Fig. 21.

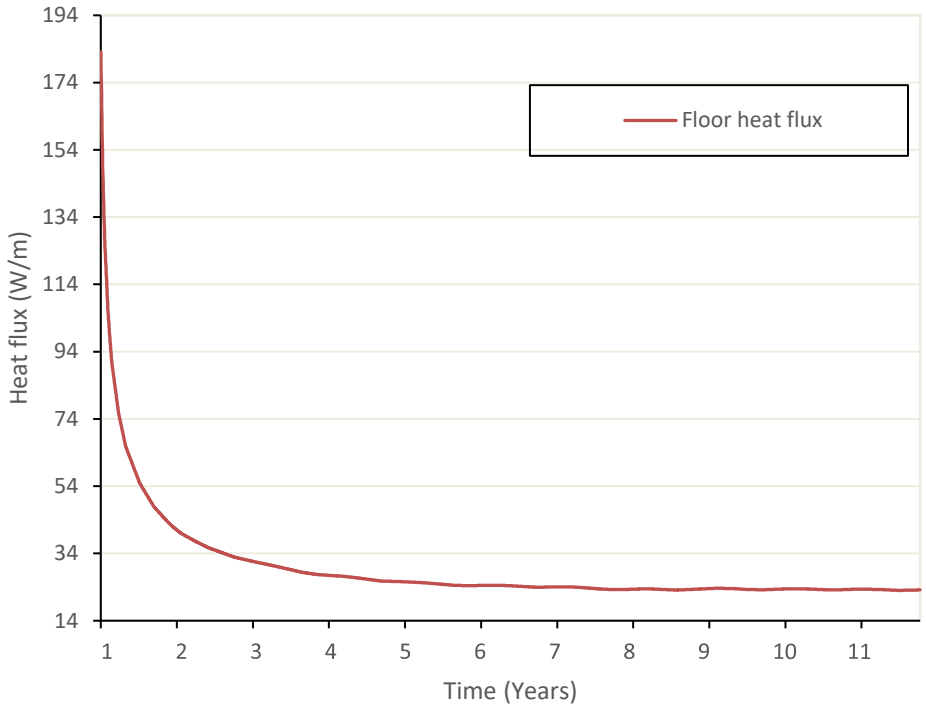

Fig. 21 Stabilization of heat flux through floor structure

Results of simulation presented in Fig. 22 show temperature distribution at different months of the year. Zero degree isotherm profile decreases in January closer to the building reaching 1.0m depth at the outer surface of the wall. Two meters away from the wall, soil demonstrates deeper frost penetration at a depth of 2.0 m.

Two curves in figures Fig. 23 and Fig. 24 show annual variation of heat flux through basement wall and floor. During summer time heat flow in walls reduces to 21 W/m, while it increases at winter months until 76 W/m. Heat flow in floor slabs is somewhat less, approximately 23 W/m and almost does not change over the year.

Overall heat loss is calculated by summarizing total area of walls and floor subjected to heat transmission. Using given heat loss per running meter obtained from simulation, the total heat loss is calculated multiplying this value by length of the structure's perimeter and by time. Resulting

74m running metres were accounted for floor structure and 122 m for walls. Table 7 provides values of heat loss through wall and floor structures, respectively, when approach 1 is employed.

Table 7 – Summary of heat loss during the year of simulation using Approach 1

Parameter	Overall heat flux (W/m)	Energy loss (kWh)	Estimated cost (CAD) (8.896¢ per kWh)*
Heat loss through floor	8,475	15,050	1,204
Heat loss through wall	18,035	52,800	4,224
Total	26,510	67,850	5,428

*-Commercial rates provided by Manitoba Hydro, accessed on 01/08/2018 ("www.hydro.mb.ca," 2018)

a) January

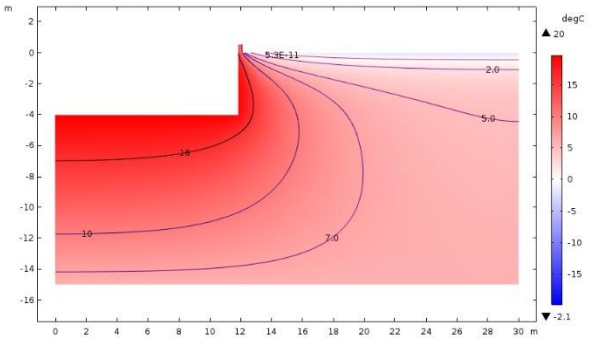

b) February

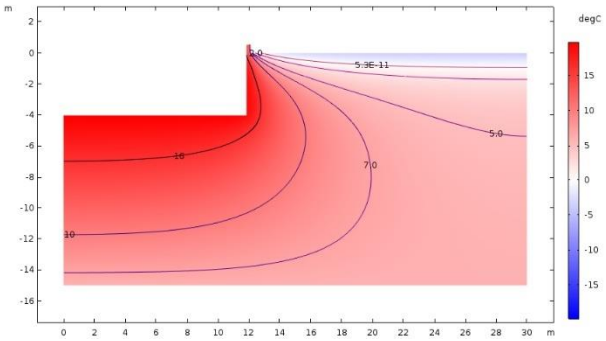

c) March

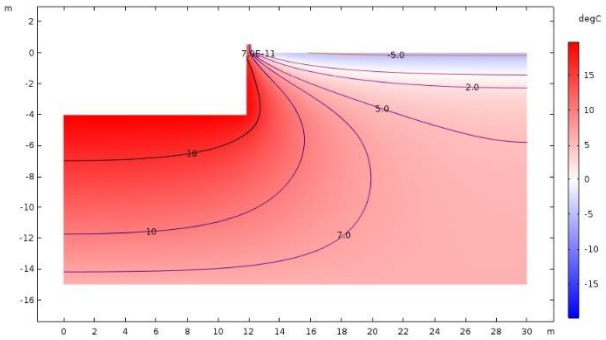

d) April

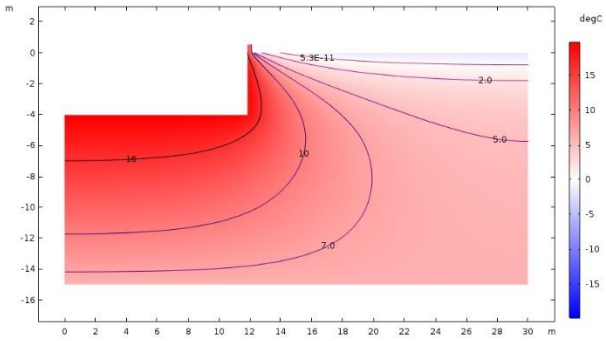

e) May

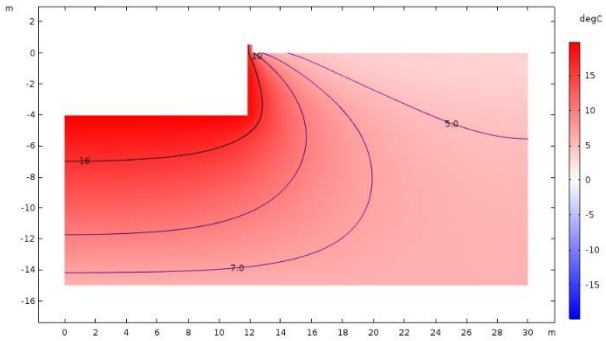

f) June

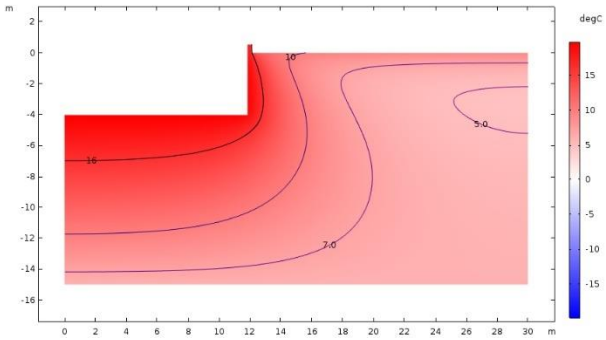

g) July

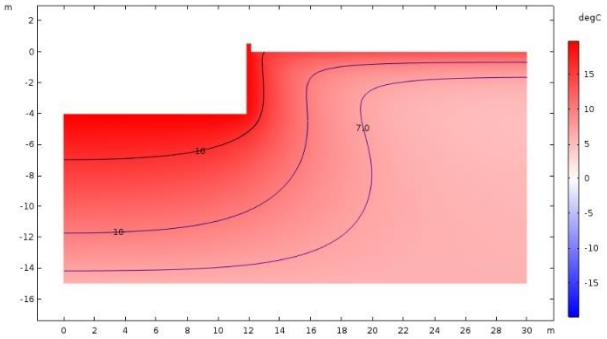

j) October

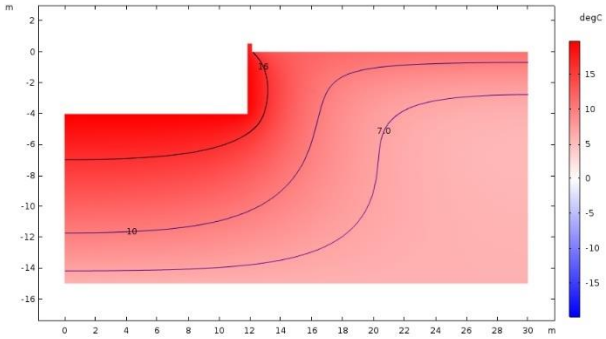

h) August

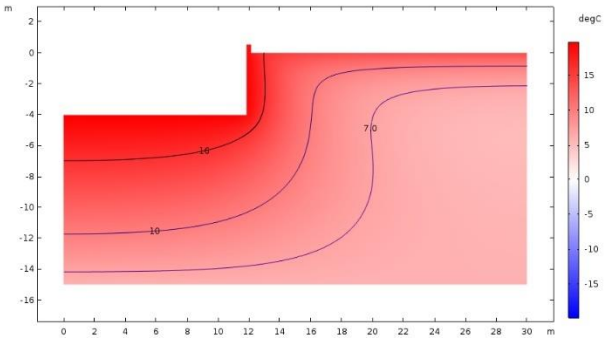

k) November

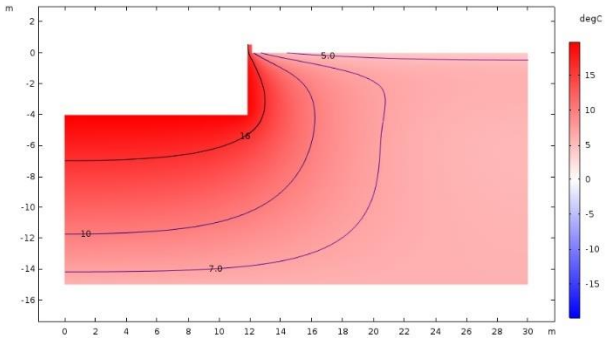

i) September

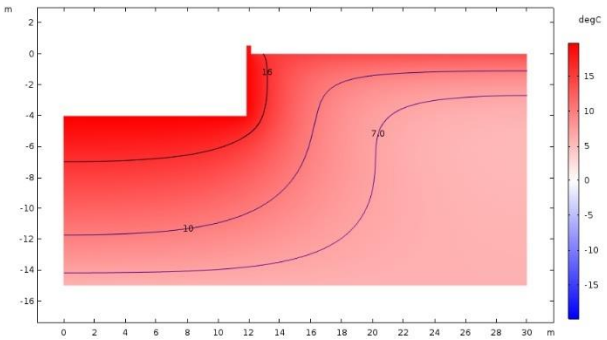

l) December

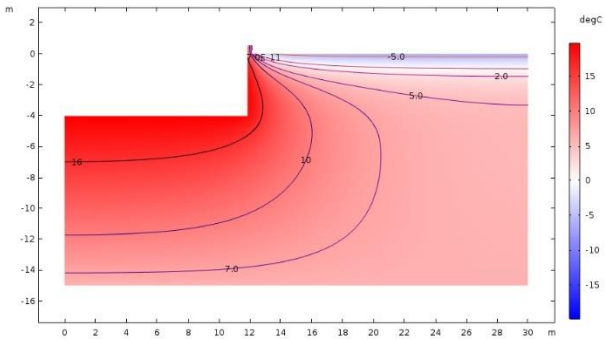

Fig. 22 Distribution of temperature isotherms in January-December. (Thermal properties are constant)

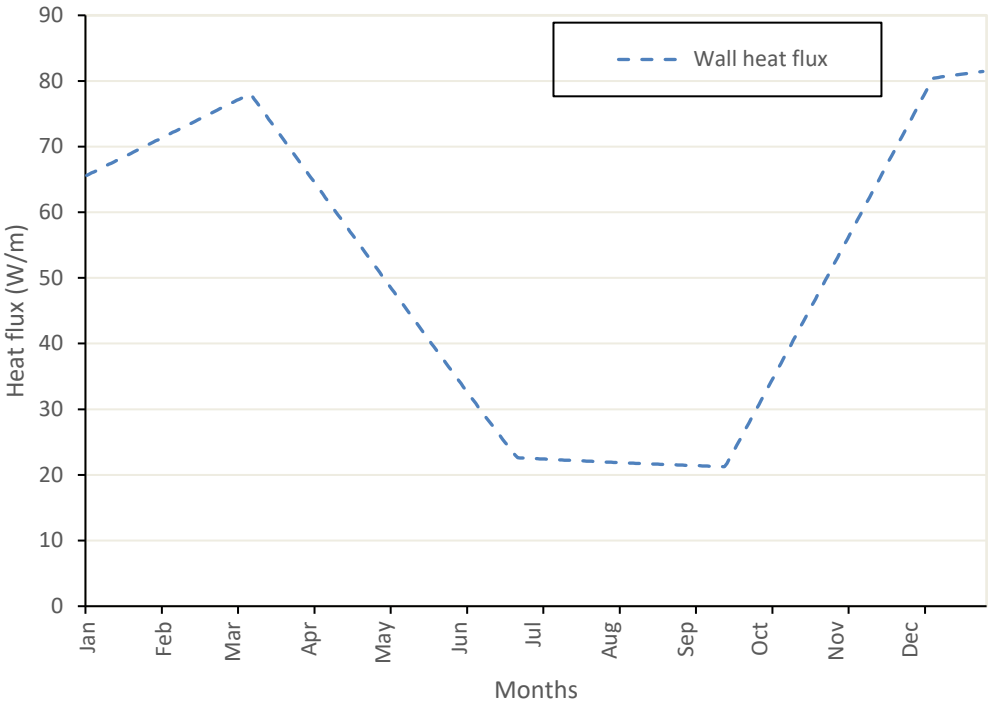

Fig. 23 Heat flux through wall over design period. Approach 1

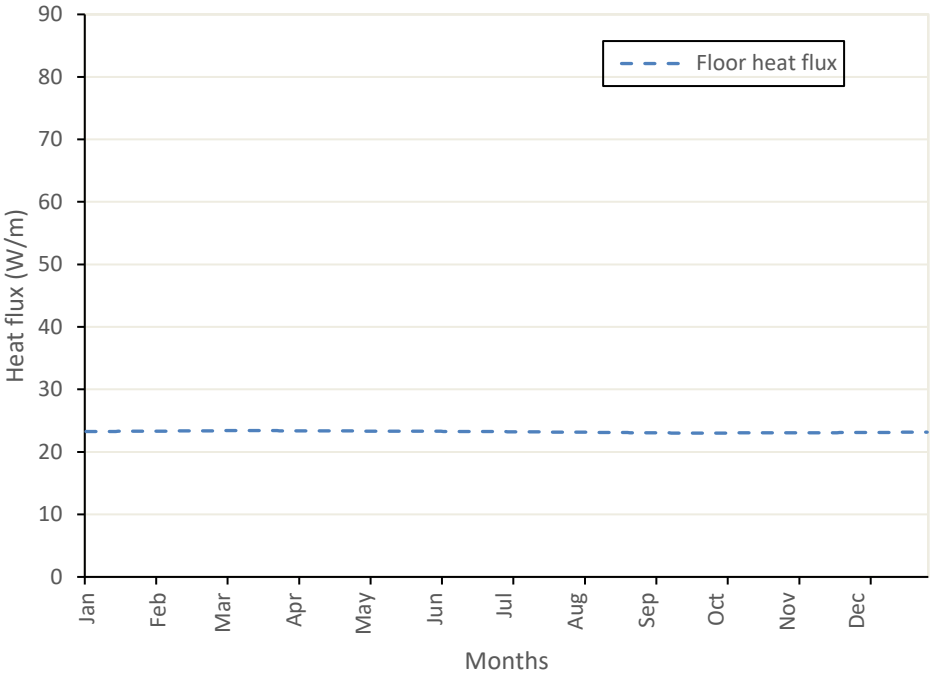

Fig. 24 Variation of total floor heat flux over design period. Approach 1

3.2.4. Heat Loss Simulation Using Approach 2

In the second approach, the thermal parameters k, C and ρ, vary for frozen and unfrozen states. This model aims to treat soil's thermal properties as fully saturated porous medium. Porewater content subjected to freezing yields Eq. [3] (Zhu & Michalowski, 2005) described in Chapter 3.1.3. In this equation, water content is formulated as an exponential function of temperature and validated as described in Chapter 3.1.4. Fully saturated condition is considered where water is introduced as sum of liquid and solid phase. Freezing water becomes ice with properties introduced in Table 8. Soil is considered as compound material consisted of soil grains, water and ice. Each fraction contributes to properties of soil by means of volumetric content. Density of ice and water are assumed as 1000 kg/m^3 to avoid volume change. Material properties are summarized in Table 8.

Table 8 –Material properties

Material	Thermal conductivity k (W/m·C^0)	Heat capacity C_p (J/kg·C^0)	Density ρ (kg/m^3)
Concrete	1.8	880	2300
Insulation	0.041	1450	34
Backfill material (Crashed stone ~20mm)	1.273	1650	1700
Soil particles	2.5	867	2650
Water	0.6	4188	1000
Ice	2.2	2117	1000

Results obtained from this simulation were compared to the previous solution where constant properties of soil were assumed (Fig. 25 and Fig. 26).

Heat flow through wall (Fig. 25) appears more intensive in fluctuation and magnitude rather than through floor structure. It varies in a range of 24 to 77 W/m in the model with constant properties and 23 to 152 W/m in the model with phase change. Heat flux through floor built-up (Fig. 26) is relatively flat and slightly fluctuates in a range of less than one W/m. Approach 1 with constant properties demonstrates average 23.2W/m of floor's heat loss while second model shows 32 W/m.

Calculated heat flux was used to estimate energy loss by integrating total area of walls and floor surface in contact with soil. Heat flux influenced by phase change demonstrated massive increase of energy loss through basement walls compared with Approach 1 (from 52,800 to 92,825 kWh). The same trend was observed in floor structure where the increase was approximately 75%. Energy heating demands of entire Stanley Pauley building refers to 380 MWh annually (Saaly, Maghoul, & Kavgic, 2018). Energy dissipation through foundation calculated with Approach 2 accounts to 30% of that value. However, it does not represent original design but only gives a quantitative measure of energy dissipation of worse case scenario of uninsulated basement. This value will be used for comparative analysis in further calculations. Temperature distribution in soil and ice content and are show in Fig. 27 and Fig. 28.

Table 9 – Comparative analysis of two methods for base case

Parameter	Overall heat flux (W/m)	Overall energy loss (kWh)	Estimated cost (CAD) (as 8.896¢ per kWh)
Heat loss through floor	8,475/11,920	15,050/21,170	1,204/1,884
Heat loss through wall	18,035/31,711	52,800/92,825	4,224/8,261
Total	26,510/43,631	67,850/114,022	5,428/10,145

*- Approach 1(numerator) /Approach 2 (denominator)

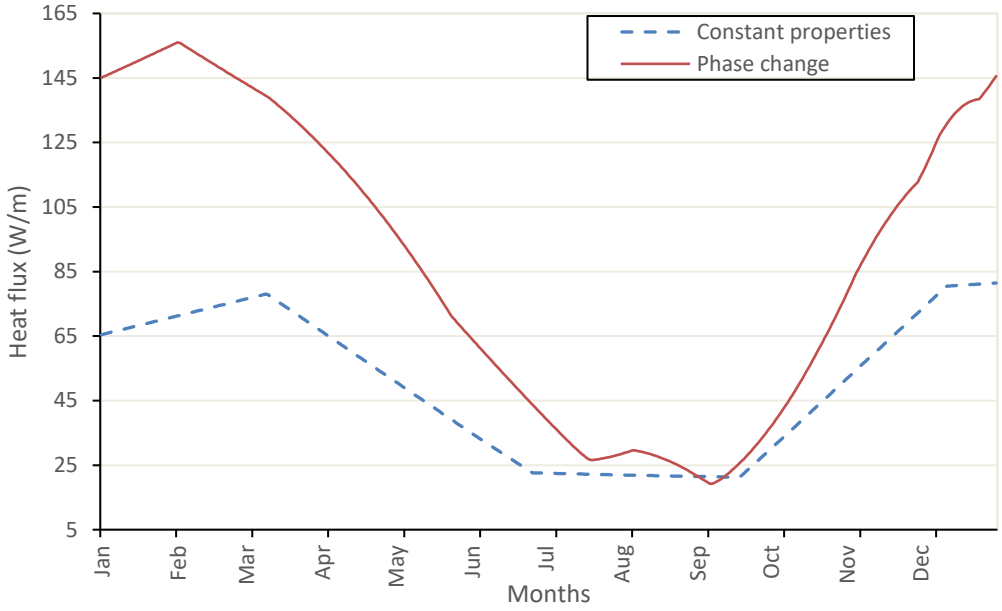

Fig. 25 Heat flux through wall. Predicted using constant properties and phase change approach

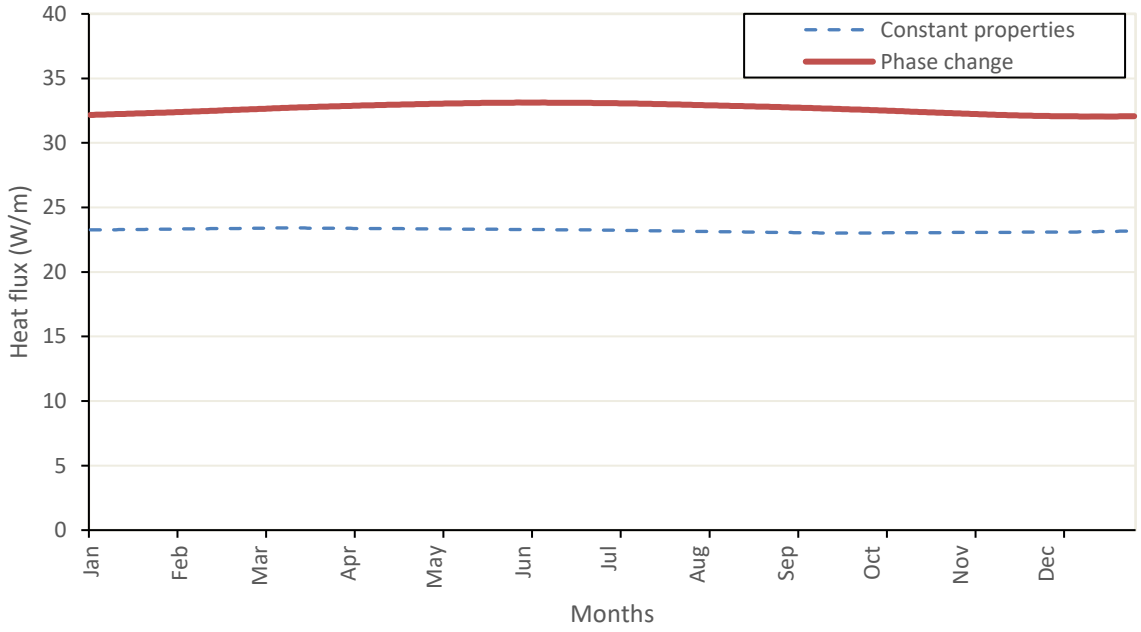

Fig. 26 Variation of total floor heat flux. Predicted using constant properties and phase change approach

a) January

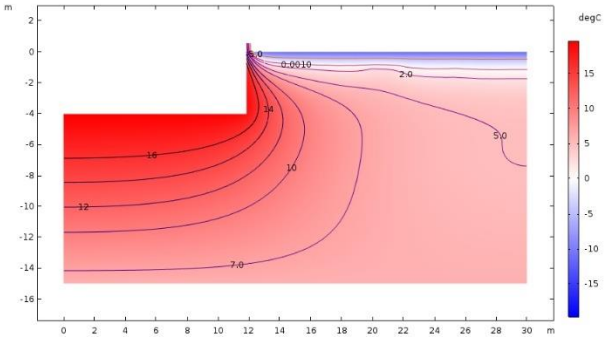

b) February

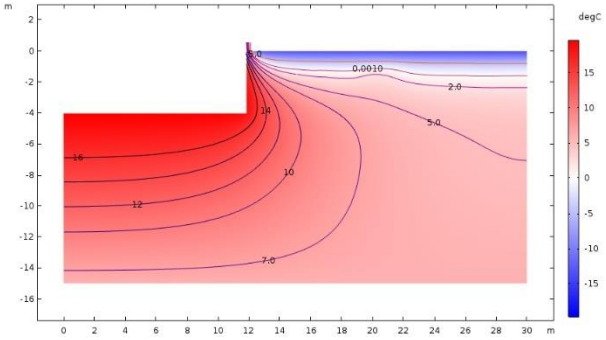

c) March

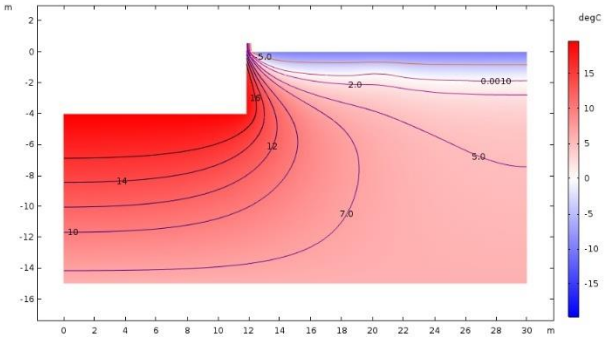

d) April

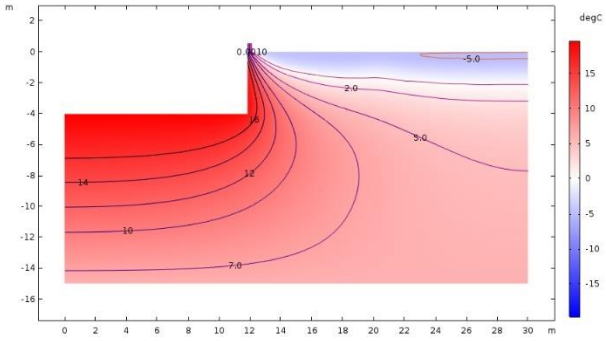

e) May

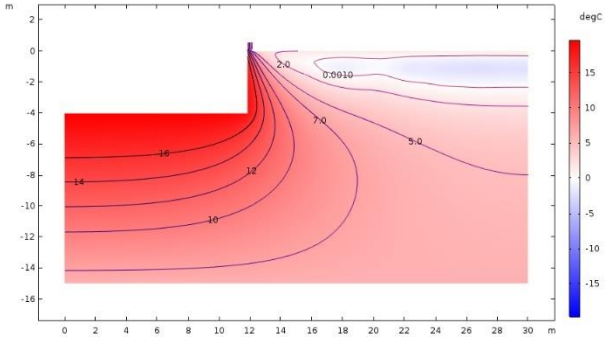

f) June

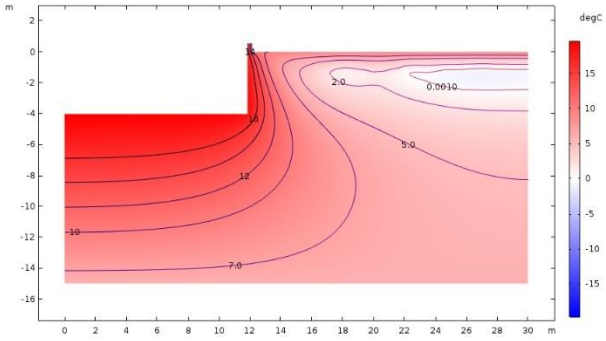

g) July

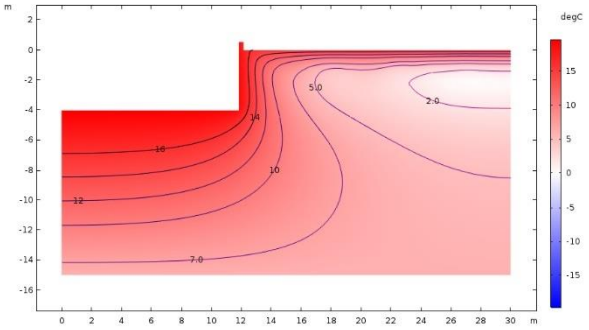

j) October

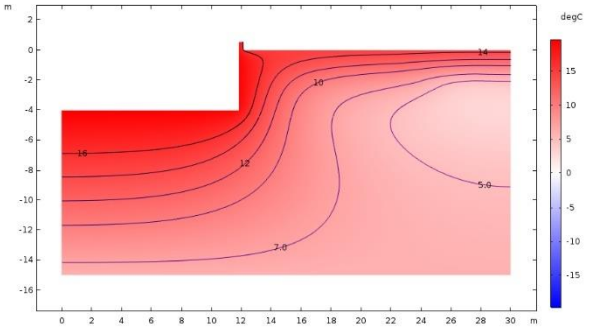

h) August

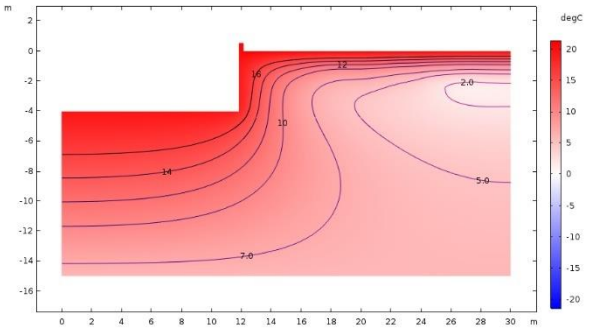

k) November

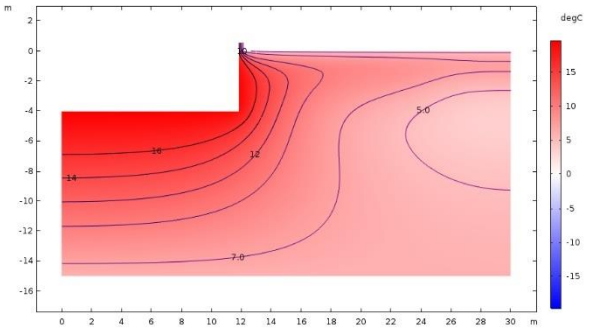

i) September

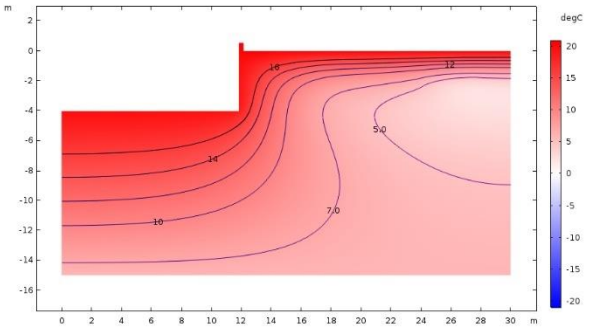

l) December

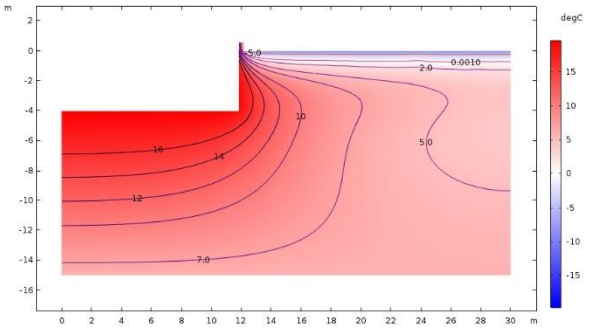

Fig. 27 Distribution of temperature isotherms in January-December

a) January

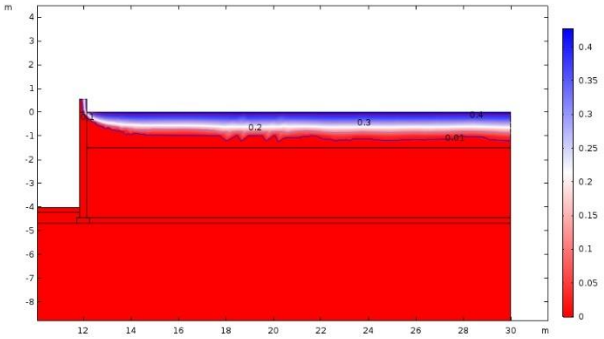

b) February

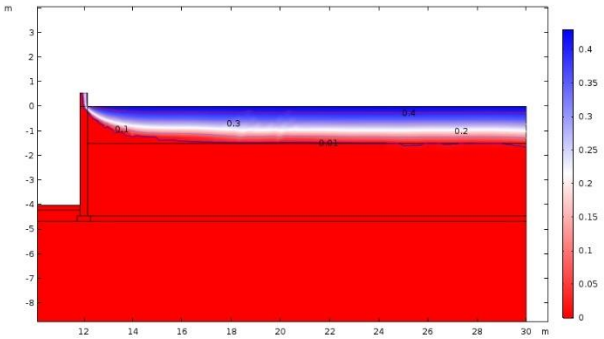

c) March

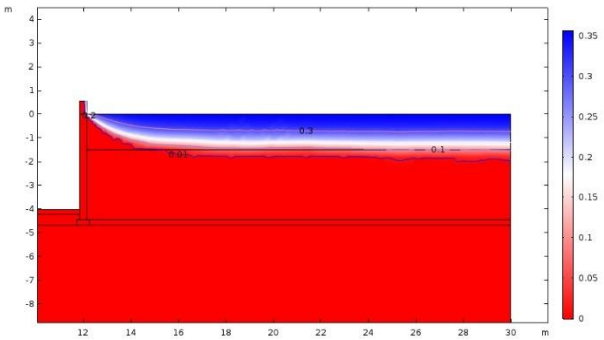

d) April

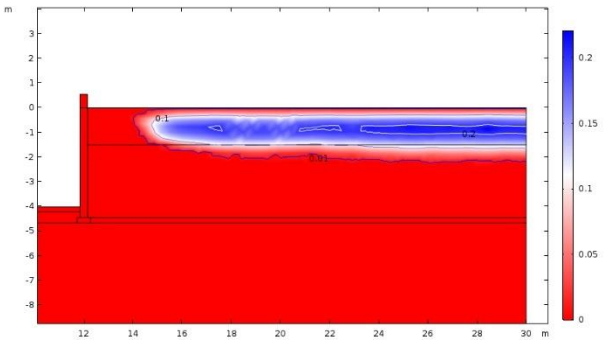

e) May

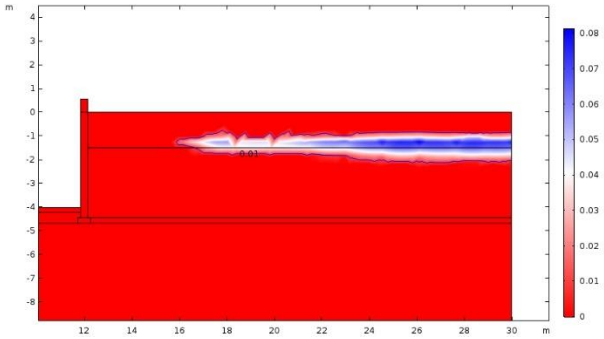

f) June-October

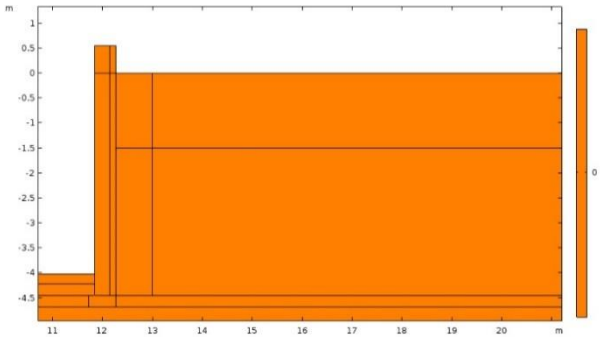

j) November (end of month)

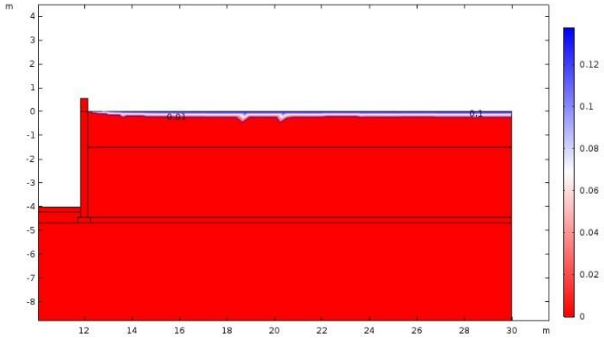

h) December

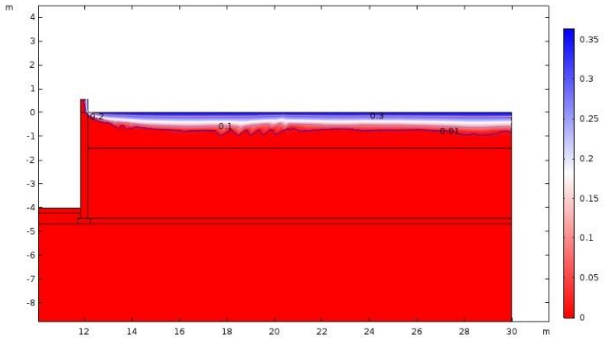

Fig. 28 Distribution of ice content over the year

3.3. Model Performance Designed Based on Project Documentation Parameters

Similar study was performed with respect to instructions provided by design insulation. A typical basement cross-section based on the project documentation is illustrated in Fig. 29.

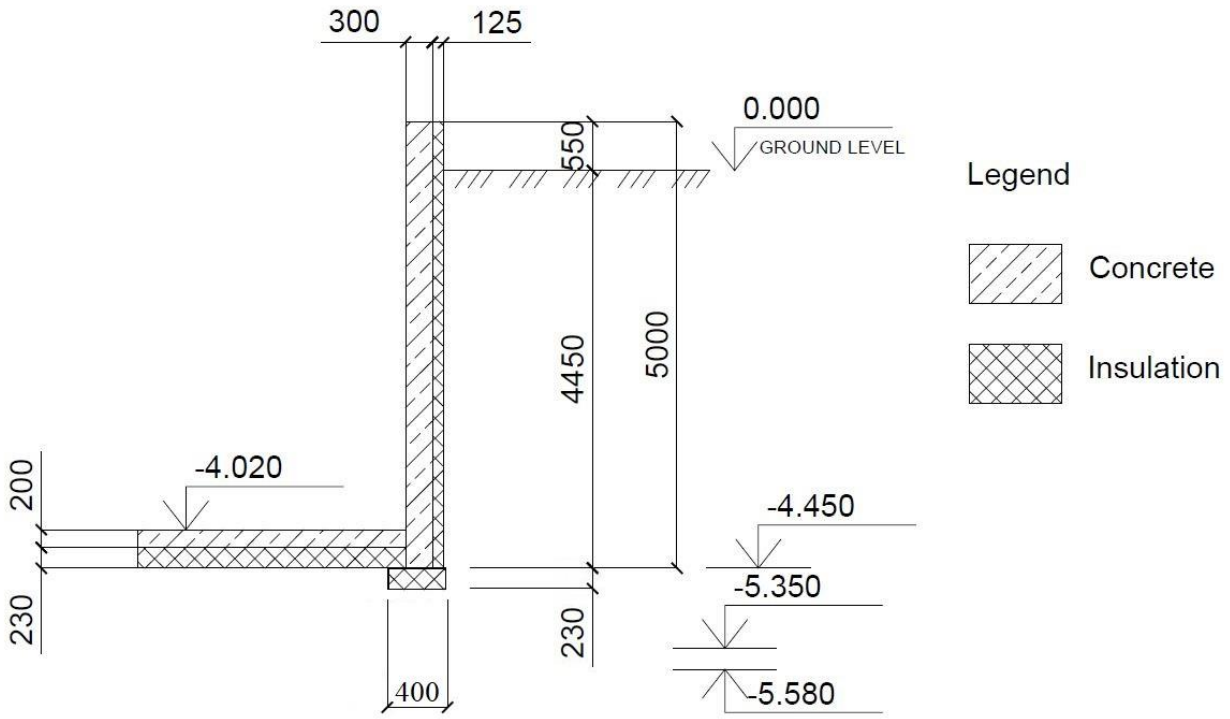

Fig. 29 Cross-section of the basement (in mm)

During construction phase, the reinforced concrete slab of the basement floor was poured over the void forms of 230 mm height. Void forms are often made of honeycomb cardboard panels (Becker & Moore, 2006) stiff enough to carry the load from freshly poured concrete. Later, they tend to degrade due to weathering making voids beneath the concrete slab. Since air captured beneath the concrete slab has very low thermal conductivity, it is assumed that void forms have properties similar to insulation panels attached to basement walls. In simulation, it is assumed that basement

walls have the insulation of 125 mm while floor slab 230 mm. Material properties of structural elements (concrete, insulation) have been assigned as listed in

Table 8.

3.3.1. Mesh Generation

Automatic physics-controlled sequence type with fine mesh refinement generates mesh as presented in Fig. 30. Size of the mesh is adapted to the size of domain elements, so the meshing becomes more dense at smaller elements and corner points.

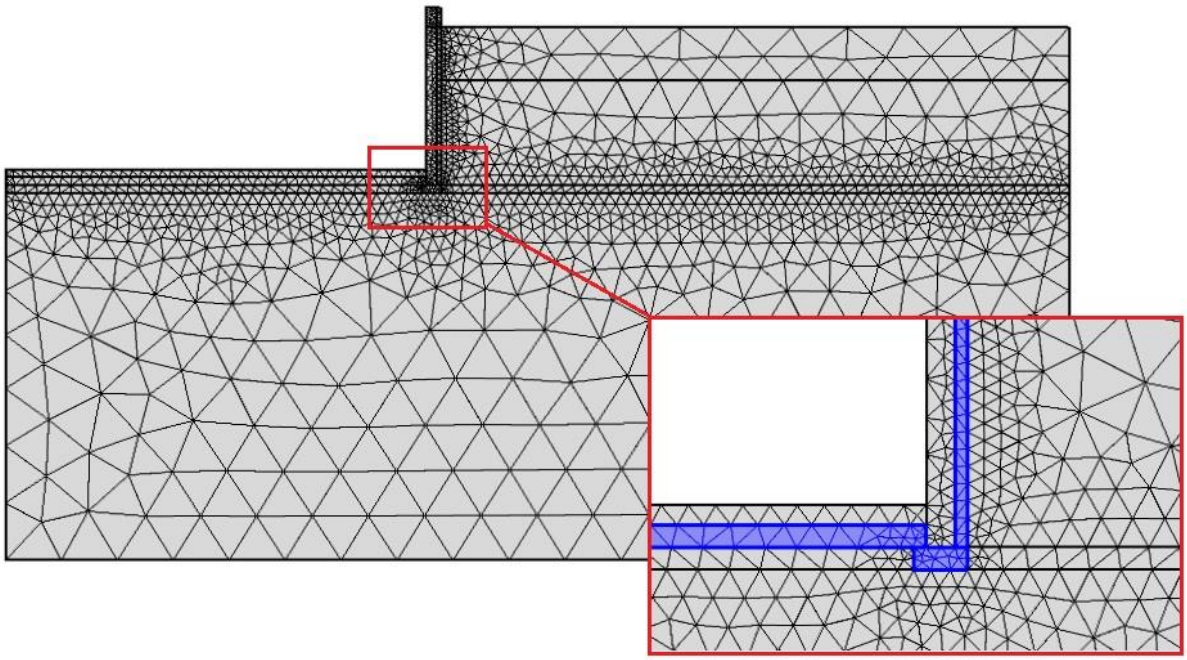

Fig. 30 Mesh refinement of insulation.

3.3.2. Heat Loss Simulation Using Approach 1

Results of simulation presented in Fig. 33 show temperature distribution at different months of the year. Freezing profile in January decreases closer to the building reaching 1.0m depth at the outer

surface of the wall. Two meters away from the wall soil demonstrate deeper frost penetration at a depth of 2.0 m.

Two curves in figures Fig. 31 and Fig. 32 show annual variation of heat flux through basement wall and floor. During summer time heat flow reduces to 10 W/m, while it increases at winter months until 29 W/m. Heat flow in floor structures is somewhat less, approximately 14 W/m and almost does not change over the year. Overall heat loss is calculated as described in paragraph 3.2.3. Table 10 provides values of heat loss through wall and floor structures, respectively, when approach 1 is employed.

Table 10 – Summary of heat loss during the year of simulation using Approach 1

Parameter	Overall heat flux (W/m)	Energy loss (kWh)	Estimated cost (8.896¢ per kWh)
Heat loss through floor	5,060	8,990	720
Heat loss through wall	6,303	18,455	1,475
Total	13,980	27,445	2,195

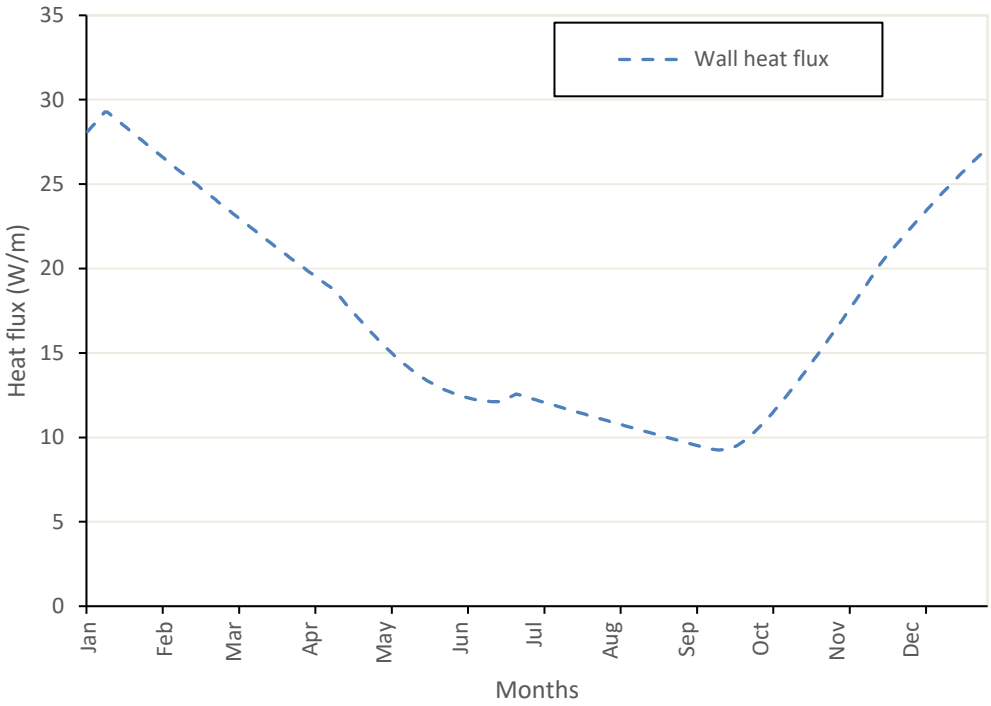

Fig. 31 Heat flux through wall over design period

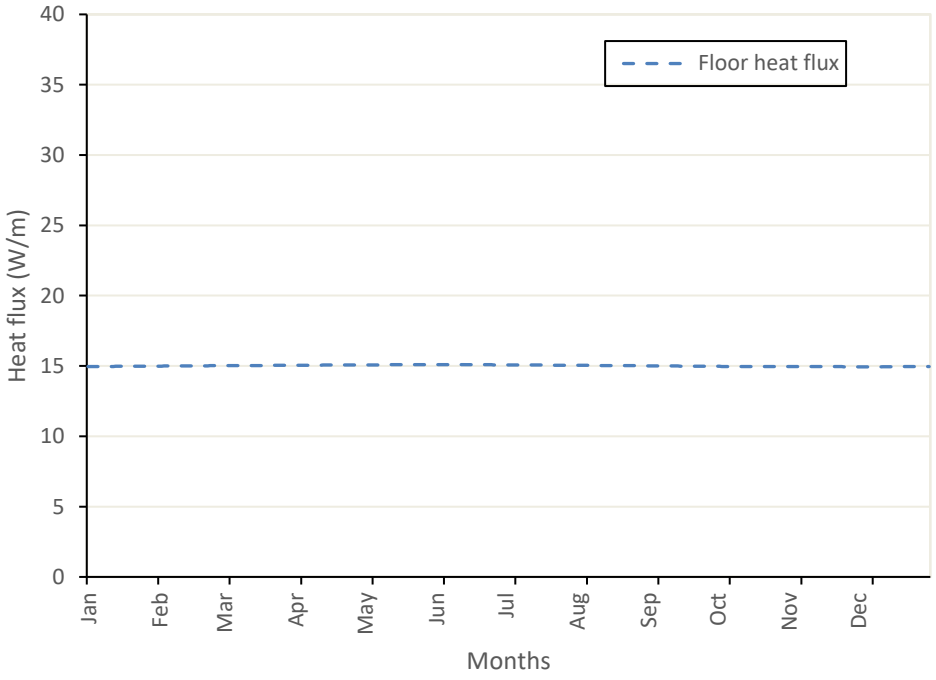

Fig. 32 Variation of total floor heat flux over design period

a) January

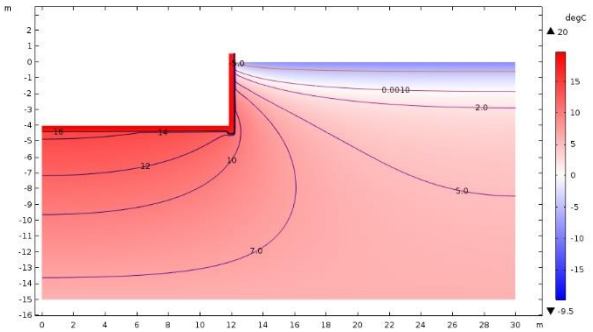

b) February

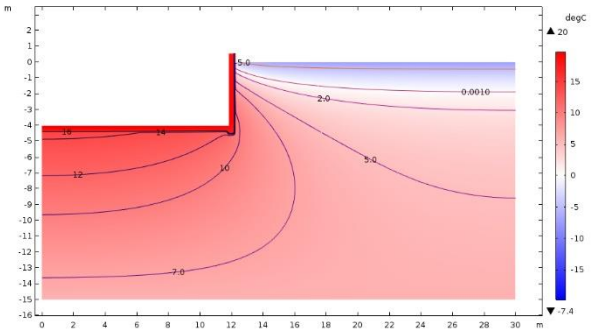

c) March

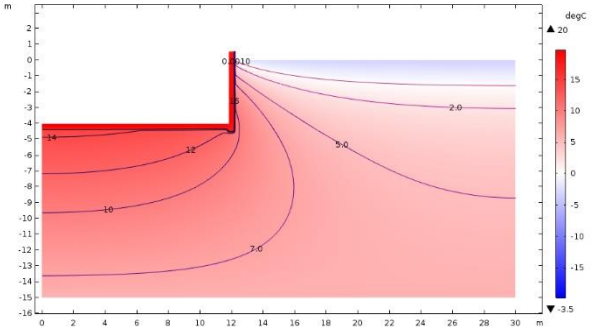

d) April

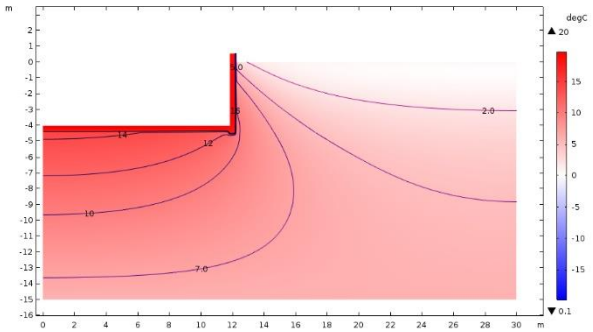

e) May

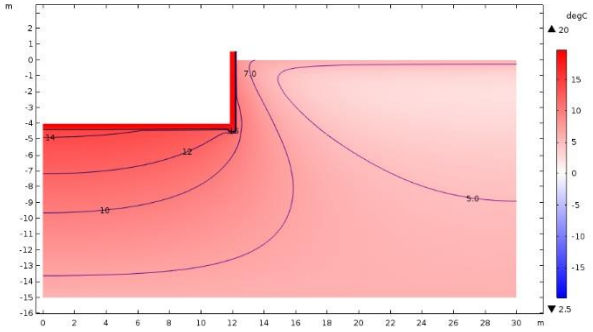

f) June

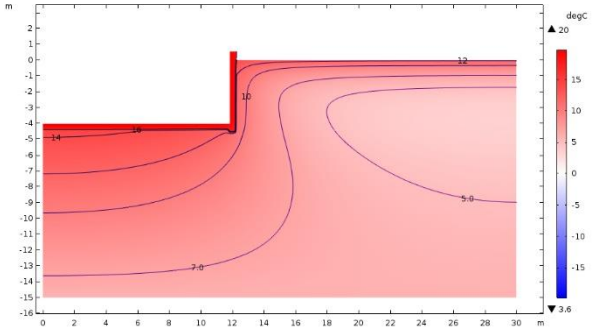

g) July

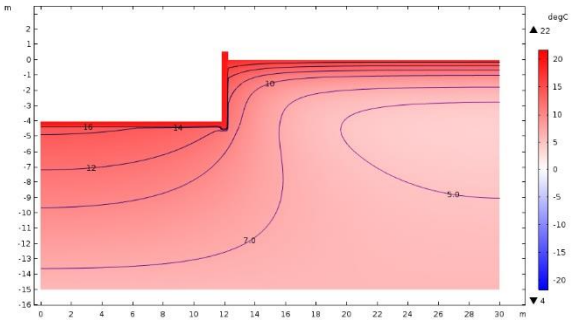

j) October

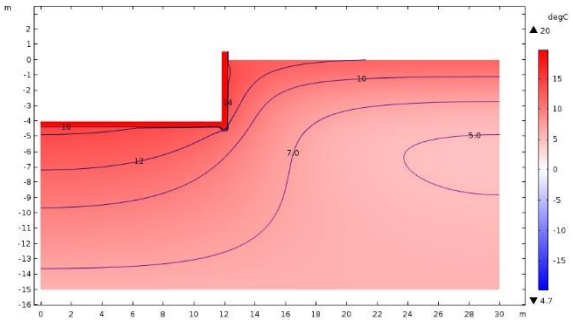

h) August

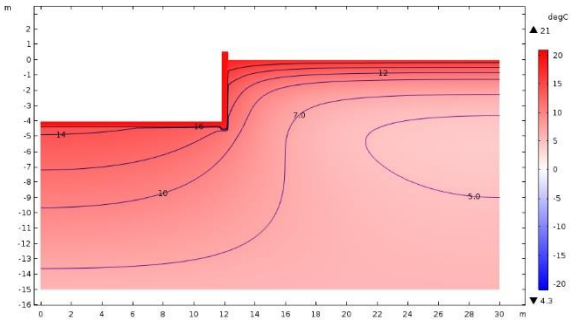

k) November

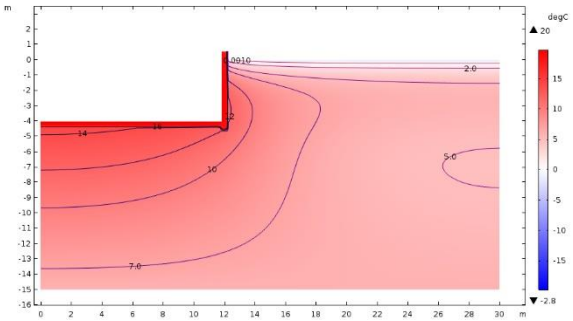

i) September

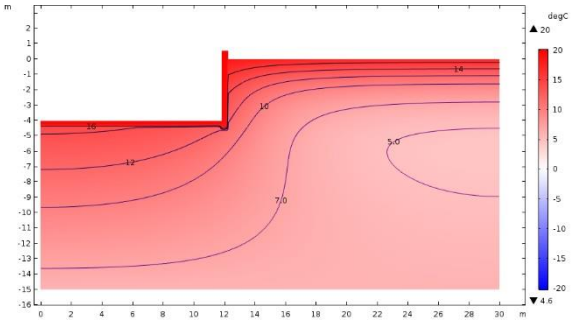

l) December

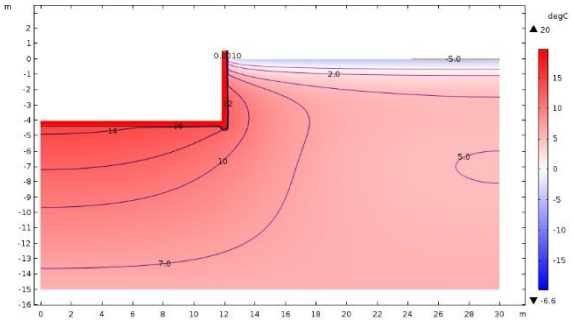

Fig. 33 Distribution of temperature isotherms in July-December

3.3.3. Heat Loss Simulation Using Approach 2

Results obtained from this simulation were compared to the previous solution where constant properties of soil were assumed. Effect of phase change resulted in more severe heat transfer in soils and deeper frost penetration.

Heat flow through wall appears more intensive in fluctuation and magnitude rather than through floor structure. It varies in a range of 11 to 37 W/m (Fig. 34) in the model with constant properties and 11 to 37 W/m in the model with phase change (Fig. 35). Heat flux through floor built-up is relatively even and slightly fluctuates in a range of less than one W/m. Approach 1 demonstrates average 13.8W/m while second shows 16.2 W/m (Fig. 35).

Calculated heat flux was used to estimate energy loss by integrating total area of walls and floor surface in contact with soil. Heat flux influenced by phase change resulted in 34% increase of energy loss through basement walls. The same trend was observed in floor structure where the increase was approximately 17%. Overall, heat loss through wall's and floor surfaces was increased by 29% (from 27,445 to 35,425 kWh) compared to results obtained in Approach 1 (Table 11). Compared to the results calculated in section 3.2.4 insulation of basement gave an expected reduction of heat loss by magnitude more than three times (from 114,022 to 35,425 kWh). Energy dissipation through foundation calculated with phase change approach accounts to 8.9% of heating demands (380 MWh) of the whole envelope including superstructures. This means that almost 9% of the heat used during the year would be transmitted into the soil through insulated buried structures. Temperature distribution in soil and ice content and are shown in Fig. 36 and Fig. 37.

Table 11 – Comparative analysis of two methods

Parameter	Overall heat flux (W/m)	Overall energy loss (kWh)	Estimated cost (CAD) (as 8.896¢ per kWh)
Heat loss through floor	5,061/5,930	8,990/10,530	800/936
Heat loss through wall	6,303/8,500	18,455/24,895	1,642/2,215
Total	11,364/14,430	27,445/35,425	2,442/3,151

*- Approach 1 (numerator) / Approach 2 (denominator)

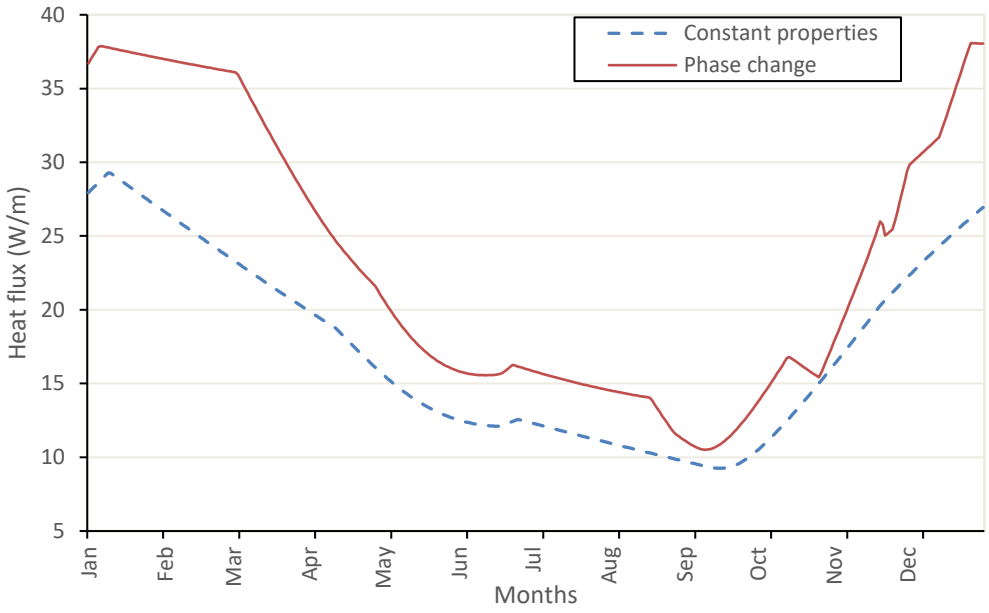

Fig. 34 Heat flux through wall. Predicted using constant properties and phase change approaches

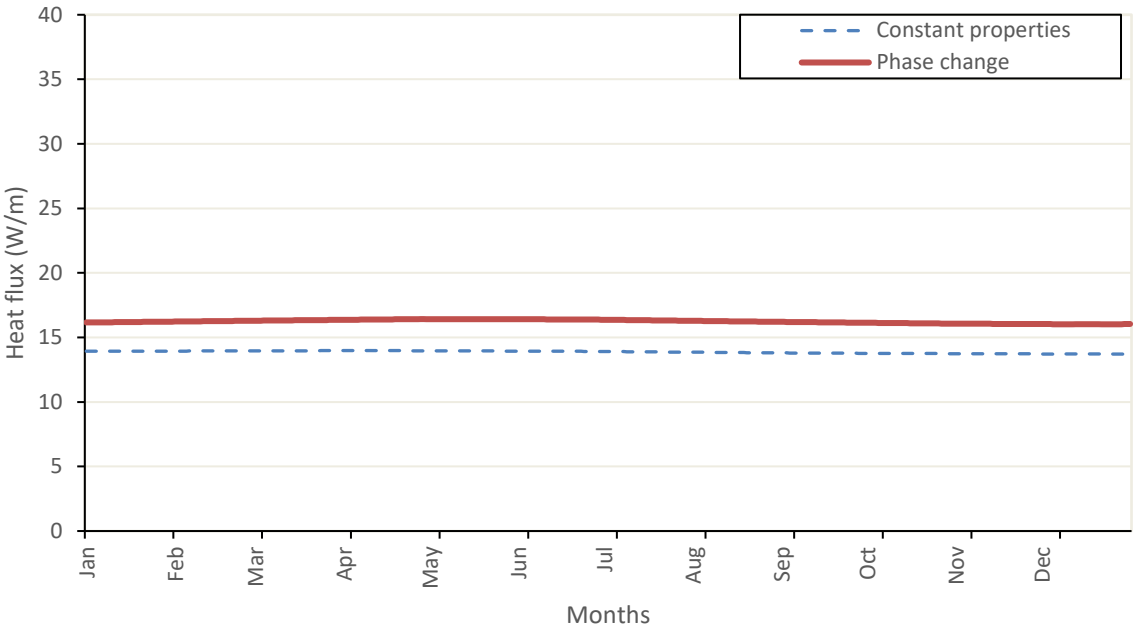

Fig. 35 Variation of total floor heat flux. Predicted using constant properties and phase change approaches

a) January

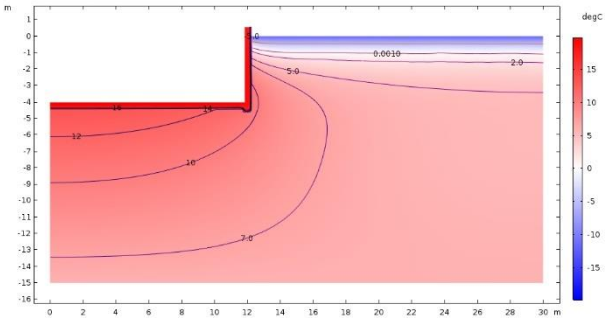

b) February

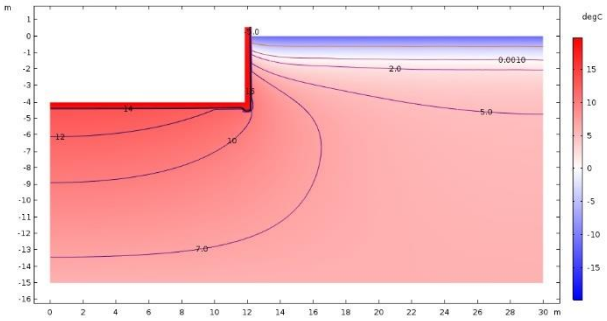

c) March

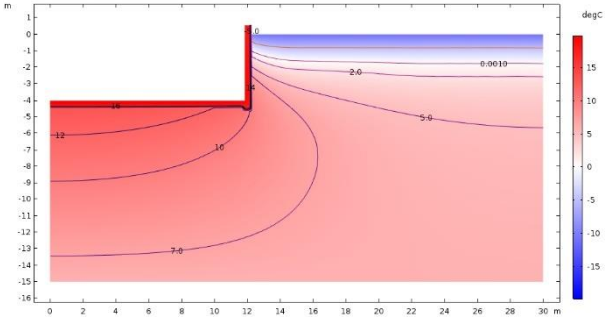

d) April

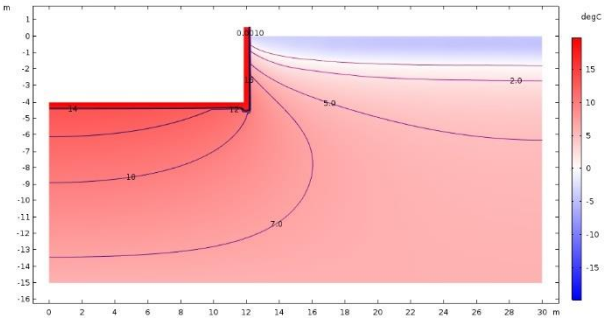

e) May

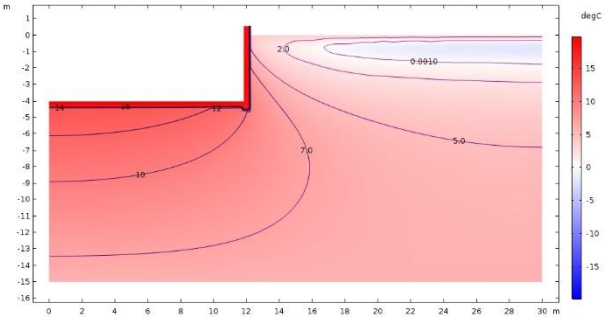

f) June

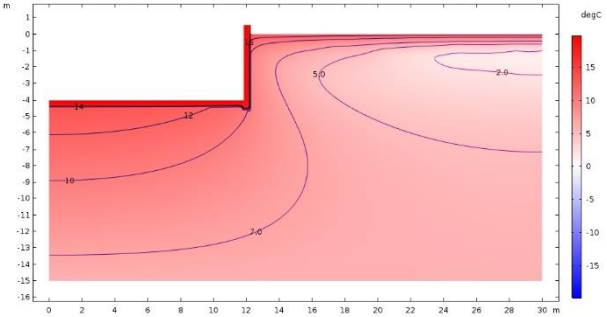

g) July

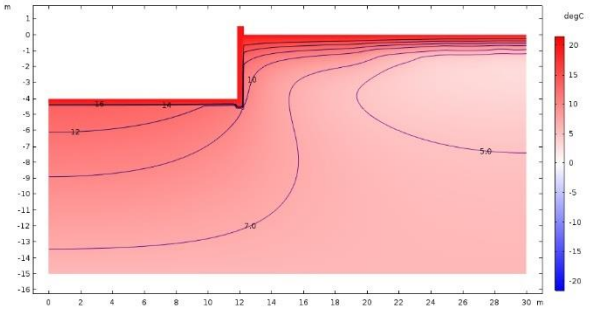

j) October

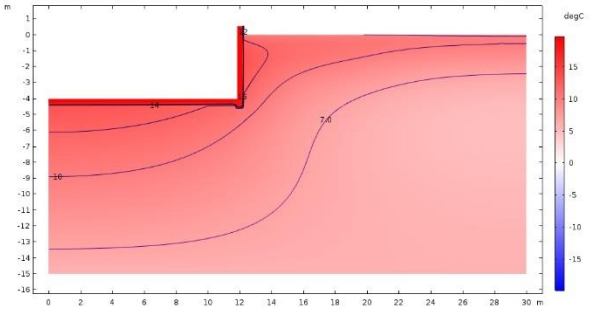

h) August

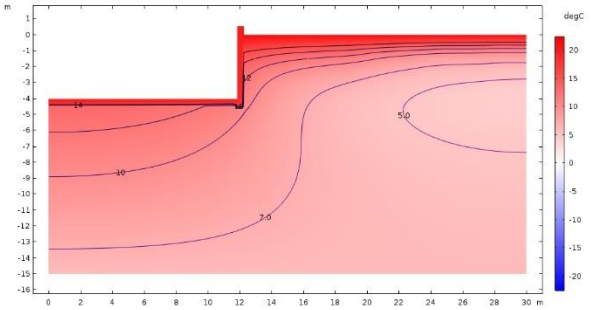

k) November

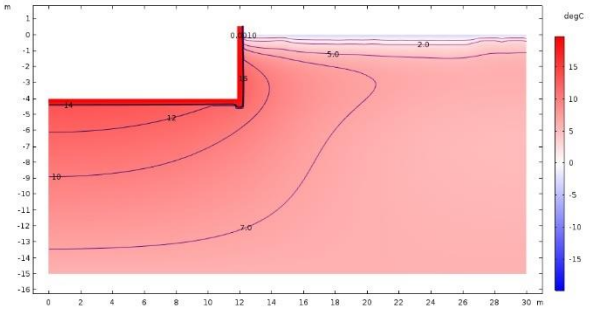

i) September

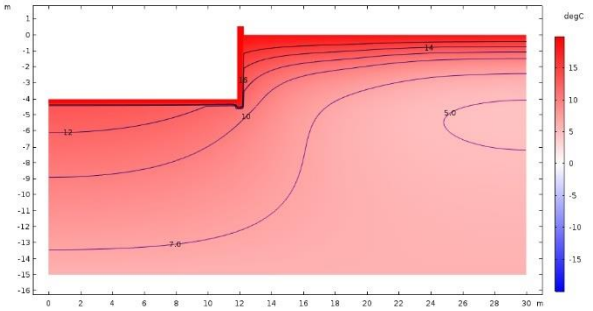

l) December

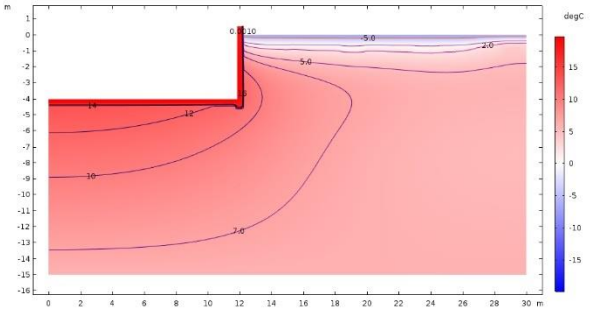

Fig. 36 Distribution of temperature isotherms in January-December

a) January

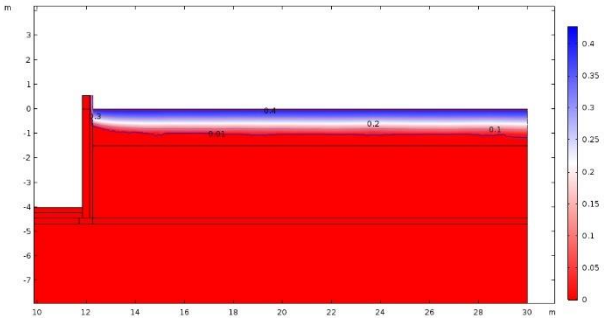

b) February

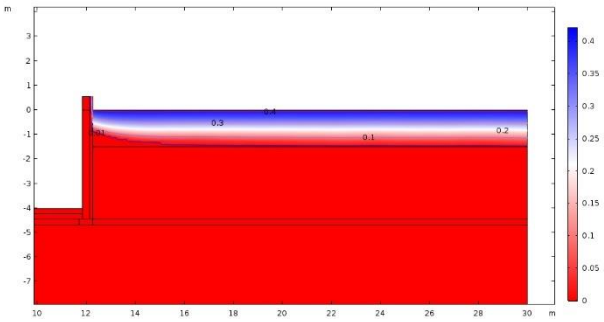

c) March

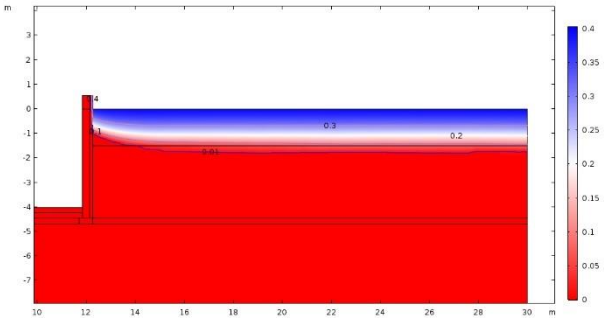

d) April

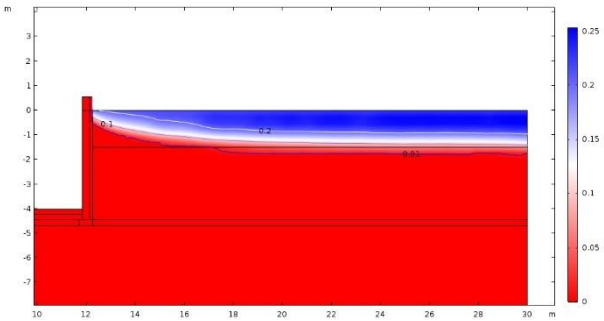

e) May

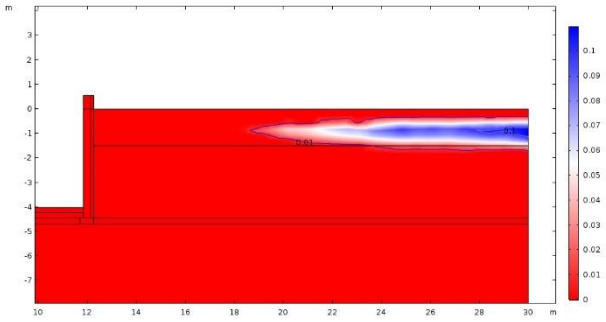

f) June-October

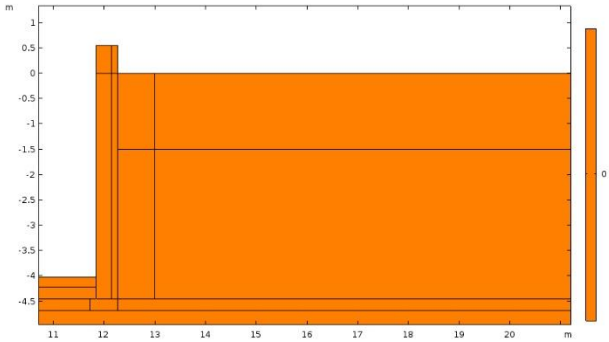

j) November (end of month)

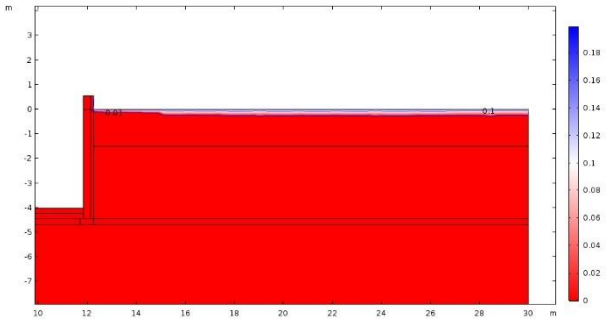

h) December

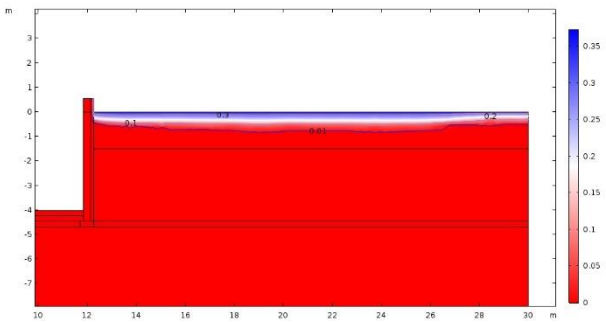

Fig. 37 Distribution of ice content over the year

4. Mitigation Strategies for Heat Loss through the Basement Structure

In this chapter, different mitigation strategies for heat loss through the basement structure will be addressed. The alternatives studied in this study include 1) adding a vertical layer of granular backfill with a drainage system close to the basement wall, 2) placing additional insulation around the basement, 3) considering snow pack around the building as insulating material. An economic analysis is performed to study the effectiveness of these strategies.

4.1. Mitigation Strategy 1: Backfill Material around Foundation

This section aims to reflect reality of the design practice by taking into consideration a layer of granular backfill material close to the basement structure. The effect of backfill material is studied in this approach to see how heat transfer is affected when new material is introduced (Fig. 38).

4.1.1. Model Description

The model takes into account the effect of phase change in heat transfer (Approach 2) and has a similar formulation as described in section 3.3.3.

Crushed stone with ¾ inch fraction was used for backfilling (

Table 8). A trench of 700 mm around the basement? was filled with such materials until the depth of the basement floor. Main purpose of granular backfill is to provide proper drainage of ground and vadose water, runoff and prevent capillary suction into insulation, that is why backfilling is considered as drained material.

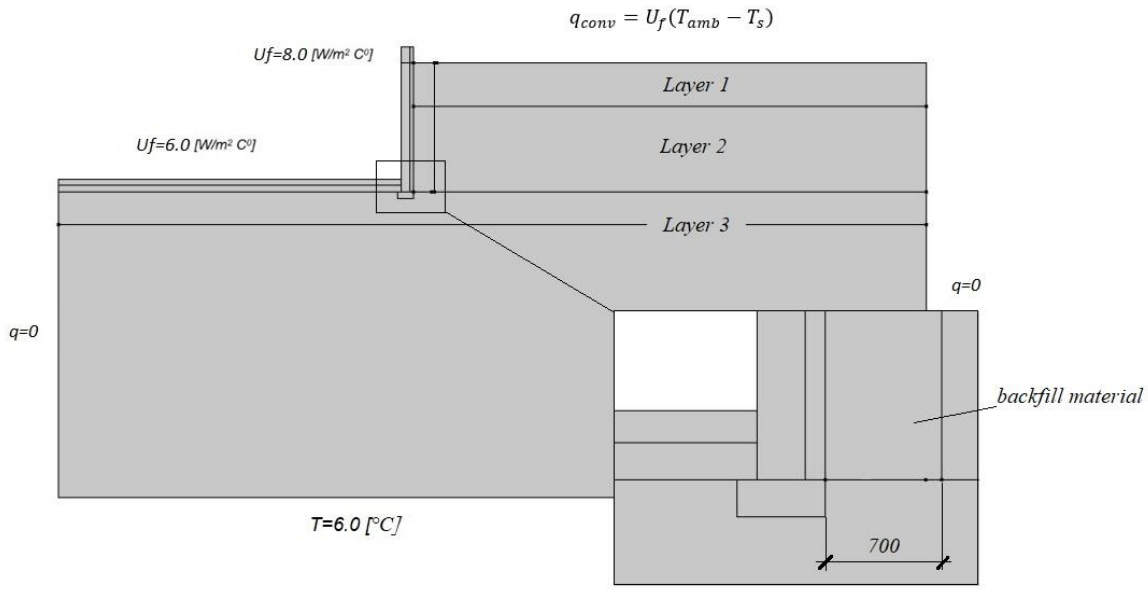

Fig. 38 French drain design

4.1.2. Results of Simulation

Backfill material demonstrate slight reduction of heat flux along the basement wall during cold seasons. In January-February it is 5-6 W/m lower than estimated without placing backfill. Heat flux through floor built-up demonstrates almost identical matching with slight variation in less than fraction of degrees Celsius.

Heat flux influenced by backfilling (Fig. 39 and Fig. 40) resulted in a tiny 6% drop of energy loss through basement walls.

Table 12 – Comparative analysis of two methods

Parameter	Overall heat flux* (W/m)	Overall energy loss* (kWh)	Estimated cost (CAD) (8.896¢/ kWh)**
Heat loss through floor	5,900/5,930	10,510/10,530	935/936
Heat loss through wall	7,820/8,500	22,785/24,895	2,027/2,215
Total	13,720/14,430	33,295/35,425	2,962/3,151

*-w/ backfilling (numerator) /Project design, Approach 2 (denominator)
**-Commercial rates provided by Manitoba Hydro, accessed on 01/08/2018 ("www.hydro.mb.ca," 2018)

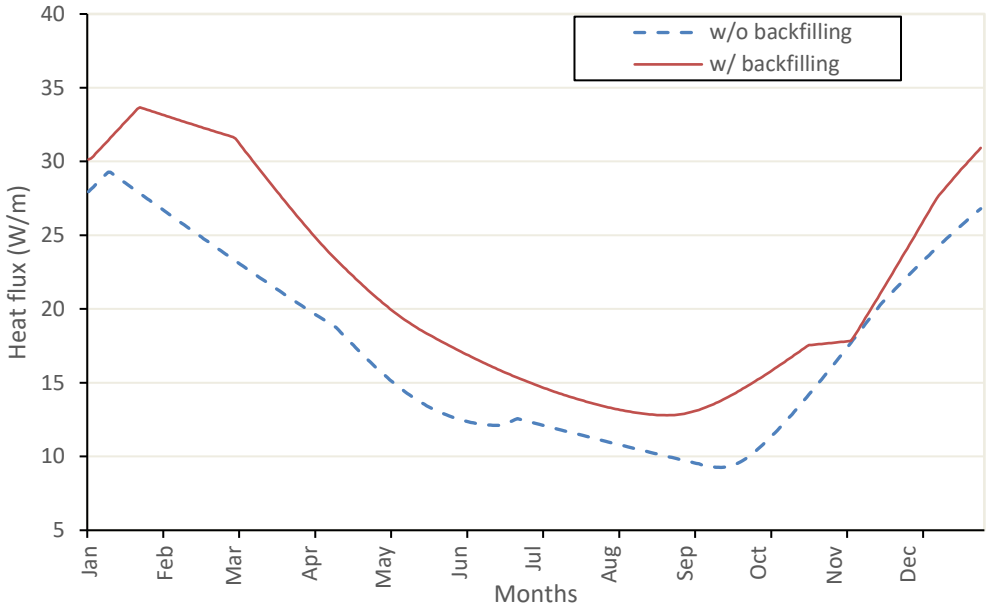

Fig. 39 Heat flux through wall.

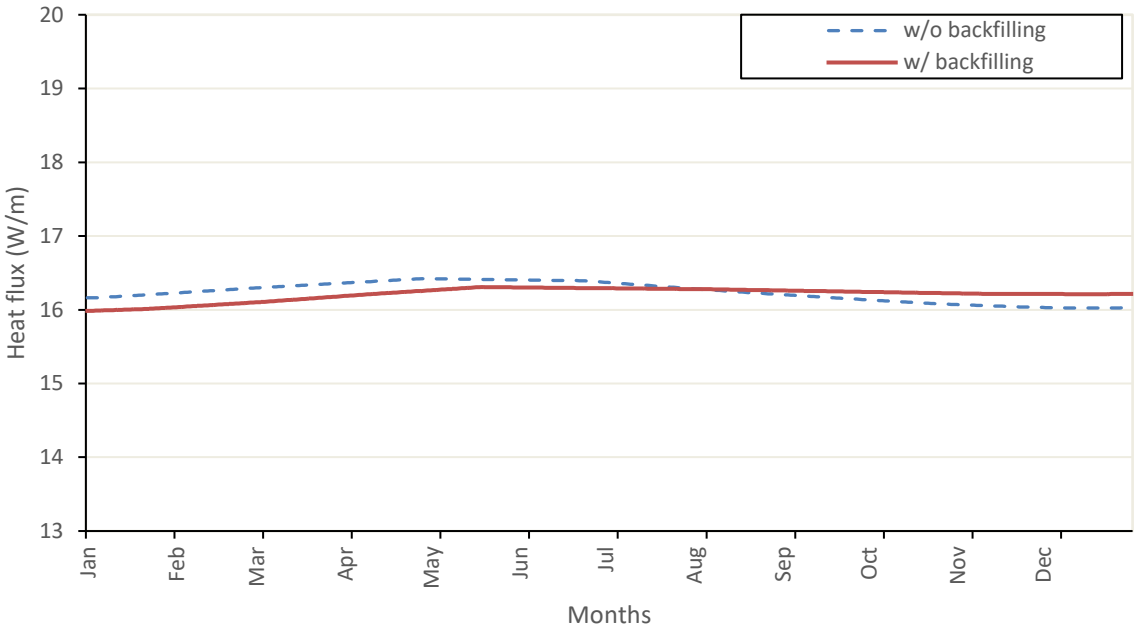

Fig. 40 Variation of total floor heat flux constant properties and phase change approach

4.2. Mitigation Strategy 2: Additional Insulation around the Basement Structure

This section aims to provide analysis of additional insulation applied to the basement to reduce heat dissipation. Since overall heat loss of the basement estimates 9% (Para. 3.3.3) of all energy demands required for heating it is of great interest to find out whether the increase of insulation will demonstrate significant improvement.

4.2.1. Model description

The model takes into account the effect of phase change on heat transfer (Approach 2) and has a similar formulation as described in section 3.3.3. Alternative insulation is designed to minimize heat flux towards the ground and reduce energy loss in whole. Solution consists of an additional 100 mm layer of insulating material buried horizontally half-meter below grade and 1.2 m in width (Fig. 41).

This can be in accordance with the recommendations provided by Canadian Foundation Engineering Manual (4th edition), which proposes the utilization of rigid boards, fabricated from extruded polystyrene. Closed cell insulation is laid down with the slope which allows to direct groundwater away from building. Use of polystyrene boards is allowed in absence of contact with hydrocarbons.

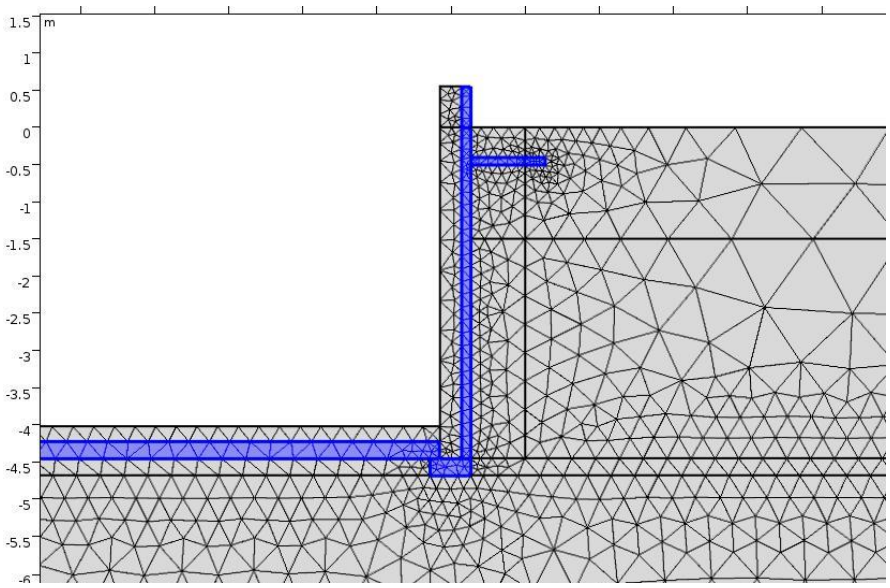

Fig. 41 Insulated pavement

4.2.2. Results of Simulation

Results obtained from the simulation were compared with heat loss calculated from initial insulation design using Approach 2.

Heat flux along the basement wall varies in a range of 10 to 25 W/m over the year, which is 10 W/m less than estimated without additional insulation (Fig. 42). Heat flux through floor built-up demonstrates slight reduction reaching average 16W/m (Fig. 43).

Heat flux influenced by additional insulation (Fig. 41) resulted in 31% drop of energy loss through basement walls (Table 13). The same trend was observed in floor structure where decrease was approximately 2% (from 10,350 to 10,530 kWh). Overall, energy dissipation was reduced by 22% due to the applied insulation. As can be seen from Fig. 44, horizontal insulation reduces depth of frost penetration in area adjacent to the basement. This, in turn, implies reduction of temperature gradient beneath the insulated pavement which results in overall reduction of heat dissipation.

Table 13 – Resulting energy loss after alternative insulation design

Parameter	Overall heat flux (W/m)	Overall energy loss (kWh)	Estimated cost (CAD) (as 8.896¢ per kWh)
Heat loss through floor	5,800/5,930	10,350/10,530	921/936
Heat loss through wall	5,822/8,500	16,955/24,895	1,508/2,215
Total	11,622/14,430	27,305/35,425	2,430/3,151

*- Additional insulation (numerator) /Original design, phase change (denominator)

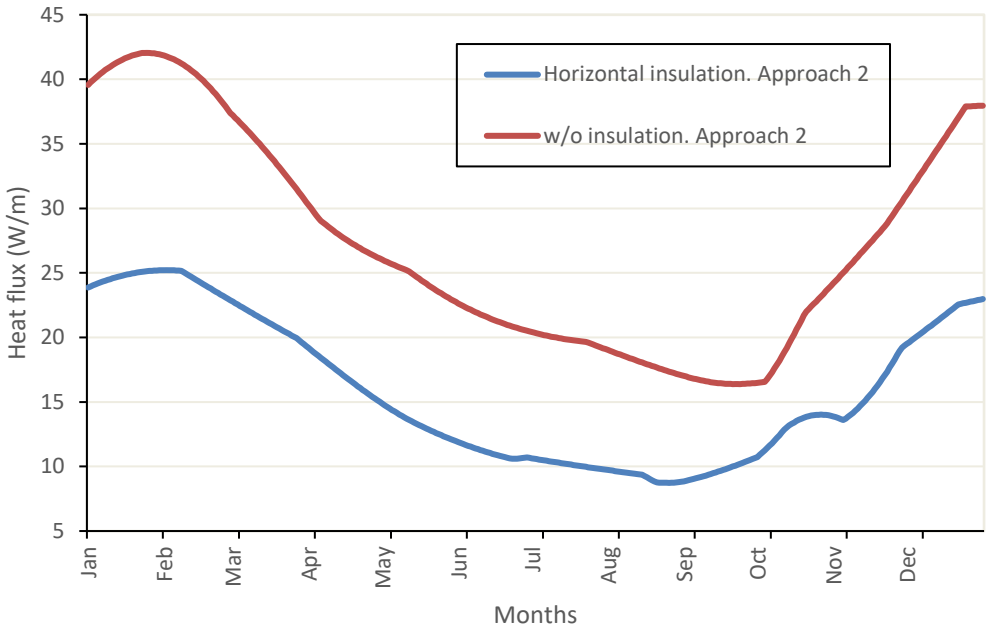

Fig. 42 Heat flux through wall. Predicted using constant properties and phase change

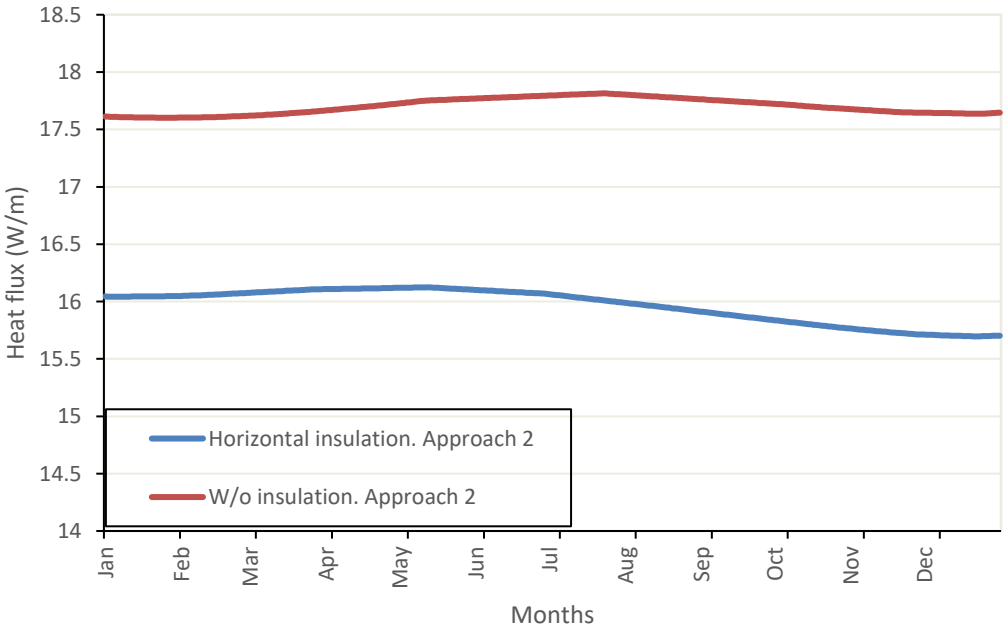

Fig. 43 Variation of total floor heat flux. Predicted using constant properties and phase change approach

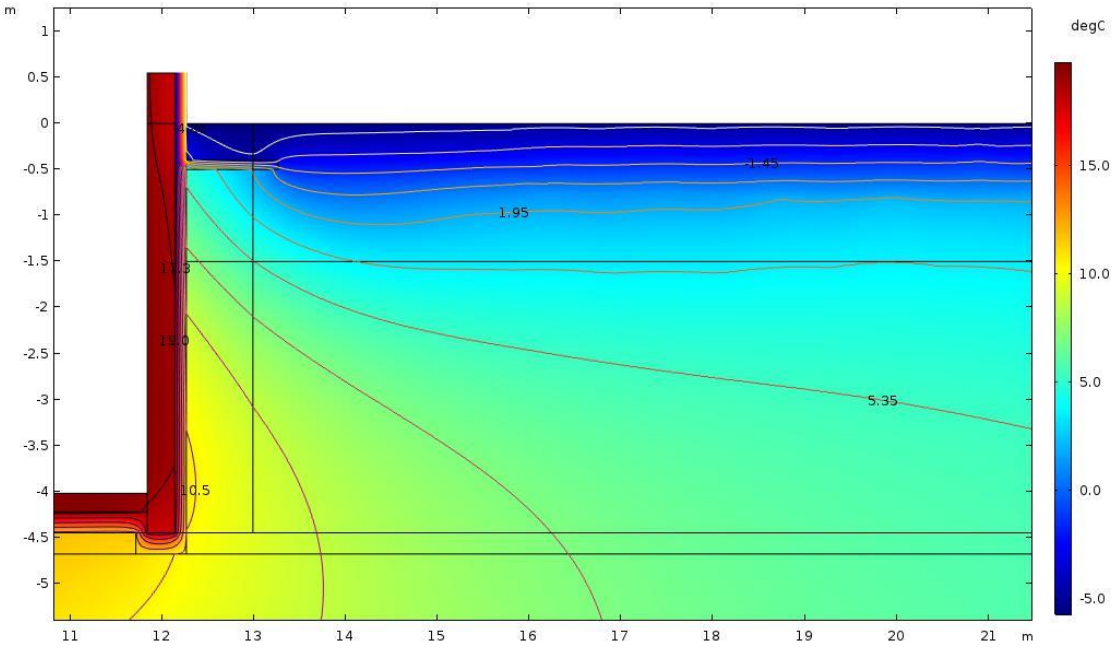

Fig. 44 Effect of horizontal insulation on frost penetration (February)

4.3. Mitigation Strategy 3: Effect of Snowpack around the Building.

4.3.1. Model Description

The model has a similar formulation as described in section 3.3.3. In this scenario snow is collected right beside the building during the winter maintenance and acts as insulation. Snow action is only reasonable for winter time when negative temperatures prevail.

Snow pack has very uneven properties which mostly depend on density, crystalline structure and grain to grain contact. Shoveled snow is much denser that fresh one and has higher thermal conductivity which vary from 0.12 W/mK and 0.54 W/mK for porosities from 0.4 to 0.68 (Côté, Rahimi, & Konrad, 2012). Newman (1995) refers snow thermal conductivity in a range of 0.046 W/mK for fresh snow and 0.326 W/mK for old, dense snow.

In this model it is assumed that snow pack exists only during the winter time from December-February (Fig. 45). Snow pile has the 0.4m height and 1.1m width, $k = 0.465\ [W/mK]$, $C_p = 2043$ [J/kg·K], $\rho = 560\ [\frac{kg}{m^3}]$

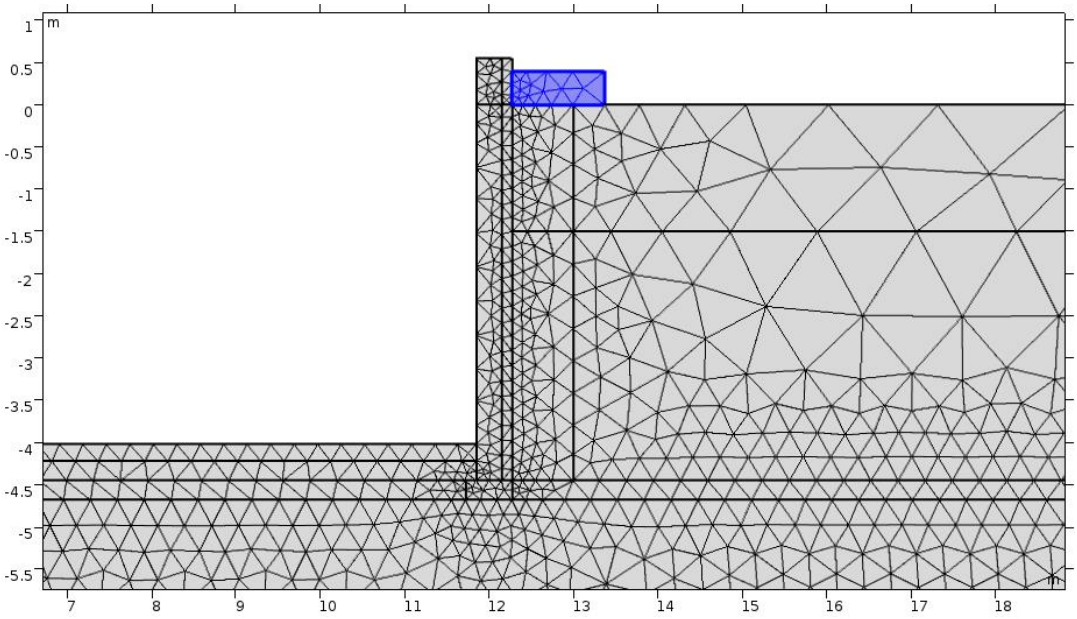

Fig. 45 Modelling snowpack during winter months

4.3.2. Results of Simulation

Results obtained from the simulation were compared with heat loss calculated from initial insulation design (para. 4.1) using Approach 2. Results summarized in

Table 14 do not show significant reduction of heat exchange either through wall nor floor (Fig. 46 and Fig. 47). Total heat flux dropped from 13,720 to 13,058 W/m. Total energy losses resulted in slight drop from 35,425 to 31,3540 kWh. Economic benefits from snow pack reaches 11% savings on energy (Fig. 46)

Table 14 – Comparative analysis of two methods

Parameter	Overall heat flux* (W/m)	Overall energy loss* (kWh)	Estimated cost (CAD) (8¢/ kWh)*
Heat loss through floor	5,870/5,900	10,452/10,530	930/936
Heat loss through wall	7,188/7,820	20,902/24,895	1,860/2,215
Total	13,058/13,720	31,354/35,425	2,790/3,151

*-w/ snowpack (numerator) /Original design, phase change (denominator)

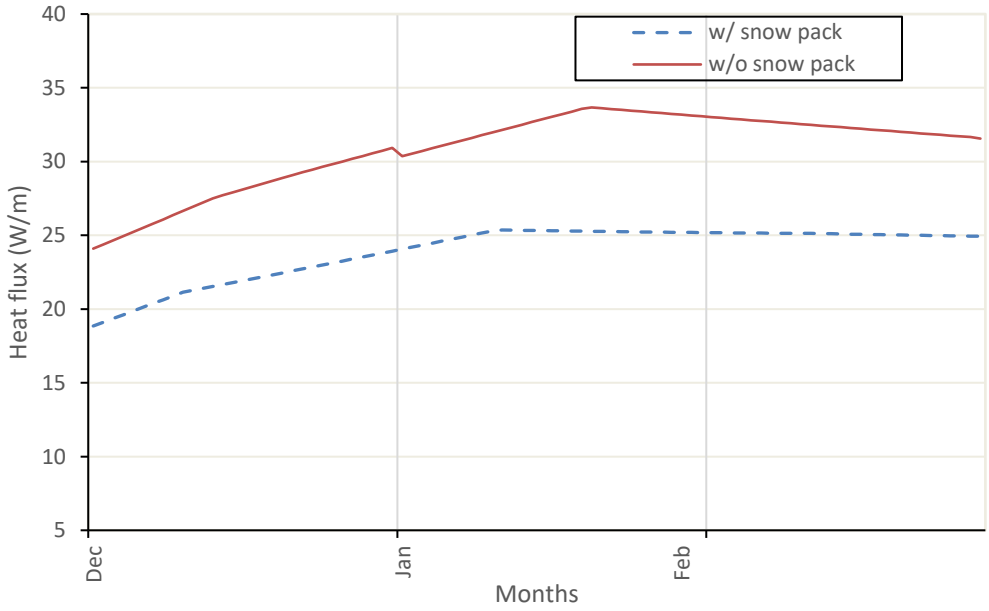

Fig. 46 Heat flux through wall esimated for snow pack and without it

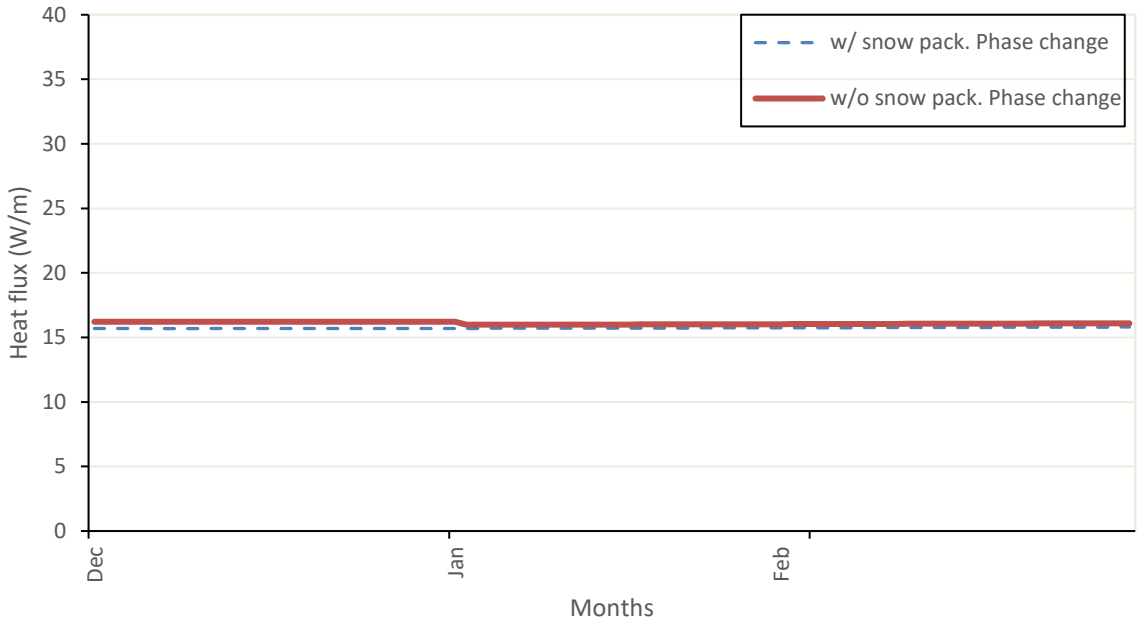

Fig. 47 Variation of total floor heat flux. Predicted using phase change approach for snow pack conditions and without it.

4.4. Comparison of Results

Heat transfer in soils has been studied and applied to real case study by running two numerical models. Results obtained from both models showed that phase change plays a significant role in prediction of heat loss. The Model in which phase change wasn't considered demonstrated underestimated values of heat loss and more shallow frost penetration depth. In contrast, the model with considering phase change and variable water content demonstrated increase in overall energy loss. Frost depth reached in some points up to 2.0 m.

First, Approach 2 (phase change) shows that uninsulated basement loses 3.8 times more heat rather than one with 125mm of insulation applied on walls and 230mm on floor. Under the same conditions Approach 1 demonstrates difference in 2.5 times.

5. Summary and Conclusion

Heat transfer in soils has been studied and applied to real case study by running two numerical models. Numerical models were implemented in COMSOL Multiphysics software based on application of heat transfer physics incorporated into Heat Transfer in Porous Medium module. Additionally, ice and water content relations were assigned via external variables.

First approach represents basic solution to formulate soils properties as fixed values taken from direct measurements made at site or lab. Fact that thermal properties of frozen ground differ from thawed one motivated us to conduct a series of tests to evaluate its properties after freezing and later use this data in calculations. Another approach (numerical model) was introduced based on described in literature formulation of variable porewater content as an exponential function of negative temperature imposed to the ground. Understanding physic of water migration at freezing soils and fact that water does not freeze completely at temperatures below 0 ^{o}C motivated us to run the second model for comparative analysis. Heat transfer equation addresses jump of heat source during phase change when latent heat is released during freezing of water.

Laboratory measurements showed that thermal properties of soils encountered at the construction site were within the range described in literature. This gives an idea that thermal properties of soils may be taken from literature after proper classification. It is recommended to repeat measurements several times on different specimens for better statistical analysis and to avoid invalid values to be used. It was observed that one out of six measurements tend to be less adequate and precise than the average.

The real case study was simulated according to project documentation. Frost penetration reaches 1.6 m meters when calculated using Approach 2 and 1.8m after Approach1 is employed.

In addition, to mitigate energy loss through the basement enclosure, different scenarios were studied. Results of simulations are summarized in Fig. 48. Use of backfill material had a slightly positive impact on energy performance as the heat loss were decreased from 35,425 to 33,295 kWh (6%).

Alternative mitigation strategies such as additional horizontal insulation buried at 1.2 m below the ground surface in combination with backfill material demonstrated significant reduction in heat flux by 21%. Colder seasons with lower ambient temperatures and higher wind velocities may increase convective heat flux and result in increased energy consumption.

Cost analysis is summarized in Fig. 49. It demonstrates that uninsulated basement has significant heat loss (10,145$ annually) which is three times higher rather than insulated. Mitigation strategies with back filling and snow pack brought economic effect of 6% and 11% respectively. Additional insulation reduces expenses up to 2,430$.

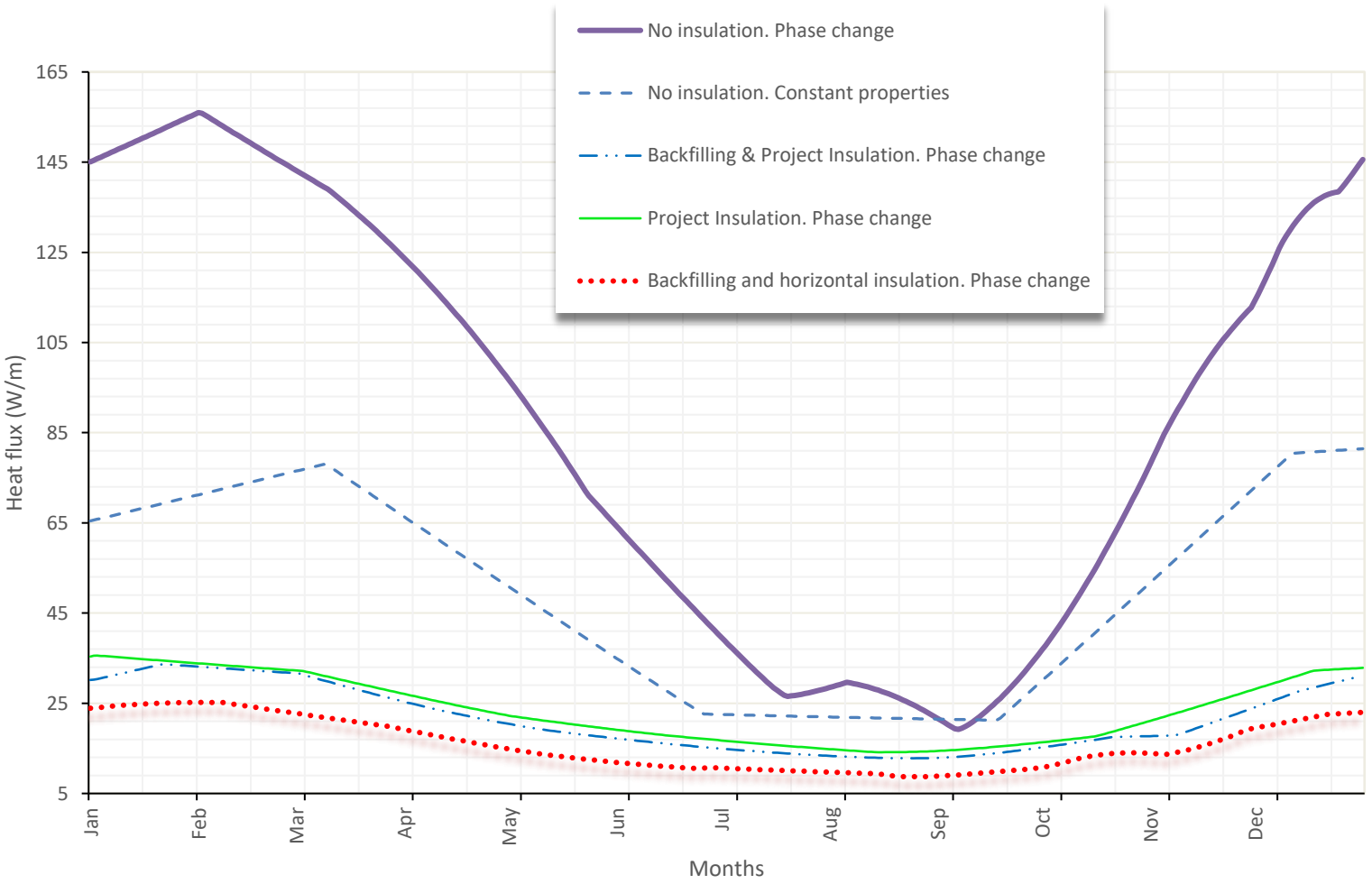

Fig. 48 Summary of wall heat loss from all simulations.

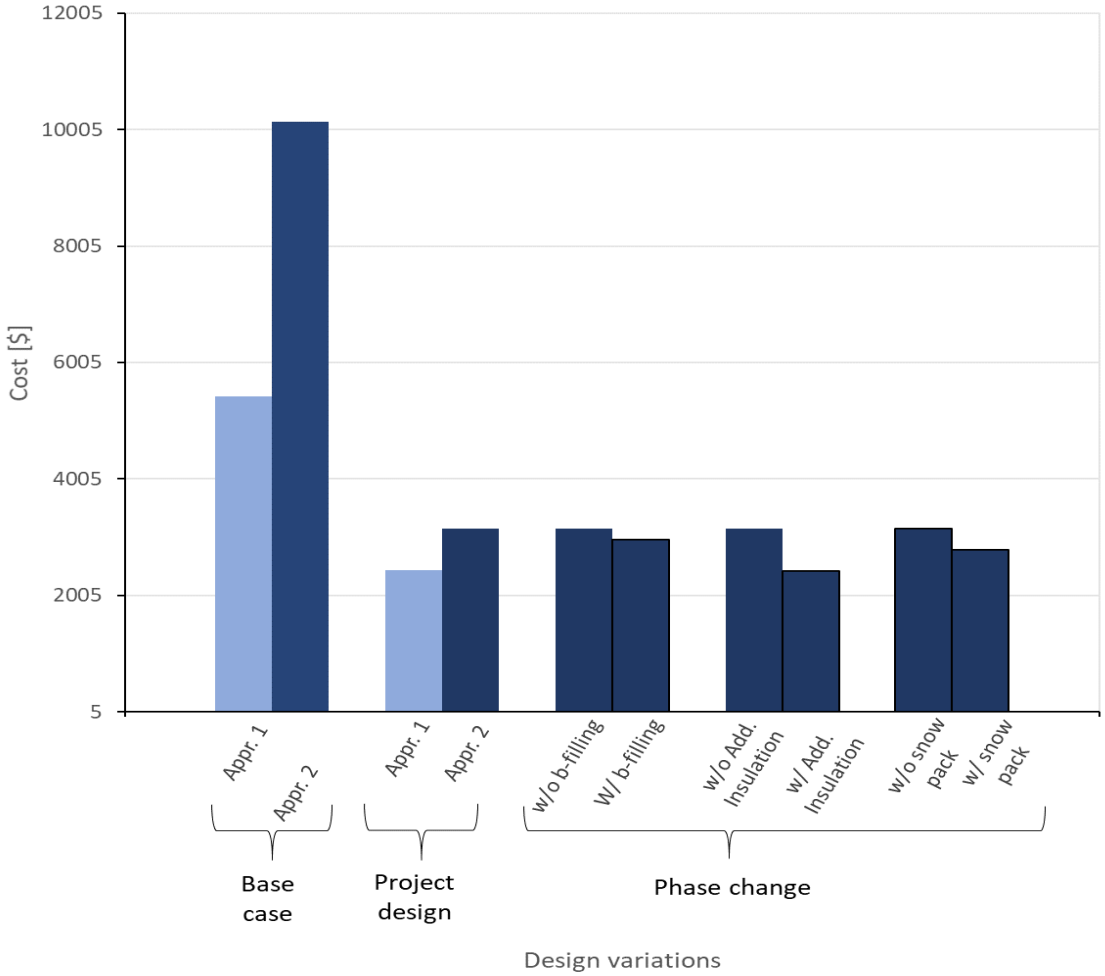

Fig. 49 Annual expenses on heat loss for different designs

Overall, the designed model gives a robust solution for heat loss prediction with relatively low computation time and qualification required. Resulting 35MWh of annual energy loss was predicted in Stanley Pauley basement part of the building which according to some preliminary calculation gives about 10% of all energy demands required for heating. Additional insulation of pavement all around perimeter of the building may reduce this value to somewhat 7%.

5.1.1. Limitations

Fully saturated condition is considered where pores are filled either with water or ice depending on temperature distribution. This fact may result in more intensive heat exchange as water and ice have significantly higher conductivity rather than air.

Problem was solved in 2D definition which makes heat flux distribution in *x* and *y* directions only. Solving problem in 3D may result in faster heat exchange. Geometry was simplified for better meshing , thus piles and pile caps were not modelled. The thermal effect of adjacent buildings was not considered.

5.1.2. Recommendations and Future Work

For future work, it appears to be interesting to design such problem which allows implementing coupled heat and mass transfer for heat loss calculation to determine the effect of degree of saturation of surrounding soil on the energy performance of basement structures.

It might be of great interest to analyse mentioned above problem in 3D definition to evaluate the effect of adjacent buildings on the thermal regime of the Stanley Pauley building.

REFERENCES

Ananyan, A. A. (1959). Structural interacting of water with rock. *Proceedings of Higher Education Institutions*, (1–2), 14.

Andersland, O. B., & Ladanyi, B. (2013). *An introduction to frozen ground engineering*. Springer Science & Business Media.

ASTM. (2013). ASTM D7015-13 Standard Practices for Obtaining Intact Block (Cubical and Cylindrical) Samples of Soils. *Standard Practices for Cycle Counting in Fatigue Analysis*, *D7015-13*.

ASTM. (2015). ASTM D1587/D1587M-15 Standard Practice for Thin-Walled Tube Sampling of Fine-Grained Soils for Geotechnical Purposes. *Standard Test Method for Measurement of Particle Size Analysis of Soils. ASTM, Philadelphia, Pennsylvania, USA*.

ASTM International. (2000). ASTM D4220/D4220M-14 - Preserving and Transporting Soil Samples. *ASTM International*, *D4220-14*, 1–11.

Becker, D. E., & Moore, I. D. (2006). Canadian foundation engineering manual. Canadian Geotechnical Society, Alliston, Ont.

Beskow, G. (1935). Soil freezing and frost heaving with special attention to roads and railroads. *The Swedish Geological Society, C*, (375), 23–91.

Bobko, K., Maghoul, P., & Kavgic, M. (2018). Energy Performance of Below-Grade Envelope of Stanley-Pauley Building in Winnipeg. In *GeoEdmonton 2018*.

Brooks, R., & Corey, T. (1964). Hydraulic Properties Of Porous Media. *Hydrology Papers, Colorado State University*, *24*.

Chuhanov, Z. F. (1974). High-speed method of intensive convectional heat and mass transfer. *Proceedings of the Academy of Sciences*, *10*, 1341–1356.

Côté, J., Rahimi, M., & Konrad, J.-M. (2012). *Thermal conductivity of compacted snow*. *Cold Regions Engineering 2012: Sustainable Infrastructure Development in a Changing Cold Environment*.

Dall'Amico, M. (2010). *Coupled water and heat transfer in permafrost modeling*. University of Trento.

Decagon. (2013). KD2 Pro thermal properties analyzer operator's manual version 4. *Decagon Devices, Pullman, WA*.

Deru, M. (2003). *Model for Ground-Coupled Heat and Moisture Transfer from Buildings*. National Renewable Energy Laboratory (NREL), Golden, CO.

Deru, M. P., & Kirkpatrick, A. T. (2002). Ground-Coupled Heat and Moisture Transfer from Buildings: Part1–Application. *Journal of Solar Energy Engineering*, *124*(1), 10.

Domenico, P. A., & Schwartz, F. W. (1998). *Physical and chemical hydrogeology*. Wiley.

Duffy, M. J., Hiller, M., Bradley, D. E., Keilholz, W., & Thornton, J. W. (2009). TRNSYS-features and functionalitity for building simulation 2009 conference. In *11th International IBPSA Conference-Building Simulation* (pp. 1950–1954).

Eckert, E. R., & Drake, R. M. (1961). *Heat and mass transfer*. *M.L. Gosenergoizdat*.

EnergyPlus. Version 8.9.0 Documentation. (2018).

Essex, D., Joe, K., Arvinder, H., Russell, L., Daniel, F., Kaeryn, G., … John, R. (2017). *Project Manual. Volume I of II Stanley Pauley Engineering Building 97 Dafoe Road* (Vol. I). University of Manitoba.

Farouki, O. (1992). *European foundation designs for seasonally frozen ground*. COLD REGIONS RESEARCH AND ENGINEERING LAB HANOVER NH.

Ferguson, G., & Woodbury, A. D. (2004). Subsurface heat flow in an urban environment. *Journal of Geophysical Research: Solid Earth*, *109*(B2).

First Nations housing. (2018). Retrieved from https://www.sac-isc.gc.ca/eng/1100100010715/1521125087940

Flerchinger, G. N., Seyfried, M. S., & Hardegree, S. P. (2006). Using soil freezing characteristics to model multi-season soil water dynamics. *Vadose Zone Journal*, *5*(4), 1143–1153.

Fredlund, D. G., Sheng, D., & Zhao, J. (2011). Estimation of soil suction from the soil-water characteristic curve. *Canadian Geotechnical Journal*, *48*(2), 186–198.

Fukuda, M., Kim, H., & Kim, Y. (1997). Preliminary results of frost heave experiments using standard test sample provided by TC8. In *Proceedings of the international symposium on ground freezing and frost action in soils, Lulea, Sweden* (Vol. 25, p. 30).

Gorochov, E. N. (2015). *Development of theory and methods of virtual modelling of temperature-cryogenic regime of earth-and-rockfill dams in cryolithic zone.* Nizhny Novgorod State University of Architecture and Civil Engineering.

Hagentoft, C.-E. (1988). Heat loss to the ground form a building. Slab on the ground and cellar. Thèse de doctorat, Lund Institute of Technology, Lund, Suède, 216 p.

Hansson, K., Šimůnek, J., Mizoguchi, M., Lundin, L.-C., & Van Genuchten, M. T. (2004). Water flow and heat transport in frozen soil. *Vadose Zone Journal*, *3*(2), 693–704.

Islam, M. D. (2015). Experimental and numerical study on flow and heat transport in partially frozen soil.

Jame, Y.-W. (1977). *Heat and mass transfer in freezing unsaturated soil*.

Janssen, H., Carmeliet, J., & Hens, H. (2004). The influence of soil moisture transfer on building heat loss via the ground. *Building and Environment*, *39*(7), 825–836.

Jumikis, A. R. (1966). *Thermal soil mechanics*.

Kays, W. M., Crawford, M. E., & Weigand, B. (2005). *Convective heat and mass transfer*.

Krarti, M., Chuangchid, P., & Ihm, P. (2004). Analysis of heat and moisture transfer beneath freezer foundations-Part II. *Journal of Solar Energy Engineering*, *126*(2), 726–731.

Kurylyk, B. L., & Watanabe, K. (2013). The mathematical representation of freezing and thawing processes in variably-saturated, non-deformable soils. *Advances in Water Resources*, *60*, 160–177.

Kutateladze, S. S. (1990). *Heat transfer and hydrodynamic drag. Manual*. Energoatomizdat.

Lebedev, P. D., & Petrov-Denisov, V. G. (1966). fluid dynamic theory, heat and mass transfer in small porous particles. *Heat and Mass Transfer. Collection of Research Papers.*, *5*, 146.

Maghoul, P. (2017). Numerical Simulation for Foundations Energy Efficiency in Cold Region. In *Poromechanics VI* (pp. 715–723).

Maghoul, P. (2017). Numerical Simulation for Foundations Energy Efficiency in Cold Region. *Poromechanics 2017 - Proceedings of the 6th Biot Conference on Poromechanics*, (June). https://doi.org/10.1061/9780784480779.088

Maghoul, P., Kavgic, M., & Bobko, K. (2017). Modeling of Thermal Performance of Foundation Walls in a Cold Climate.

Milligan, S. (2010). *2006 Aboriginal population profile for Kamloops by Shelly Milligan.* Ottawa, Ont.: Statistics Canada, Social and Aboriginal Statistics Division.

Moore, S. (2015). Thanks to $5 million gift electrical engineering is growing again! *UM Today*. Retrieved from http://news.umanitoba.ca/thanks-to-5-million-gift-electrical-engineering-is-growing-again/

Mualem, Y. (1976). A new model for predicting the hydraulic conductivity of unsaturated porous media. *Water Resources Research*, *12*(3), 513–522.

Newman, G. (1995). *Heat and mass transfer in unsaturated soils during freezing.* University of Saskatchewan, Saskatoon, Sask.

Parkin, G., von Bertoldi, A. P., & McCoy, A. J. (2013). Effect of tillage on soil water content and temperature under freeze–thaw conditions. *Vadose Zone Journal*, *12*(1).

Rubinšteĭn, L. I. (1971). *The stefan problem* (Vol. 27). American Mathematical Soc.

Saaly, M., Maghoul, P., & Kavgic, M. (2018). Performance Analysis of a Proposed Geothermal Pile-Based HVAC System for a Building in Cold Regions. Elsevier.

Shoop, S. A., & Bigl, S. R. (1997). Moisture migration during freeze and thaw of unsaturated soils: modeling and large scale experiments. *Cold Regions Science and Technology*, *25*(1), 33–45.

Šimůnek, J., Šejna, M., & Van Genuchten, M. T. (1996). The HYDRUS-2D software package for simulating water flow and solute transport in two-dimensional variably saturated media. Version 1.0. *US Department of Agriculture Riverside, California*.

Spiga, M., & Vocale, P. (2014). Effect of Floor Geometry on Building Heat Loss Via the Ground. *Heat Transfer Engineering*, *35*(18), 1520–1527.

Taylor, G. (2012). Assessment of Sustainable and Cultural Housing Design in the Clayoquot Sound First Nations: A Decision Framework for Residential Housing Developments.

Tian, H., Wei, C., Wei, H., & Zhou, J. (2014). Freezing and thawing characteristics of frozen soils: Bound water content and hysteresis phenomenon. *Cold Regions Science and Technology*, *103*, 74–81.

Timofeev, V. N. (1962). Heat transfer in a lump materials. *VNIIMP-Metallurgy*, (8), 472–494.

Tsytovich, N. A. (1975). *Mechanics of frozen ground*. Scripta Book Co.

Van Genuchten, M. T. (1980). A closed-form equation for predicting the hydraulic conductivity of unsaturated soils 1. *Soil Science Society of America Journal*, *44*(5), 892–898.

Watanabe, K., & Wake, T. (2009). Measurement of unfrozen water content and relative permittivity of frozen unsaturated soil using NMR and TDR. *Cold Regions Science and Technology*, *59*(1), 34–41.

www.hydro.mb.ca. (2018). Retrieved August 1, 2018, from https://www.hydro.mb.ca/accounts_and_services/rates/commercial-rates.shtml

Zhang, M., Yuan, J., & Wang, R. (2011). Effect of well pair distance of ground water heat pump on the changes of geo-temperature field due to aquifer energy extraction. In *Electrical and Control Engineering (ICECE), 2011 International Conference on* (pp. 5877–5882). IEEE.

Zhang, Y. (2014). Thermal-Hydro-Mechanical Model for Freezing and Thawing of Soils.

Zhu, M., & Michalowski, R. L. (2005). Simulation of heat transfer in Freezing soils using Abaqus. In *Abaqus Users' Conference* (pp. 1–7).

Appendix 1- Graphic Materials of Laboratory Tests

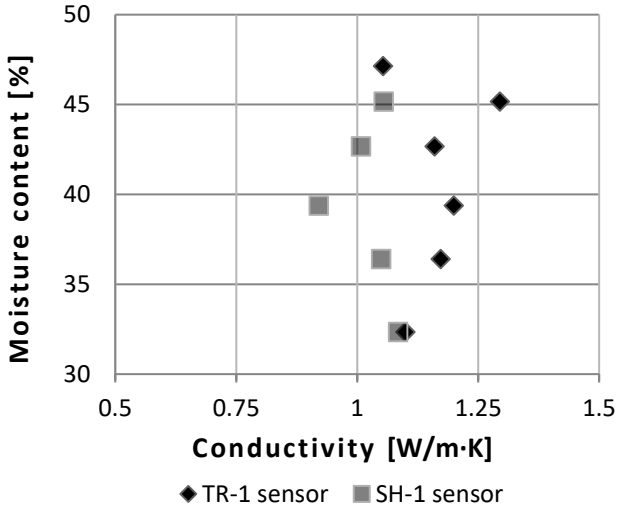

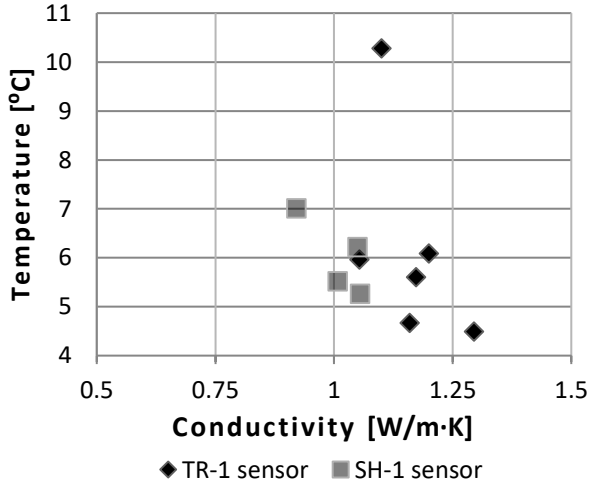

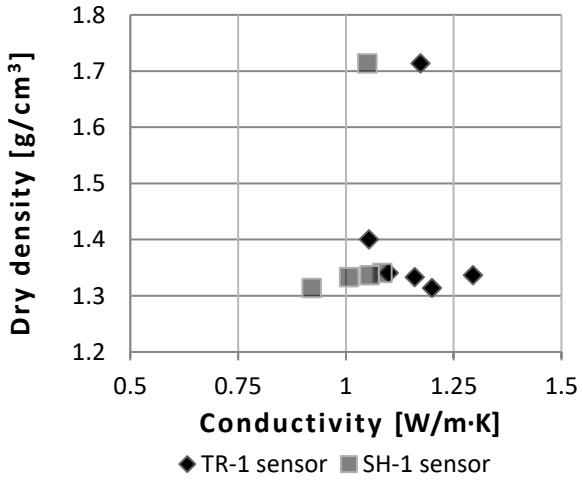

Fig. 50- Conductivity relation to physical properties of Layer 1 (Black clays -1.5m)

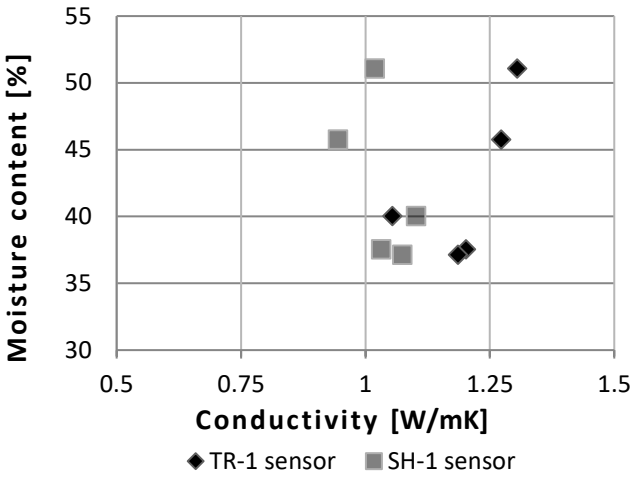

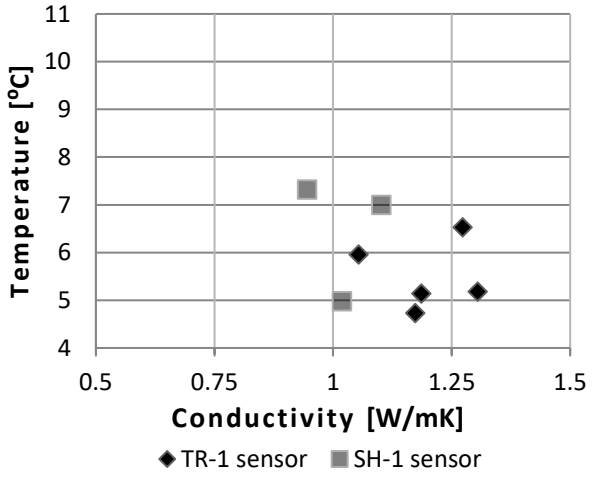

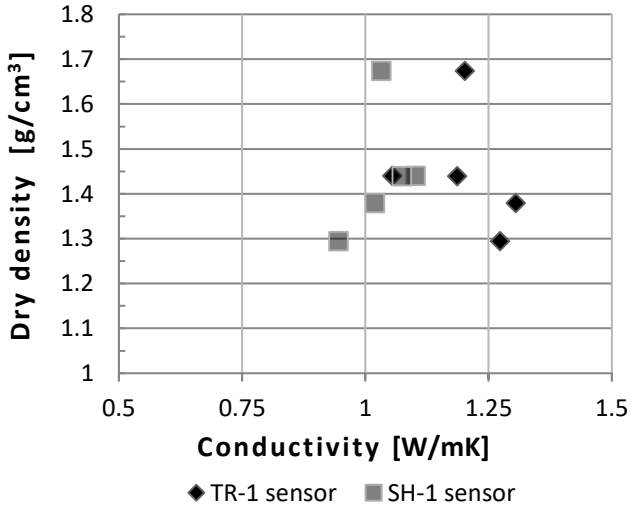

Fig. 51- Conductivity relation to physical properties of Layer 2 (Brown clays)

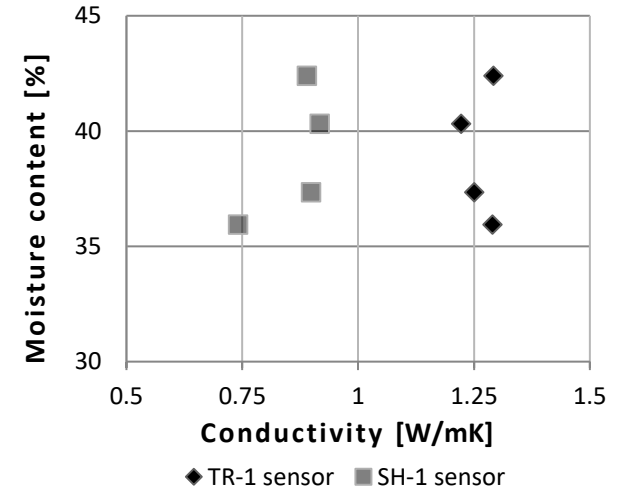

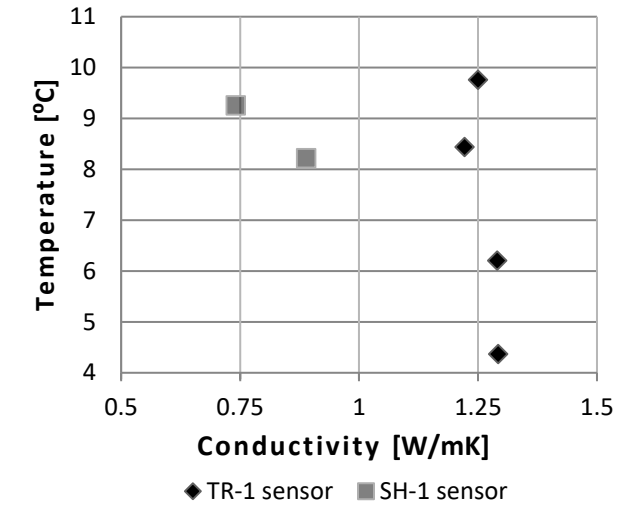

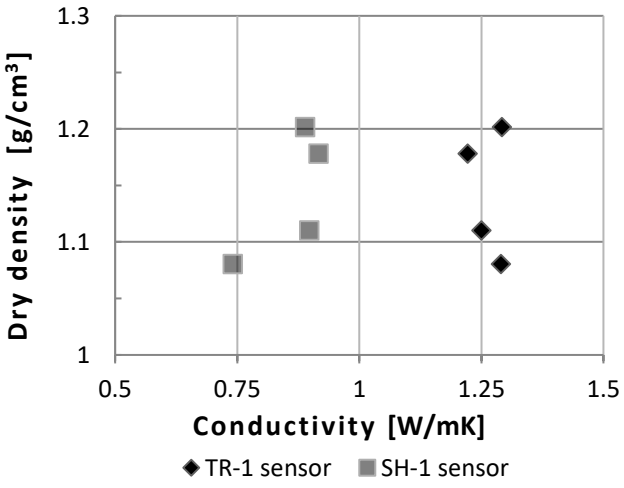

Fig. 52- Conductivity relation to physical properties of Layer 2 (Brown clays)

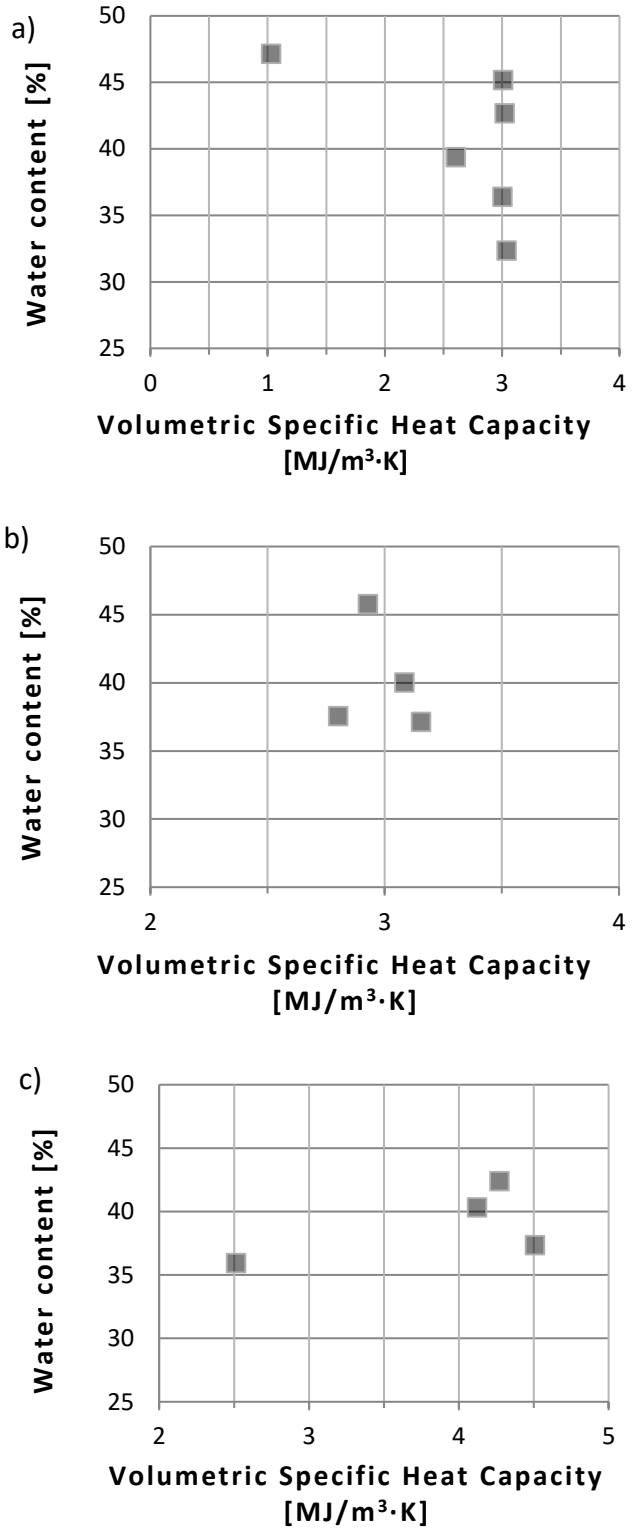

Fig. 53- Volumetric specific heat capacity related to water content of soil's samples

a)-Layer 1 *b)*-Layer 2 *c)*-Layer 3